A Quasi-Thermal-Mechanical-Biological Model of the Ste-Sophie, QC Landfill

by

James Thomas Doyle

A thesis submitted to the Faculty of Graduate and Postdoctoral Affairs in partial fulfillment of the requirements for the degree of

Master of Applied Science

in

Environmental Engineering

Carleton University
Ottawa, Ontario

ABSTRACT

A landfill located in Ste-Sophie, QC was instrumented with sensors measuring temperature, oxygen concentration, and settlement. A quasi-thermal-mechanical-biological conceptual model was developed and a corresponding numerical model was set-up in COMSOL Multiphysics to simulate the temperatures within the vertical waste profile. Thermal conductivity was varied with depth and time in the waste profile. An aerobic heat generation model was proposed that related the aerobic heat generation rate to the oxygen concentration measured near the surface. An anaerobic heat generation model presented in the literature was included in the model. The heat generation rate was dependent on waste temperature and the total energy expended. Corresponding field data were collected and the simulated temperatures were in good agreement with measured field temperatures. A heat budget was computed showing that aerobic and anaerobic heat generation accounted for 36% and 64% of total heat generation, respectively, during the filling stages of landfill operation.

ACKNOWLEDGEMENTS

I would like to thank my supervisor, Dr. Paul Van Geel, for all of his teaching, insight, and support on this project. I would also like to thank the research group of Dina Megalla, Alyssa Gladish, Courtney Berquist, and Katie Murray for all of their help.

TABLE OF CONTENTS

ABSTRACT ii
ACKNOWLEDGEMENTS iii
LIST OF TABLES vii
LIST OF FIGURES viii
LIST OF APPENDICES x
1.0 INTRODUCTION 1
1.1 Scope of Work 2
2.0 LITERATURE REVIEW & BACKGROUND INFORMATION 4
2.1 Landfill Introduction 4
2.2 Landfill Design 6
2.2.1 Cover System 6
2.2.2 Working Landfill 7
2.2.3 Landfill Gas Collection System 7
2.2.4 Leachate Collection System 8
2.2.5 Composite Liner System 8
2.3 Waste Stabilization 9
2.3.1 Hydrolysis 11
2.3.2 Acidogenesis 12
2.3.3 Acetogenesis 13
2.3.4 Methanogenesis 13
2.4 Factors Affecting Waste Stabilization 14
2.4.1 Waste Composition 15
2.4.2 Moisture 16
2.4.3 Temperature 16
2.4.4 Oxygen 17
2.4.5 pH 18
2.4.6 Nutrients 18
2.4.7 Bacteria 19
2.5 Heat Transfer & Generation in Landfills 19
2.5.1 Specific Heat 19
2.5.2 Thermal Conductivity 20
2.5.3 Conduction 23

2.5.4 Convection 23
2.5.5 Radiation 24
2.5.6 Heat Generation 26
2.5.7 Latent Heat 32
2.6 Settlement of Waste 33
2.7 Landfill Modelling 37
3.0 STE-SOPHIE LANDFILL EXPERIMENTAL SETUP & FIELD DATA 44
3.1 Experimental Set-up at the Ste-Sophie, Quebec Landfill 44
3.2 Temperature Field Data 49
3.3 Oxygen Field Data 52
3.4 Settlement Field Data 53
4.0 LANDFILL QUASI-THERMAL-MECHANICAL-BIOLOGICAL CONCEPTUAL MODEL & NUMERICAL MODEL SETUP 54
4.1 Heat Transfer within the Waste 55
4.1.1 Specific Heat 56
4.1.2 Thermal Conductivity 57
4.2 Conduction from Underlying Soil 58
4.3 Surface Heat Flux 59
4.4 Anaerobic Heat Generation Rate 59
4.5 Aerobic Heat Generation Rate 62
4.6 Numerical Model Setup in COMSOL Multiphysics 64
4.7 Mechanical Settlement 66
5.0 LANDFILL QUASI-THERMAL-MECHANICAL-BIOLOGICAL MODEL RESULTS AND DISCUSSION 68
5.1 Mechanical Settlement 68
5.2 Numerical Model Results & Predicted Temperatures 69
5.3 Comparison with Second Bundle Column 73
5.4 Heat Budget Analysis 75
5.5 Model Sensitivity Analysis 79
6.0 MODELLED AIR INJECTION TEST 86
7.0 LANDFILL SURFACE STUDY 89
7.1 Surface Study Experimental Set-up 89
7.2 Surface Study Results & Discussion 96
8.0 CONCLUSIONS & RECOMMENDATIONS FOR FUTURE WORK 107

8.1 Conclusions 107
8.2 Recommendations for Future Work 109
REFERENCES 111

LIST OF TABLES

Table 1: Factors Affecting Landfill Gas Production (Modified from El-Fadel, 1991) 15
Table 2: Summary of Heat Generation Values found in Literature 31
Table 3: Composite Compressibility Model Parameters From Literature 37
Table 4: Date of Data Collection Commencement for Instrument Bundles 49
Table 5: Hanson Cell D Heat Generation Parameters 60
Table 6: Model Simulation Periods 65
Table 7: Heat Budget 76
Table 8: Sensitivity Analysis Results 81

LIST OF FIGURES

Figure 1: Total Global MSW Disposal (2012) [Modified from Hoornweg and Bhada-Tata, 2012]5
Figure 2: Anaerobic Digestion Process Schematic (Modified from Waste-to-Energy Research and Technology Council, 2009) 10
Figure 3: Composition of Landfill Gas through Aerobic and Anaerobic Digestion Processes in a Typical Landfill (Modified from Agency for Toxic Substances & Disease Registry, 2001) 11
Figure 4: Factors Affecting Waste Stabilization (Modified from Rees, 1980) 14
Figure 5: Heat Budget for the first 10.5 months of waste placement at the Ste-Sophie, QC landfill cell (with permission from Bonany, 2012) 42
Figure 6: Overhead view of Ste-Sophie Landfill 45
Figure 7: Instrument bundle used at the Ste-Sophie Landfill 46
Figure 8: Waste Lift Heights and Bundle Locations 47
Figure 9: Cross Sectional View of Bundles in Landfill 48
Figure 10: Temperature profiles of Bundles 1-12 50
Figure 11: Oxygen Data for Bundles 1-12 52
Figure 12: Settlement of Bundles 1-12 53
Figure 13: THMB Conceptual Model 54
Figure 14: Conceptual Model of Heat Transfer Processes within and around Landfill 55
Figure 15: Thermal conductivity variance with depth and time 58
Figure 16: Heat Generation vs. Energy Expended 61
Figure 17: 3D Plot of heat generation dependent upon temperature and energy expended 62
Figure 18: Bundle 9 Temperature & Oxygen Data 63
Figure 19: Bundle 11 Temperature & Oxygen Data 63
Figure 20: Actual and Modelled Settlement Values 68
Figure 21: Actual and Modelled Odd-numbered Bundle Temperatures 69
Figure 22: Expended energy at each of the bundle locations over time 71
Figure 23: Temperature profiles with depth at the following dates: a) December 12, 2010; b) January 27, 2011; c) August 22, 2011; d) March 14, 2012; e) January 9, 2013; f) May 23, 2014 72
Figure 24: Actual and Modelled Even-numbered Bundle Temperatures 74
Figure 25: Specific Heat Sensitivity Analysis a) -20%, b) -10%, c) base model, d) +10%, e) +20% 83
Figure 26: Thermal Conductivity Sensitivity Analysis a) -20%, b) -10%, c) base model, d) +10%, e) +20% 84
Figure 27: Oxygen Injection Point Source Location 87
Figure 28: Oxygen Injection Test Results 88
Figure 29: Overhead Schematic of Surface Monitoring Station Set-Up 90
Figure 30: Surface Monitoring Station Set-Up 91
Figure 31: Excavation of waste pods 93
Figure 32: Sensor installation into excavated wall of waste pod 93
Figure 33: Clean sand grain size distribution 94
Figure 34: Filling of sand cover on pod 1 95
Figure 35: Surface monitoring station on June 23rd, 2015 96
Figure 36: Oxygen Concentration at a Depth of 40 cm for Pod 1 (Clean Sand) 97
Figure 37: Oxygen Concentration at a Depth of 40 cm for Pod 2 (WM Interim Cover) 97

Figure 38: Oxygen Concentration at a Depth of 40 cm for Pod 3 (2% Clay, Sand) 98
Figure 39: Pod 1 saturated cover (June 26, 2014). Pooled water is visible at a depth of 10 cm. ... 99
Figure 40: Oxygen content in the cover of pods 1 and 3 (D=15 cm) and just below the cover of pod 2 (D=40 cm) 100
Figure 41: Pod 1 temperature, heat flux, and rainfall data 102
Figure 42: Pod 2 temperature data 102
Figure 43: Pod 3 temperature, heat flux, and rainfall data 103
Figure 44: Temperatures at a depth of 40 cm in pods 1-3 103
Figure 45: Temperatures at a depth of 60 cm in pods 1-3 104
Figure 46: Temperatures at a depth of 75 cm in pods 1-3 104
Figure 47: Pod 2 oxygen and temperature 105
Figure 48: Plastic liner placed above pods 106

LIST OF APPENDICES

APPENDIX A – ENGINEERING DRAWINGS……..……115

1.0 INTRODUCTION

Solid waste management is an important and essential part of human life. In 2010, Canadians sent approximately 25 million tonnes of waste to be disposed of in landfills. This is equivalent to 729 kg per capita per annum, which ranks Canadians 17th out of 17 OECD countries (Giroux, 2014).

A successful solid waste management strategy involves minimizing the generation of waste at the source; recovery, reuse, and recycling of waste materials; and proper management of waste at disposal. In 2010, Canadians diverted just 24.5% of municipal solid waste generated, meaning that 75.5% of municipal solid waste was sent to be disposed of in landfills (Giroux, 2014). This massive amount of waste (25 million tonnes in 2010) poses many environmental and social challenges including:

- Where to dispose of the waste
- Management of landfill gas production
- Threat of leachate to contaminate groundwater
- Stabilization and settlement (reducing the contamination lifespan of landfills)
- Reclamation of land for other uses

The cold Canadian climate is another challenge involved in the management of solid waste. During cold winter months, municipal waste that is placed curbside may be frozen by the time it is collected. Frozen waste placed in the landfill can stay frozen for many months or even years (Bonany et al., 2013a; 2013b) due to being insulated at cold temperatures by subsequent waste layers placed above. Cold or frozen temperatures inhibit biological activity in the waste, therefore not allowing temperatures to rise and

waste to be decomposed. This results in a longer contaminating lifespan of the landfill as well as a slower rate of settlement. Gaining a greater understanding of the heat transfer and heat generation within a landfill situated in a northern climate can lead to better waste management practices for waste management operators to use. The overall goal of this thesis is to advance this insight and understanding.

1.1 Scope of Work

This research focuses on the stabilization of landfills in northern climates such as Canada. Instrumentation was installed in a landfill in Ste-Sophie, QC starting in late 2009 and has been successfully recording temperature, settlement, oxygen, piezometer, and total earth pressure data to present day. The goal of this work was to advance the work of Bonany (2012) and Megalla (2015). Bonany (2012) first developed a one-dimensional heat transfer model simulating the first two years of temperature data. Surface heat flux, conduction from the landfill base, latent heat, and heat generation were all considered in the model. Megalla (2015) continued the work of Bonany (2012) by modelling subsequent waste lifts, improving the conceptual model, and presenting a model application to illustrate the effects of a different waste placement schedule on waste temperature.

In this thesis, a quasi-thermal-mechanical-biological coupled landfill model is presented that uses Bonany (2012) and Megalla (2015) as a foundation. The model simulates temperatures within a waste profile in a landfill over time, as waste is added and settles. Heat transfer from above, below, and within the landfill are considered in the model. Heat generation due to aerobic and anaerobic decomposition is also considered. This work intends to provide further insight into the heat transfer and generation processes that

are ongoing in a landfill. Data from the Ste-Sophie, QC landfill has been used to calibrate the model that is presented in this thesis. Due to the cold Canadian climate, the model must consider frozen waste and the thawing process it undergoes in the landfill. The major improvements made in this thesis to the models presented by Bonany (2012) and Megalla (2015) include:

- The inclusion and coupling of an anaerobic heat generation model
- Improved aerobic heat generation term
- The inclusion of a settlement model of the waste over time
- Improved thermal properties, including variation of thermal conductivity with depth and time

The thesis is organized into the following sections:

- Section 1.0: Introduction
- Section 2.0: Literature Review and Background Information
    - A review of relevant information on landfills and landfill heat transfer and heat generation research
- Section 3.0: Ste-Sophie Landfill Experimental Setup and Field Data
    - A description of the in-field experimental setup and corresponding field data
- Section 4.0: Landfill Quasi-Thermal-Mechanical-Biological Conceptual Model and Numerical Model Setup

    - Detailed description of the conceptual model and description of procedures and assumptions made in the development of the model in COMSOL Multiphysics
- Section 5.0: Landfill Quasi-Thermal-Mechanical-Biological Model Results & Discussion
    - Model results compared against measured field data, a heat budget of the model, and a model sensitivity analysis
- Section 6.0: Modelled Air Injection Test
    - Study of potential effects of injecting oxygen into the landfill
- Section 7.0: Landfill Surface Study
    - Overview of surface field instrumentation set-up and data to evaluate surface heat fluxes
- Section 8.0: Conclusions & Recommendations for Future Work

The surface monitoring station field data and the modelling of the data (Section 7.0) were originally the focus of the author's MASc research. When the data did not indicate the expected trends and the issues related to the data could not be resolved, it was decided by the author and his supervisor to shift the focus of the author's MASc to the modelling of the instrument bundle data.

2.0 LITERATURE REVIEW & BACKGROUND INFORMATION

2.1 Landfill Introduction

Landfills date as far back as 500 BC when ancient Greeks realized the need to dispose of waste outside city limits (Murray, 1995). In 2012, the world's population produced 1.3

billion tonnes of municipal solid waste, and that number is expected to grow to 2.2 billion tonnes by 2025 (Hoornweg and Bhada-Tata, 2012). Currently, landfilling is still the most common method of municipal solid waste disposal as seen in Figure 1.

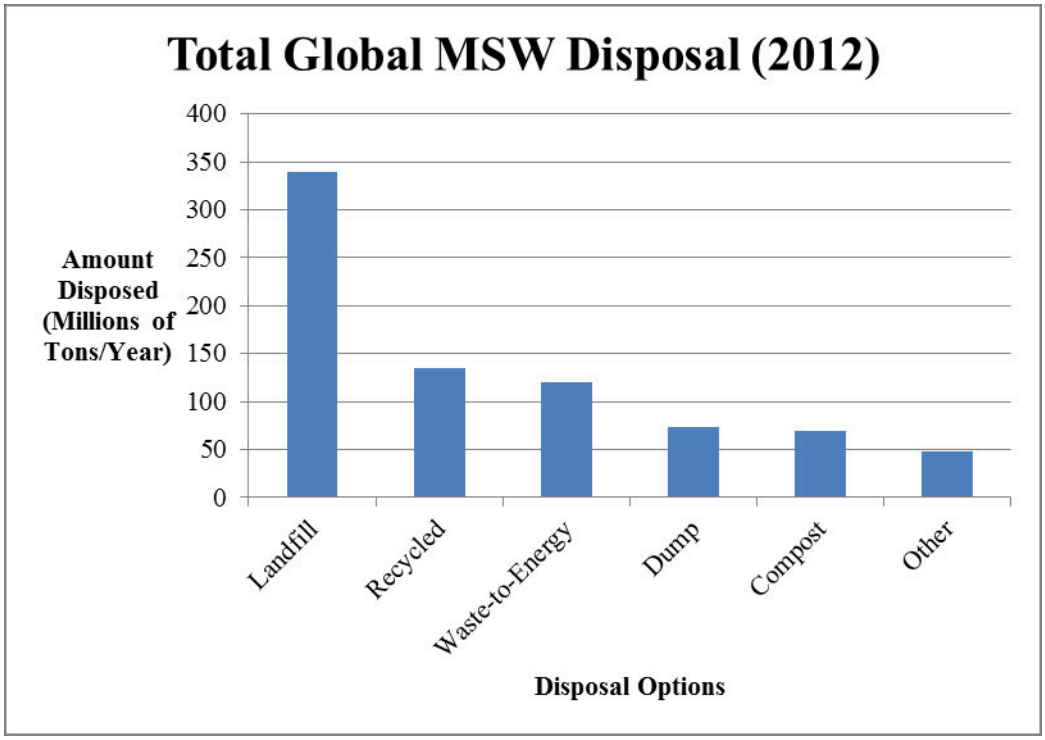

Figure 1: Total Global MSW Disposal (2012) [Modified from Hoornweg and Bhada-Tata, 2012]

Mismanagement of municipal solid waste disposal in landfills can lead to environmental and human health effects such as:

- Global warming effects due to the release of methane (a greenhouse gas produced during the anaerobic decomposition of waste)
- Contamination of ground and drinking water due to the seepage of contaminants from the landfill
- Vast land use
- Production of odours
- Other environmental, human health, and social effects

The sheer volume of waste disposed of in landfills, coupled with the fact that improper management of landfills can lead to negative effects, results in investigations to better the management and operation of modern landfills.

2.2 Landfill Design

Modern landfills are engineered systems designed to protect human and environmental health. There are many components of design, all of which are in place to make the disposal and storage of waste as safe as possible. The following are the main components of landfill design:

- Cover System
- Working Landfill
- Landfill Gas Collection System
- Leachate Collection System
- Composite Liner System

2.2.1 Cover System

The final cover system controls the amount of water that is allowed to percolate into the waste as well as the amount of landfill gas that leaves the waste. Because moisture is a key parameter in the generation of leachate and landfill gas, as well as the stabilization of the landfill, the design of the cover is pertinent to good landfill design (Rowe, 2011). A typical permeable landfill cover design allows for 0.15-0.2 m/a of percolation through the cover, which is simply done through the use of a compacted soil layer. This amount of moisture allows for biodegradation to occur, but also allows generation of a reasonable amount of leachate that can be handled by the leachate collection system without a large build-up of leachate head and potential environmental issues. A permeable cover design

however does not do a good job at controlling the egress of landfill gas (Rowe, 2011). An alternate approach to cover design is a low permeability cover, which often includes a plastic liner to limit percolation and resulting leachate, and to reduce landfill gas emissions. This cover design can reduce the amount of biological activity in the landfill if sufficient moisture has not accumulated in the landfill before cover placement. Lower biological activity results in lower amounts of leachate and gas collection; and associated costs (Rowe, 2011).

2.2.2 Working Landfill

Waste is placed in the landfill in what are known as lifts; or layers of waste that are compacted in small areas. Landfills commonly use interim daily soil covers placed at the end of each day on top of the waste to limit odours, vermin, and migration of waste due to the wind. Some landfills use interim daily plastic covers that cover the waste at the end of each day and are then rolled back at the start of the next workday (Indiana Department of Environmental Management, 2013).

2.2.3 Landfill Gas Collection System

Landfill gas is produced due to the biodegradation of the waste (process discussed in more detail in Section 2.3). Landfill gas is primarily comprised of carbon dioxide and methane, in approximately equal proportions. Nitrogen, oxygen, hydrogen, water vapour, and various volatile organic compounds (VOCs) are also found in trace amounts. When emitted from the landfill, landfill gas has significant environmental impacts (primarily due to the high greenhouse gas effect of methane). Landfill gas can also be an explosive hazard if concentrations build up within the landfill. In 1986 in Derbyshire, UK, landfill gas, in a landfill cell without gas collection, migrated through the subsurface to the basement of a nearby dwelling and caused a severe explosion (Williams and Aitkenhead,

1991). For these reasons, modern landfills collect landfill gas through a series of horizontal and vertical wells throughout the waste. The collected landfill gas can either be burned off to minimize the environmental impacts, or, due to the high concentration of methane, landfill gas can also be a useful resource to nearby local industry (Rowe, 2011).

2.2.4 Leachate Collection System

Leachate is liquid primarily generated from percolated rain water (also generated from water that is the by-product of biological reactions in the waste) that filters through the waste and collects contaminants. To collect the leachate, at least one leachate collection system is installed at the base of modern engineered landfills. Leachate collection systems are a series of perforated pipes, surrounded by gravel, that collect leachate by means of gravity and remove it (by pumps) to a leachate treatment facility. The goal of a leachate collection system is to remove leachate from the landfill to reduce the hydraulic head on the liner system. Reducing the hydraulic head will reduce the hydraulic gradient across the liner system and therefore reduce the volume of leachate that may escape from the landfill.

2.2.5 Composite Liner System

A major concern for landfills is leachate escaping from the bottom barrier of the landfill and migrating into groundwater and local drinking water. To minimize the risk of this possibility, landfills have an engineered composite liner system underneath the leachate collection system to provide resistance to the migration of contaminants, both by the advection of leachate due to leachate head above the liner and by diffusion of contaminants due to concentration-driven movement. There are two main types of composite liner systems used in modern landfills: compacted clay liners (CCLs) overlain by a geomembrane, and geosynthetic clay liners (GCLs) overlain by a geomembrane.

Compacted clay liners are made up of 0.6-1.2 m of compacted clay while geosynthetic clay liners are made up of 5-10 mm of low-permeability bentonite clay that swells when moist, encased between two geotextiles. Both liner systems are constructed and overlain by a geomembrane (1.5-2 mm thick high density polyethylene (HDPE)), a non-woven geosynthetic to protect the geomembrane and a protective drainage layer of sand (Rowe, 2011).

2.3 Waste Stabilization

Waste stabilization is a collection of chemical and physical processes that reduce the contaminating potential of a landfill and converts toxic substances into stable forms. Waste is fully stabilized once the landfill no longer has the potential to contaminate the surrounding environment. (Sharma & Lewis, 1994; US EPA, 1998)

The waste stabilization process occurs in two main steps. The first step, aerobic decomposition, occurs due to the presence of oxygen in the waste, when the waste is first placed. Once all available oxygen is used up and the aerobic process is halted, anaerobic decomposition commences (El-Fadel, 1991) (See Figure 3). The exception is near the surface of landfills, where diffusion of oxygen through the upper layer can allow for aerobic conditions to proceed for longer periods. Since the anaerobic process generally persists for a much longer period than the aerobic process, this is what controls the stabilization of waste. The by-product of the anaerobic process is landfill gas.

The anaerobic process is quite complex and occurs in four main stages:

- Hydrolysis
- Acidogenesis

- Acetogenesis
- Methanogenesis

These processes are described in the subsequent sections. It is important to note that although these processes occur in succession for given portions of waste, all of the processes are ongoing throughout the landfill at any given time. The hydrolysis step is the rate-limiting step, controlling the rate at which landfill gas is produced. At any particular location throughout a landfill however, one step may be dominant (El-Fadel, 1991). In general, the anaerobic degradation process takes more complex organic matter (such as polymers like cellulose) and breaks it down into simpler organic matter (such as monomers like glucose) and eventually into carbon dioxide and methane. Figure 2 is a schematic of the anaerobic digestion process, detailing the breakdown of organic matter through the four stages.

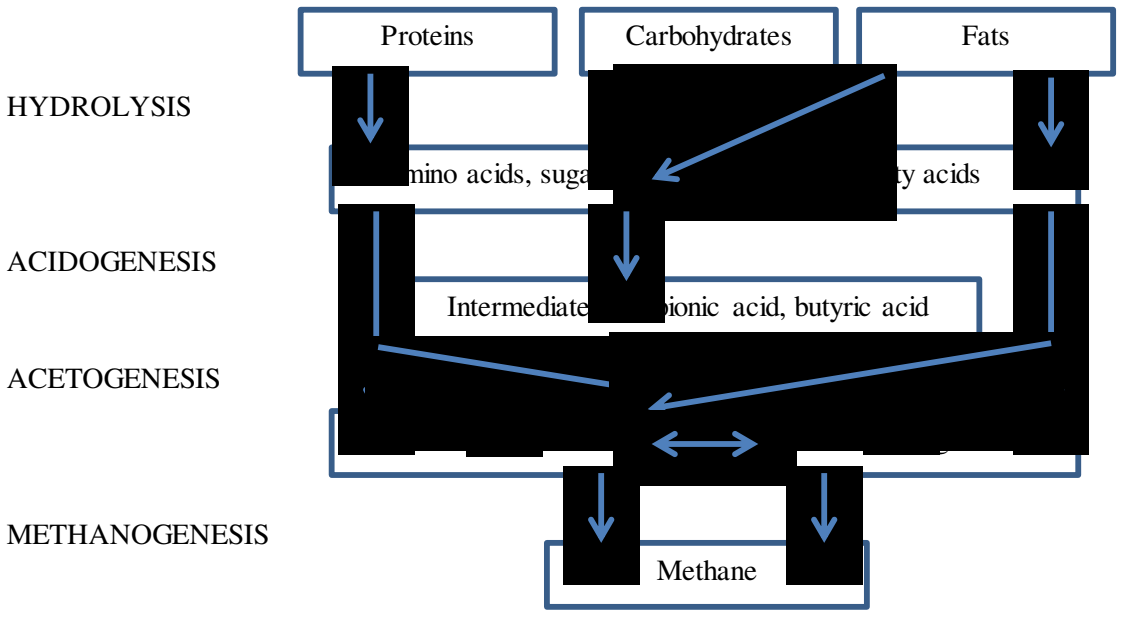

Figure 2: Anaerobic Digestion Process Schematic (Modified from Waste-to-Energy Research and Technology Council, 2009)

As these processes are ongoing, the composition of landfill gas being produced due to the decomposition of the waste changes over time. Figure 3 shows the change in composition of landfill gas over time.

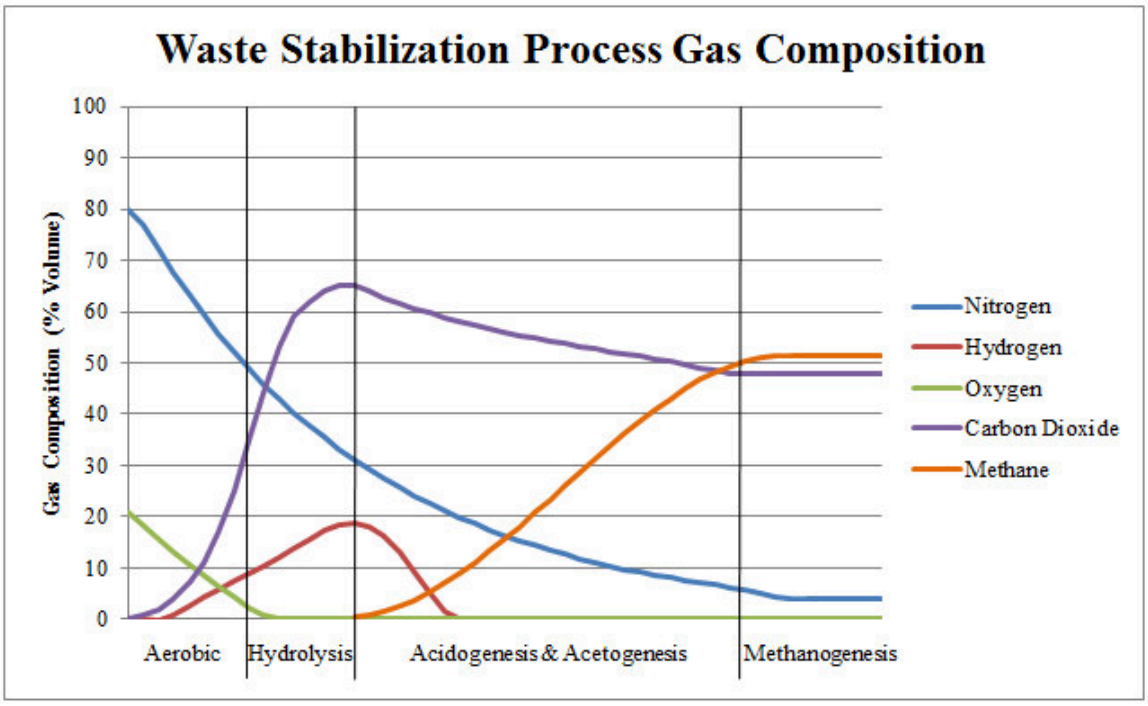

Figure 3: Composition of Landfill Gas through Aerobic and Anaerobic Digestion Processes in a Typical Landfill (Modified from Agency for Toxic Substances & Disease Registry, 2001)

As can be seen in Figure 3, the oxygen in the waste is depleted by the start of the anaerobic process. During hydrolysis, hydrogen is produced and then consumed by microbes during the acidogenesis stage. Carbon dioxide is produced throughout the entire process, eventually steadying at 45-60% during the methanogenesis stage. Methane, produced by methanogens during methanogenesis, steadies at 45-60% as well.

2.3.1 Hydrolysis

Hydrolysis is the rate-limiting and most important step in the production of landfill gas through the anaerobic process (El-Fadel, 1991; Halvadakis, 1983; Gholamifard, 2008). During hydrolysis, polymeric materials (e.g. lipids, proteins, carbohydrates, and fats) are

broken down into simple sugars, alcohols, amino acids, and long fatty acid chains. The breakdown is facilitated by microbial species that produce three major types of enzymes known as cellulases that break down cellulosic material. These three enzymes are Endoglucanases, Exoglucanases, and B-Glucanases (El-Fadel, 1991).

2.3.2 Acidogenesis

Acidogenesis transforms the sugars, alcohols, amino acids, and fatty acid chains that were produced during hydrolysis into short chain volatile fatty acids, ketones, alcohols, hydrogen gas, and carbon dioxide gas (El-Fadel, 1991; Waste-to-Energy Research and Technology Council, 2009). Two main types of acidogenic bacteria exist. Hydrogen producing acidogens digest alcohols and fatty acids into mainly acetic acid, butyric acid, propionic acid, hydrogen, and carbon dioxide. The second type is hydrogen consuming acidogens. These microbes digest carbohydrates, hydrogen, and other organic compounds to form acetic acid (El-Fadel, 1991; Waste-to-Energy Research and Technology Council, 2009). The two types of microbes work in concert with each other as the hydrogen formed by the first type of microbes feeds the second type of microbes. The carbon dioxide, unused hydrogen, and acetic acid skip the acetogenesis stage and are consumed by methanogenic bacteria. The remaining butyric acid, propionic acid, long-chain fatty acids, alcohols, and other organic compounds are further broken down during acetogenesis.

The formation of carboxylic acids (e.g. acetic acid, butyric acid, propionic acid) during acidogenesis produces the majority of heat that is generated during the anaerobic digestion process (El-Fadel et al., 1996b).

2.3.3 Acetogenesis

As mentioned above, the remaining products of acidogenesis are further broken down by acetogens into carbon dioxide, hydrogen, and acetic acid. The reactions of acetogenesis will only proceed if the partial pressure of hydrogen is less than 10^{-4} atm. Therefore the presence of hydrogen-consuming microbes in the acidogenesis phase is extremely critical to acetogenesis (El-Fadel, 1991). When the remaining long-chain fatty acids are consumed by the acetogens, the pH is increased to a level where methanogenesis is able to occur (Ahring, 2003).

2.3.4 Methanogenesis

Methanogenesis transforms the carbon dioxide, hydrogen, and acetic acid produced during acidogenesis and acetogenesis into methane and carbon dioxide. There are two main groups of methanogenic bacteria: acetotrophic (or acetoclastic) methanogens and hydrogenotrophic (or hydrogen-utilizing) methanogens (El-Fadel, 1991, Bareither et al., 2013). The acetotrophic methanogens consume acetic acid to form methane and carbon dioxide according to the following reaction:

$$CH_3COOH \rightarrow CH_4 + CO_2 \quad (\mathbf{1})$$

The hydrogenotrophic methanogens consume hydrogen and carbon dioxide to form methane and water according to the following reaction:

$$4H_2 + CO_2 \rightarrow CH_4 + 2H_2O \quad (\mathbf{2})$$

As can be seen in Figure 3, the concentration of carbon dioxide slightly decreases during methanogenesis, while the concentration of methane significantly increases. The hydrogenotrophic bacteria play an important role in regulating the partial pressure of hydrogen which governs the entire anaerobic process (El-Fadel, 1991). The acetotrophic

bacteria produce approximately 70% of the methane in landfill gas (El-Fadel et al., 1996a).

2.4 Factors Affecting Waste Stabilization

A number of different factors play a part in the stabilization of waste/generation of landfill gas. Figure 4 is an influence diagram modified from Rees (1980) that shows the factors and relationships that affect the production of biogas and therefore stabilization of waste. The importance of the movement/presence of moisture in the waste is recognized as the focal point of the factors.

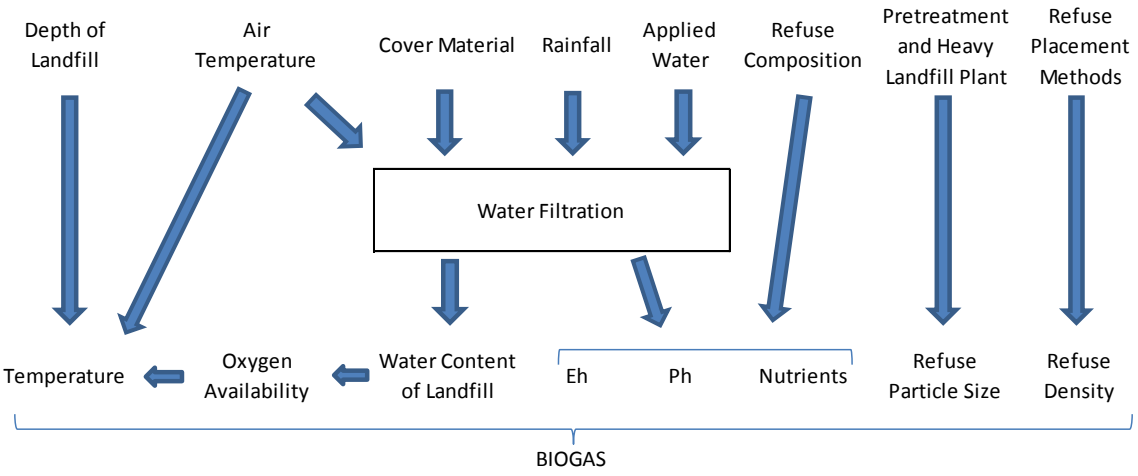

Figure 4: Factors Affecting Waste Stabilization (Modified from Rees, 1980)

El-Fadel (1991) categorized factors affecting the production of landfill gas into three categories: external, internal, and operational/waste management variables. These variables are shown in Table 1.

Table 1: Factors Affecting Landfill Gas Production (Modified from El-Fadel, 1991)

External Variables	air temperature precipitation topography hydrogeology atmospheric pressure
Internal Variables	refuse composition moisture content refuse density nutrients microbial population temperature pH alkalinity/buffering refuse particle size oxygen concentration methane concentration carbon dioxide concentration toxics, heavy metals
Operational/Waste Mangement Variables	refuse treatment refuse compaction applied water leachate recirculation surface vegetation gas recovery

The following sections detail some of the most critical factors in the stabilization of waste.

2.4.1 Waste Composition

The composition of waste plays a role in how the waste stabilization process works, as the constituents that are digested through aerobic or anaerobic digestion are from the waste. Different locations and different landfills can have different waste compositions, depending on the local culture, economy, and industry; as well as what type of waste the landfill receives (e.g. municipal solid waste, institutional & commercial waste, construction & demolition waste, etc.) and the recycling and diversion programs in place.

In terms of the anaerobic digestion process, waste composition influences the potential availability of usable substrates as well as toxic inhibitors (El-Fadel, 1991).

2.4.2 Moisture

In general, moisture content is considered the most critical variable in the waste stabilization process. Generally, greater moisture content results in faster waste stabilization and greater landfill gas production. Moisture provides an aqueous environment that is necessary for the anaerobic degradation process, as well as providing a method for mass transfer of nutrients and microbes throughout the landfill, and buffering of pH (Warith, 2003; El-Fadel, 1991). For hydrolysis to occur, a sufficient amount of moisture for microbial activity is required (Karthikeyan & Joseph, 2007). Moisture can be controlled operationally by the addition of water or leachate recirculation. These practices have been found to enhance the waste stabilization process (El-Fadel, 1991; Townsend et al., 2008; Warith, 2003). Warith (2003) reports that greater movement of moisture through the use of leachate recirculation can increase gas production rates by 25-50%. Too much moisture addition can however inhibit the anaerobic degradation process as high moisture contents can stimulate acidogenesis to the point where the onset of methanogenesis is delayed. Rapid moisture infiltration may also impede methanogenesis itself (El-Fadel, 1991). Optimum moisture content has been reported as 60% or greater on a wet mass basis (Karthikeyan & Joseph, 2007; Rees, 1980).

2.4.3 Temperature

Temperature is an interesting factor in waste stabilization as higher temperatures both drive landfill gas production and are generated by the degradation process. Anaerobic activity and gas production rates have been shown to improve with increased

temperatures in both the mesophilic and thermophilic optimal temperature ranges. Mesophilic bacteria (mesophiles) are those that excel under moderate temperatures. Thermophilic bacteria (thermophiles) are those that excel under higher temperatures. The optimum temperature range for mesophilic bacteria has been reported as 40 ^{o}C (Rees, 1980), 30 ^{o}C to 40 ^{o}C (El-Fadel, 1991), 35 ^{o}C to 45 ^{o}C (Hanson et al., 2006), 34 ^{o}C to 40 ^{o}C (Townsend et al., 2008), and 34 ^{o}C to 45 ^{o}C (Karthikeyan & Joseph, 2007). The optimum temperature range for thermophilic bacteria has been reported as 50 ^{o}C to 55 ^{o}C (El-Fadel, 1991), 50 ^{o}C to 60 ^{o}C (Hanson et al., 2006), and up to 70 ^{o}C (Townsend et al., 2008). Ward (1983) reported that for every 10 ^{o}C increase in temperature, landfill gas generation rates double.

Hanson et al. (2006) studied the effects of placement conditions on decomposition of municipal solid waste in cold climates. A landfill in Anchorage, Alaska was studied. A 7 m thick layer of waste (insulated both above and below) was placed during freezing conditions. The central portion of this layer remained frozen two years after placement. No decomposition or gas generation was found in the frozen waste. A one-dimensional thermal model was used to analyze temperature distribution in the landfill, and it was concluded that thinner waste lifts would promote higher temperatures throughout the landfill and therefore earlier onset of biodegradation.

2.4.4 Oxygen

The availability of oxygen has an obvious effect on the rate at which aerobic decomposition proceeds. The absence of oxygen renders aerobic decomposition non-existent. During the anaerobic digestion process, the presence of oxygen inhibits degradation (Haarstrick et al., 2003; El-Fadel, 1991) due to facultative anaerobes

(microbes capable of producing energy through aerobic or anaerobic reactions depending on the presence of oxygen) out-competing methanogens (Hedrick & White, 1993). If extensive pumping of landfill gas is conducted in a landfill, air may be drawn into the anaerobic zone, resulting in the inhibition of the methanogenesis stage (Warith, 2003).

2.4.5 pH

The anaerobic digestion process is sensitive to the pH of waste. An acidic pH can increase the solubility of many constituents, which can result in the inhibition of both the acidogenesis and methanogenesis stages (El-Fadel, 1991; Warith, 2003). El-Fadel (1991) recognized 6-8 as the optimum range for anaerobic decomposition. Warith (2003) recognized a pH of 6.7-7.5 as optimum, while noting that anything outside of the range 6-8 has a serious effect on methane production. Townsend et al. (2008) noted 6.8-7.4 as the optimum range for anaerobic decomposition. Water addition or leachate recirculation can be used to manage the pH of a landfill (El-Fadel, 1991; Townsend et al., 2008).

2.4.6 Nutrients

Bacteria involved in the degradation process require nutrients to survive. Increased nutrient concentrations in the waste result in a healthier and larger bacterial population. Nutrients include hydrogen, nitrogen, sodium, potassium, calcium, magnesium, phosphorous, and other metals (El-Fadel, 1991). Although these nutrients are found throughout most landfills, inadequate mixing of the waste within a landfill may result in local nutrient limited areas (Warith, 2003). Leachate recirculation can provide improved distribution of nutrients. On the opposite end of the spectrum, heavy metals, sulfides, and other toxic pollutants can inhibit biological activity within a landfill (El-Fadel, 1991).

2.4.7 Bacteria

The bacteria involved in methanogenesis are found within the waste and soil placed within a landfill. Adding other sources of bacteria, such as municipal sludge or waste water, can result in earlier onset of methanogenesis and increased bacterial counts (El-Fadel, 1991; Warith, 2003).

2.5 Heat Transfer & Generation in Landfills

The ability of materials to store and transport heat is dependent upon their thermal properties, particularly specific heat and thermal conductivity. The thermal properties of municipal solid waste in a landfill can vary greatly depending on a number of different factors and are critical when modelling the heat transfer and heat budget of a landfill.

Heat is transferred to, from, and within a landfill by the three main heat transfer processes: conduction, convection, and radiation. Heat can also be generated in a landfill due to aerobic or anaerobic decomposition.

2.5.1 Specific Heat

Specific heat is a measure of the energy needed to increase the temperature of a unit mass by one degree. Because of the difference in molecular structure between different materials, a different amount of heat energy is required to heat a material to a specific temperature (American Heritage, 2011). Greater specific heats result in more energy needed to change the temperature of a material. Specific heat is commonly expressed in J/kg•K. Rees (1980) estimated the specific heat for waste as the same as that of sawdust. Rees (1980) also considered a change in specific heat with change in moisture content. Lefebvre et al. (2000) report that values for specific heat range from 1900 J/kg•K to 3000 J/kg•K, however in subsequent landfill modelling a specific heat of 600 J/kg•K was

calculated through numerical analysis (Lanini et al., 2001). Yoshida & Rowe (2003) used a specific heat of 1939 J/kg•K for unsaturated waste and 2363 J/kg•K for saturated waste in modelling a Tokyo landfill. Hanson et al. (2006) used a value of 719 J/kg•K for waste and 1783 J/kg•K for soil cover layers in a landfill heat budget model of a landfill in Anchorage, Alaska, USA. Hanson et al. (2013) used a value of 2000 J/kg•K for waste and 2800 J/kg•K for soil cover layers in a subsequent landfill heat budget model for a landfill in Michigan, USA. Faitli et al. (2014) attempted to quantify the thermal parameters of waste by proportionally weighting the thermal parameters of all components (waste constituents as well as moisture and air fractions) within a waste sample. Using 17 different waste samples, Faitli et al. (2014) found specific heat to range from 1750 J/kg•K to 3140 J/kg•K. In a 2D thermal model, Zambra et al. (2011) used a specific heat of 3320 J/kg•K for compost. Bonany et al. (2013a) used a specific heat of 1000 J/kg•K in a landfill heat budget model. Bonany et al. (2013b) used a specific heat of 1400 J/kg•K in a subsequent landfill heat budget model. Megalla (2015) built upon the work of Bonany et al. (2013a, 2013b) and recalibrated the model using a specific heat of 800 J/kg•K.

2.5.2 Thermal Conductivity

Thermal conductivity is a measure of the ability of a substance to conduct heat. More specifically, it is the rate at which heat can be transferred through a given material, through a unit area. Thermal conductivity is commonly expressed in W/m•K. It is difficult to estimate the thermal conductivity of municipal solid waste, as the waste is

very heterogeneous and therefore the thermal conductivity can vary throughout (Faitli et al., 2014).

Rees (1980) estimated the thermal conductivity for waste as the same as that of sawdust, 0.08 W/m•K. Lefebvre et al. (2000) used thermal shock probes placed in waste to attempt to measure the thermal properties. A range in thermal conductivity of 0.06 W/m•K to 0.25 W/m•K was found using the thermal shock probes (Lanini et al., 2001), and values of 0.1 W/m•K and 0.17 W/m•K were used in modelling (Lefebvre et al., 2000; Lanini et al., 2001). Lefebvre et al. (2000) also stated that thermal conductivity varies with moisture within porous media such as municipal solid waste, however were not able to reasonably correlate thermal conductivity to moisture, likely due to the heterogeneous nature of the waste and not a large enough sample size. Neusinger et al. (2005) used a thermal conductivity of 1 W/m•K in modelling the heat transfer through a landfill. Neusinger (2005) also modelled the effects of a landfill gas leak on the thermal profile of a landfill. The gas leak caused the drying of the landfill, and therefore thermal conductivity was affected as thermal conductivity is a function of moisture in the waste. The modelled thermal conductivity was varied accordingly within the area of the gas leak, and a thermal conductivity ranging from 0.3 W/m•K to 2.0 W/m•K was used. Gholamifard et al. (2008) used a thermal conductivity of 0.4 W/m•K for dry wastes at placement and a thermal conductivity of 0.6 W/m•K to 0.8 W/m•K for a landfill with leachate recirculation (and therefore higher moisture content and better moisture distribution throughout). Hanson et al. (2006) used a thermal conductivity of 0.23 W/m•K for waste and 2.35 W/m•K for soil within a landfill heat budget model. Hanson et al.

(2013) used a thermal conductivity of 1.0 W/m•K for waste and 2.5 W/m•K for soil. Hanson et al. (2013) values were computed using laboratory and field thermal probe experiments; as well as data from literature. Yoshida & Rowe (2003) and Rowe et al. (2010) used a different thermal conductivity for waste that was exposed to or not exposed to air. Waste exposed to air (unsaturated waste) was assigned a thermal conductivity of 0.35 W/m•K while waste not exposed to air (saturated waste) was assigned a thermal conductivity of 0.96 W/m•K. Faitli et al. (2014) attempted to quantify the thermal parameters of waste by proportionally weighting the thermal parameters of all components (waste constituents as well as moisture and air fractions) within a waste sample. Using 17 different waste samples, Faitli et al. (2014) found thermal conductivity to range from 0.24 W/m•K to 1.15 W/m•K. In a 2D thermal model, Zambra et al. (2011) used a thermal conductivity of 0.18 W/m•K for compost. As waste settles and becomes more compact, its thermal conductivity will increase. Waste having greater moisture content also results in greater thermal conductivity. This is due to the fact that air spaces within the waste that cause waste to have a lower thermal conductivity are filled with moisture and increase the ability of the waste to conduct heat. The moisture profile within a landfill reaches values closer to saturation with depth. Therefore due to both the greater moisture content and greater compaction, the thermal conductivity in lower layers is greater than the thermal conductivity in higher layers of a landfill. Megalla (2015) used this approach in a heat transfer model. The top meter of waste was assigned a thermal conductivity of 0.3 W/m•K, while waste below the top meter was assigned a thermal conductivity of 0.67 W/m•K.

2.5.3 Conduction

Heat transfer by conduction can take place in solids, liquids, or gases. Conduction can be thought of as the transfer of heat from the more energetic (warmer) particles of a substance to adjacent particles that are less energetic (cooler) due to interactions between particles (Moran & Shapiro, 2008). The heat transfer due to conduction is governed by Fourier's Law:

$$Q = -kA\frac{dT}{dx} \tag{3}$$

Where Q is the heat transfer, k is the thermal conductivity, A is the cross sectional area through which heat is transferred, and $\frac{dT}{dx}$ is the temperature gradient. The negative sign implies the direction of heat transfer from high temperature to low temperature (Moran & Shapiro, 2008).

Conduction is the primary method of heat transfer within the landfill. Heat can be conducted through the solids fraction of the waste, moisture/leachate within the waste, and through air in void spaces. Since conduction is driven by the thermal conductivity (a material property) it is important to understand the composition of the waste. Seeing as an increased moisture content results in an increase in thermal conductivity (as discussed in Section 2.5.2) it is important to have a good estimation of the moisture profile within the landfill.

2.5.4 Convection

Heat transfer between a solid surface (i.e. the landfill surface) and an adjacent liquid or gas (i.e. the air overtop the landfill surface) is referred to as convection. Convection is heat transfer due to the combination of conduction within the fluid particles as well as the

bulk motion of the fluid particles over the solid surface (Moran & Shapiro, 2008). Heat transfer due to convection is governed by Newton's Law of Cooling:

$$Q = hA(T_a - T_s) \quad (\mathbf{4})$$

Where Q is the heat transfer, h is the convection coefficient, A is the cross sectional area through which heat is transferred, T_a is the ambient temperature, and T_s is the surface temperature. The convection coefficient is an empirical parameter dependent upon the two interacting media as well as the magnitude and nature of the convection (forced or free). For landfills, the convection coefficient is based on the waste/cover surface interacting with the air. The magnitude of the convection is dependent upon the movement of the fluid, therefore the wind speed. McAdams (1954) first developed an empirical relation for the overall ground surface heat transfer coefficient (including radiation) as:

$$h = 5.7 + 3.8v \quad (\mathbf{5})$$

Where h [W/m^{2}K] is the heat transfer coefficient and v [m/s] is the surface wind speed.

Watmuff et al. (1977) developed an empirical relation for just the convection coefficient:

$$h = 2.8 + 3.0v \quad (\mathbf{6})$$

2.5.5 Radiation

Radiation is emitted by matter as a result of changes in the electronic configuration of the atoms and molecules within it. The energy/heat is transported by electromagnetic waves and can be absorbed, transmitted, or reflected by other incident forms of matter (Moran & Shapiro, 2008).

Thermal radiation emitted from a blackbody surface (such as the sky in the case of landfills) is given by the Stefan-Boltzmann Law (Moran & Shapiro, 2008):

$$Q = \varepsilon A\sigma\,(T_b^4) \quad \textbf{(7)}$$

Where Q is the heat transfer due to blackbody radiation, ε is the emissivity of the radiating surface (factor from 0 to 1.0 quantifying how effective the surface is in radiating), A is the area of the radiating surface, σ is the Stefan-Boltzmann constant (5.067×10^{-8} W/m^2•K^4) for blackbody radiation, and T_b is the temperature of the blackbody surface. In the case of landfills, the incoming shortwave radiation from the sky to the landfill surface is simulated by Equation **(7)**. Megalla (2015) used the ambient temperature as an approximation of the sky temperature.

Heat can also be transferred by radiation between two surfaces depending on the properties of the two surfaces, their orientation with respect to each other, the extent to which the intervening medium scatters, emits, and absorbs radiation, and other factors. A special case that occurs is the exchange between a small surface (such as the landfill surface) and a much larger surrounding surface (such as the surrounding atmosphere). The net rate of exchange between the two surfaces is given by the following relation (Moran & Shapiro, 2008):

$$Q = \varepsilon A\sigma\,(T_a^4 - T_s^4) \quad \textbf{(8)}$$

Where Q is the heat transfer due to net longwave radiation, ε is the emissivity of the smaller surface (factor from 0 to 1.0 quantifying how effective the surface is in radiating), A is the area of the smaller surface, σ is the Stefan-Boltzmann constant (5.067×10^{-8} W/m^2•K^4) for blackbody radiation, T_a is the temperature of the surrounding surface

(atmosphere), and T_s is the temperature of the smaller surface. In the case of landfills, this relation represents the net longwave radiation exchange between the landfill surface and the atmosphere. Megalla (2015) used the ambient temperature to simulate the temperature of the surrounding atmosphere.

2.5.6 Heat Generation

Heat is generated in landfills due to biological activity occurring in the waste (El-Fadel, 1991; El Fadel et al., 1996c; Hanson et al., 2013; Bonany, 2012; Megalla, 2015). Heat is generated either by aerobic or anaerobic exothermic reactions occurring in the decomposing waste. When waste is first placed, aerobic decomposition occurs due to the presence of oxygen in the waste. Once all available oxygen is used up, anaerobic decomposition commences, however releasing a much smaller quantity of heat in comparison to aerobic decomposition (Ward, 1983; El-Fadel, 1991; Megalla, 2015). The exception is near the surface of landfills, where diffusion of oxygen through the upper layer can allow for aerobic conditions to continue.

Pirt (1978) looked at the difference in the heat generation per one kilogram of glucose consumed, depending on whether it was digested aerobically (1520 kcal generated per kg of glucose) or anaerobically (0.09 kcal generated per kg of glucose). Equations (9) and (10) below show the aerobic and anaerobic digestion of glucose, respectively.

$$C_6H_{12}O_6 + O_2 \rightarrow Biomass + CO_2 + H_2O + Heat \quad \textbf{(9)}$$

$$1kg \quad 0.53kg \quad 0.4kg \quad 0.72kg \quad 0.6kg \quad 1520kcal$$

$$C_6H_{12}O_6 \rightarrow Biomass + CO_2 + CH_4 + Heat \quad \textbf{(10)}$$

$$1kg \quad 0.056kg \quad 0.69kg \quad 0.25kg \quad 0.09kcal$$

It is important to note that the anaerobic digestion of waste does not only include Equation (10). Heat generation rates associated with anaerobic digestion of waste include the hydrolysis, acidogenesis, acetogenesis and methanogenesis reactions as well as other abiotic chemical reactions that may occur.

Due to the complexity of the waste stabilization process, and the parallel yet sequential biochemical reactions involved in anaerobic digestion (Section 2.3), estimating the heat generation at any given time and place within a landfill is a challenge. El-Fadel et al. (1996b, 1996c, 1997) developed a coupled model with biochemical, gas generation & transport, and heat generation & transport sub-models. To estimate heat generation, the net enthalpy of the overall biochemical reaction involved in the anaerobic process was used. This net enthalpy was calculated as 1023 kJ/mol of organic material converted or 255 kJ/mol of methane produced. Alternatively, the enthalpy was calculated by summing together the enthalpy of each of the stepwise biochemical reactions in the anaerobic process. When calculated in this manner, the net enthalpy was determined to be 109 kJ/mol of methane produced. Of the sequential biochemical reactions, the formation of carboxylic acids (e.g. acetic acid, butyric acid, propionic acid) generated the majority of heat during the anaerobic process, and therefore the heat generation rate was assumed proportional to the acid formation rate in the biochemical model.

Lefebvre et al. (2000) and Lanini et al. (2001) looked at the heat generation due to aerobic activity in fresh waste (within the first calendar year of placement). A heat generation term of 460 kJ/mol of O_2 was used in modelling. Temperatures up to 70^{o}C were reported to be found in the waste due to aerobic activity.

Yoshida & Rowe (2003) note that heat generation in landfills can not only be due to biodegradation, but hydration of incinerated residues (ash) as well. A heat generation term of 4.67 W/m^3 was used for aerobic decomposition and a heat generation term of 0.218 W/m^3 was used for anaerobic decomposition.

Neusinger et al. (2005) used a heat source of 1 W/m^3 to represent the heat generated from all inorganic reactions. The method of determination of this value was unclear.

Gholamifard et al. (2008) developed a model that coupled two-phase flow with biological activity and heat generation. Biological activity was dependent upon temperature, and heat generation was dependent on biological activity. Gholamifard et al. (2008) used a value of 170 kJ/mol of volatile fatty acids produced for heat generation during the hydrolysis stage and a value of 80 kJ/mol of methane produced for heat generation during the methanogenesis stage.

Hanson et al. (2006) considered heat generation in all waste above 0^oC. A stepwise heat generation rate of 2.5 W/m^3 for the first 120 days of waste placement, and 0.08 W/m^3 for the remaining time was used in a transient thermal analysis of a landfill located in Anchorage, Alaska. These rates considered aerobic and anaerobic heat generation. Hanson et al. (2008) used a similar stepwise function, but only considered heat generation in wastes ranging in temperature from 0^oC to 80^oC. Hanson et al. (2008) used the same heat generation rates for the Anchorage, Alaska landfill. Using the same numerical methodology, heat generation rates of 11.3 W/m^3 for the first 120 days of waste placement, and 0.38 W/m^3 for the remaining time were used to simulate temperatures in a landfill located in Michigan. Hanson et al. (2013) modified the

methodology for heat generation from the previous works. An exponential growth and decay function was developed to provide a more realistic representation of waste decomposition in comparison with the stepwise function:

$$H = A\left(\frac{t}{B_t + t}\right)\left(\frac{C_t}{C_t + t}\right)e^{-\sqrt{t/D}} \quad (\mathbf{11})$$

Where H is the heat generation rate (W/m^3), t is the time (days), A is the peak heat generation rate factor (W/m^3), B_t and C_t are shape factors (days), and D is the decay rate factor (days). A dual-ramped temperature scaled function was then incorporated. Peak heat generation was used when the temperature fell between 30^{o}C and 50^{o}C. From 30 ^{o}C down to 0^{o}C and 50^{o}C up to 80^{o}C a linear ramped function was used ranging from peak heat generation to no heat generation. These functions however could simulate a great deal of heat generation in certain regions of the landfill that are exposed to high temperatures during early periods, while showing minimal heat generation in regions where lower temperatures persist for longer periods of time. Due to the time-scale, cumulative simulated heat generation in these latter regions will be underestimated over time. Therefore, an energy expended model was created. The exponential growth and decay function and dual-ramped temperature function were combined to form a 3D plot. This plot was then integrated with time to form a 2D energy expended plot (heat generation vs. energy expended). This new 2D energy expended plot was then scaled for temperature by the same dual-ramped temperature function. This results in heat generation dependent on the total amount of energy previously expended from the waste at a given location and the temperature. Therefore all waste within the domain has the same amount of heat that can be generated; however the rate at which this heat is

generated differs throughout the landfill domain. This numerical methodology was performed for two landfill cells (referred to as Cell D and Cell B). The exponential growth and decay heat generation function used in the Cell D model had a peak heat generation of 1.52 W/m^3, time to peak heat generation of 87 days, and total energy expended of 104 MJ/m^3. The exponential growth and decay heat generation function used in the Cell B model had a peak heat generation of 1.16 W/m^3, time to peak heat generation of 360 days, and total energy expended of 174 MJ/m^3.

Bonany et al. (2013a) considered heat generation in waste 10^{o}C and above. A quadratic temperature dependent heat generation function was used peaking at 57^{o}C and 18 W/m^3. Bonany et al. (2013b) used the same heat generation function, but used a peak heat generation rate of 0.3 W/m^3 for anaerobic conditions and 16.5 W/m^3 for aerobic conditions. Megalla (2015) built on the work of Bonany et al. (2013a, 2013b) and used the same basic quadratic equation peaking at 57^{o}C for aerobic decomposition, however with different peak heat generation terms. The top meter of waste was always considered to be the aerobic zone. In most cases, a corresponding peak heat generation rate of 5.0 W/m^3 was used. However in a waste lift placed during warm summer months where temperatures rose above 60^{o}C, a peak generation of 50 W/m^3 was needed to simulate the elevated temperatures. 50 W/m^3 reflects heat generation rates in compost (Zambra et al., 2011) and Megalla (2015) argued increased oxygen levels measured within the top 1m of waste indicated greater oxygen diffusion or advection into the waste for this layer in comparison to the other waste lifts. Below the top meter was considered the anaerobic zone. Megalla (2015) considered a constant anaerobic heat generation rate of 0.3 W/m^3 for wastes at 10^{o}C or greater. Numerous studies have been done to quantify either the

aerobic, anaerobic, or combined heat generation. Table 2 (modified from Megalla (2015)) summarizes the various values for heat generation found in the literature.

Table 2: Summary of Heat Generation Values found in Literature

Author(s)	Quantitative Heat Generation	Analysis Approach	Aerobic/ Anaerobic
Pirt (1978)	6,360 kJ/kg glucose, 1,147 kJ/mol-O_2	Aerobic digestion of glucose	Aerobic
Pirt (1978)	0.377 kJ/kg glucose, 68 J/mol- CH_4	Complete conversion of organic fraction to CO_2 and CH_4	Anaerobic
El-Fadel *et al.* (1996c)	1023 kJ/mol- organic material converted	Enthalpy of reactants of the stoichiometric biochemical reaction	Anaerobic
El-Fadel *et al.* (1996c)	255 kJ/mol- CH_4	Enthalpy of reaction of the stoichiometric biochemical reaction	Anaerobic
El-Fadel *et al.* (1996c)	109 kJ/mol- CH_4	Stepwise biochemical reactions	Anaerobic
Lefebvre *et al.* (2000)	10 MJ/m^3	Heat accumulation in the waste	Aerobic
Yoshida *et al.* (1997)	460 kJ/mol-O_2	Enthalpy of the stoichiometric equation of biological reaction	Aerobic
Yoshida *et al.* (1997)	45 kJ/mol-CH_4	Enthalpy of the stoichiometric equation of biological reaction	Anaerobic
Yoshida and Rowe (2003)	4.67 W/m^3	Biological decomposition (equivalent glucose)	Aerobic
Yoshida and Rowe (2003)	0.218 W/m^3	Biological decomposition (equivalent glucose)	Anaerobic
Hanson *et al.* (2008)	2.5–11.3 W/m^3	step-function for waste decomposition	Aerobic
Hanson *et al.* (2008)	0.08-0.38 W/m^3		Anaerobic
Bonany *et al.* (2013b)	16.5 W/m^3	Numerical modelling to simulate the heat flux and heat generation	Aerobic
Bonany *et al.* (2013b)	0.30 W/m^3		Anaerobic
Megalla (2014)	50 W/m^3	Numerical modelling to simulate the heat flux and heat generation	Aerobic (limited oxygen diffusion)
Megalla (2014)	5 W/m^3		Aerobic (oxygen present)
Megalla (2014)	0.30 W/m^3		Anaerobic

2.5.7 Latent Heat

Latent heat is defined as the quantity of heat absorbed or released by a substance undergoing a change of state, such as ice changing to water, or water to steam, at constant temperature and pressure. It is also known as the heat of transformation (American Heritage, 2011). In the heat budget of a landfill, latent heat is the heat energy necessary to thaw frozen waste. In landfills in northern climates, latent heat can be a significant component (Bonany et al., 2013b). Minimal research has been done in determining the latent heat of waste. Hanson et al. (2010) notes that a delay in heat gain within a landfill in Alaska was seen due to the effects of latent heat. Hanson et al. (2006) used latent heat values of 32.7 kJ/kg for waste and 1.7 kJ/kg for daily soil cover in a numerical heat budget model. Andersland & Anderson (1978) developed an equation to determine the latent heat of soils:

$$L_s = L_w w \gamma_d (1 - w_u) \quad \textbf{(12)}$$

Where L_s [kJ/m^3] is the volumetric latent heat for soil, L_w [kJ/m^3] is the volumetric latent heat for water, w is the mass fraction of water content in soil, γ_d [kg/m^3] is the dry density of the soil, and w_u is the ratio of unfrozen water to total water within the soil. Bonany (2012) estimated the latent heat of partially frozen waste by assuming that approximately one eighth of the total waste volume was frozen water. Bonany et al. (2013b) used a final value of 38.2 kJ/kg for the latent heat of waste. Megalla (2015) used a similar method to that of Bonany et al. (2012, 2013b) and used a final value of 37.2 kJ/kg.

2.6 Settlement of Waste

The settlement of waste is an important consideration in the operation of landfills. Prediction of waste settlement is important to the design of landfill infrastructure; including covers, leachate collection and recirculation systems, vertical and horizontal gas wells, and any structures that may be constructed atop the landfill (Babu et al., 2010). Landfill design requirements include a maximum height to which a landfill can be filled to. Therefore, greater settlement that occurs during the period of filling results in a greater amount of waste that can be placed into the landfill, and therefore greater revenue generated for landfill operators.

Municipal solid waste settles due to mechanical, chemical, and biological processes (Babu et al., 2010; Marques et al., 2003; Park and Lee, 1997; Hettiarachchi et al., 2009). There have been many previous models developed to predict the settlement of waste over time.

Sowers (1973) used a traditional soil-mechanics model for the settlement of waste which included primary compression and secondary mechanical creep as seen in the following equation:

$$\Delta H = H_o C_C' log\left(\frac{\Delta\sigma + \sigma_o}{\sigma_o}\right) + H_o C_\alpha log\left(\frac{t_2}{t_1}\right) \quad \textbf{(13)}$$

Where ΔH is overall settlement, H_o is the initial height of the waste lift, C_C' is the coefficient of primary compression (ranging from 0.163 to 0.205), $\Delta\sigma$ is the incremental overburden pressure due to an above waste lift, σ_o is the average initial overburden pressure at the centre of the waste lift, C_α is the coefficient of secondary mechanical creep (ranging from 0.015 to 0.350), and t is the time.

Bjarngard and Edgars (1990) used a similar model to that of Sowers (1973) but split the secondary mechanical creep into two components: intermediate secondary mechanical creep (~1-200 days) and final secondary mechanical creep (~200 days +).

Gibson and Lo (1961) developed a model including primary compression and secondary mechanical creep that assumes the waste deforms under plastic conditions. Their model followed the equation:

$$\Delta H = H_o a \Delta\sigma + H_o b \Delta\sigma\left(1 - e^{-(\lambda/b)t}\right) \quad (\mathbf{14})$$

Where ΔH is overall settlement, H_o is the initial height of the waste lift, $\Delta\sigma$ is the compressive stress dependent upon waste height, density, and external loading, a is a primary compressibility parameter, b is a secondary compressibility parameter, λ/b is the rate of secondary compression, and t is the time since load application.

Edil et al. (1990) developed a time-dependent empirical model known as the power creep law model using site specific fitting parameters.

Park and Lee (1997) as well as Hettiarachchi et al. (2009) developed settlement models that incorporated biological decomposition according to first-order kinetics.

El Fadel et al. (1999) correlated settlement rates with waste biodegradation. They used the models developed by Gibson & Lo (1961), Edil et al. (1990), and 1-D consolidation theory similar to those used by Sowers (1973) and Bjarngard and Edgars (1990), and altered parameters to allow the models to account for biodegradation. El Fadel et al. (1999) also evaluated the effects of different operational procedures (including leachate recirculation, addition of water, pH buffer, and addition of biological sludge) on waste

settlement. Results showed that an increase in the moisture content of the waste (due to either leachate recirculation or water addition) resulted in increased settlement and shorter time period to complete stabilization, likely due to increased biodegradation. A correlation between gas generation (indicating biological activity) and settlement was also found. 1-D consolidation theory resulted in the best fit to the field data used by El Fadel et al. (1999).

Durmusoglu et al. (2005) looked at the correlation between gas generation and settlement, showing that biological degradation plays an important role in landfill settlement. They concluded that deformable landfills can settle up to 27% of their initial depth.

Marques et al. (2003) developed a composite compressibility model for municipal solid waste that models the settlement of a landfill over time. According to the model, overall settlement (ΔH) is dependent on three components: instantaneous compression in response to an applied load (ΔH_P), time-dependent secondary mechanical creep (ΔH_C), and time dependent biological decomposition (ΔH_B). The corresponding equations are given as follows:

$$\Delta H = \Delta H_P + \Delta H_C + \Delta H_B \quad \textbf{(15)}$$

$$\Delta H_P = H_o C_C' \log\left(\frac{\Delta\sigma + \sigma_o}{\sigma_o}\right) \quad \textbf{(16)}$$

$$\Delta H_C = H_o b \Delta\sigma\left(1 - e^{-ct'}\right) \quad \textbf{(17)}$$

$$\Delta H_B = H_o E_{DG}\left(1 - e^{-dt''}\right) \quad \textbf{(18)}$$

Where C_C' is the coefficient of primary compression, $\Delta\sigma$ is the change in vertical stress, σ_o is initial vertical stress, b is the coefficient of mechanical creep, c is the rate constant for mechanical creep, t' is the time since the application of the stress increment, E_{DG} is the total amount of strain that can occur due to biological decomposition, d is the rate constant for biological decomposition, and t'' is the time since waste placement. The final parameters used by Marques (2003) are found in Table 3.

Babu et al. (2010) developed a constitutive model for settlement that was based on critical state soil mechanics principles and first-order reaction kinetics for biological degradation. Reduced waste lift thickness was found to reduce the overall settlement. Babu et al. (2010) compared their results with other previously presented models (including Sowers (1973), Bjarngard and Edgars (1990), Gibson and Lo (1961), and Marques et al. (2003)) and found that predicted settlement can vary greatly depending upon the model chosen.

Van Geel & Murray (2015) used the equations developed by Marques et al. (2003) and fit these equations to settlement data from the Ste-Sophie, Quebec landfill. Model parameters were determined by regression analysis on the first layer of waste placed. These parameters were then used to predict settlement for the subsequent waste layers with good agreement with field data. Table 3 shows the final parameters used by Van Geel & Murray (2015).

Table 3: Composite Compressibility Model Parameters From Literature

Parameter	Marques (2003)	Van Geel & Murray (2015)
C_c'	0.106	0.0376
b (kPa^{-1})	0.00527	0.00194
c (day^{-1})	0.00179	0.02078
E_{DG}	0.159	0.1122
d (day^{-1})	0.00114	0.00406

2.7 Landfill Modelling

Numerous studies have been done to analyze various landfill processes such as heat transport, heat generation, biological activity, chemical composition/waste stabilization, landfill gas production, settlement, and more.

Rees (1980) studied the components of the thermal regime of an anaerobic landfill in an effort to optimize the methane production and waste stabilization process. This study was conducted while landfill gas collection as a resource was still in its infancy. Rees (1980) identified and quantified the heat of reaction, specific heat of water/MSW mixtures, heats of neutralization, heat losses to air and soil, solar radiation, and aerobic metabolism as the major contributions to the heat budget of a landfill.

El-Fadel et al. (1996b, 1996c, 1997) developed a coupled biological, gas, and heat generation model. The microbial ecosystem was described by biochemical and biokinetic equations. Biological activity was dependent upon temperature and growth of the microbial community according to Monod kinetics. The biochemical distribution throughout the landfill was dependent upon first order kinetics and the corresponding biological activity. Gas generation was linked to temperature and biological activity. The heat transport model was based on the one-dimensional heat transfer equation. Heat

generation was correlated to the acid formation rate as discussed in Section 2.5.6. The model was successfully validated with data from a controlled experimental landfill cell. The model can be used to estimate gas generation rates and therefore to design landfill gas collection systems. It was found that hydrolysis is the most important process governing the rate of gas production in an anaerobic landfill.

Lefebvre et al. (2000) and Lanini et al. (2001) studied the role of aerobic activity on waste temperature within the first year of waste placement. Lefebvre et al. (2000) studied a landfill cell located in France that was instrumented with thermal probes to measure temperature. The 20 m deep landfill cell of approximately 200 000 m^3, had a total heat accumulation of approximately 10 MJ/m^3. Of this value, 3% was attributed to heat transfer gains due to conduction and convection and 18.5% was attributed to heat produced due to aerobic decomposition using the initial oxygen trapped in the void space of the placed waste. The remaining heat was argued to be produced by aerobic decomposition using oxygen that diffuses through the waste surface. Anaerobic heat generation was deemed negligible in this analysis. In a subsequent publication, Lanini et al. (2001) created a lab-scale landfill cell to further test the model proposed by Lefebvre et al. (2000). Lanini et al. (2001) concluded that aerobic degradation plays a dominant role in heat generation within fresh waste, and that temperatures of up to 70^oC can be reached in the center of a landfill cell due to aerobic degradation from oxygen diffusion.

White et al. (2004) presented a complex multi-component model that simulated the transport and bio-chemical behaviour of the solid, liquid, and gas phases of a landfill. The model used linked discrete constant volumes and allowed the transfer of each phase from volume to volume. White et al. (2011) developed a one-dimensional infiltration

model to analyze the effects of leachate recirculation in landfills. White et al. (2011) found that the transfer of waste mass to leachate was mainly dependent upon the variation of hydraulic conductivity with water content, saturated and drainable water contents, and how these parameters vary with depth.

Neusinger et al. (2005) formed a 3D thermal model that considered the gas flow and water content. A surface heat flux of 20 W/m^2K out of the landfill incorporated effects due to convection and radiation. An anaerobic heat source of 1 W/m^3 was used for heat generation. A numerical analysis of the maximum temperature possible in the landfill was then performed by scaling the heat source. Using the base heat source of 1 W/m^3, maximum temperatures at the center of the landfill were found to be between 60^oC and 80^oC, depending on the thickness of the waste body. The model was validated by comparing model results to measured surface temperatures from a German landfill.

Gholamifard et al. (2008) developed a 3D, finite volume model composed of a two-phase flow model based on Darcy's law, and a biological model based on Monod kinetics. Biological activity was a function of temperature. The effects of saturation were studied in terms of biological activity; in terms of how increased saturation promotes hydrolysis and activation of methanogens.

Hanson et al. (2008) developed a 1-D transient heat transfer model. The bottom boundary condition was set as the mean annual earth temperature at 75 m below the landfill. At the surface, a sinusoidal surface temperature function was used based on measured temperatures at individual sites. These sinusoidal curves have been normalized so that ambient temperature data at any site can be input to give a sinusoidal surface

temperature curve for use in such models. To simulate waste placement, field records were used and waste was considered placed at initial temperatures equivalent to the average ambient temperature on the day of placement. Heat generation was dependent upon temperature and waste age, as is described in Section 2.5.6. The model was validated using data from landfills in Michigan, New Mexico, Alaska, and British Columbia.

Hanson et al. (2010) used the model to further analyze the previously mentioned landfills. The highest heat gain was observed in the Michigan landfill which had high precipitation/moisture conditions and high waste density. The highest heat generation was observed in a landfill in British Columbia due to high waste moisture and therefore enhanced microbial activity. Higher temperatures were found during anaerobic conditions in comparison to aerobic conditions. Over time, the thermal profile through the depth of the waste was found to be convex in shape with maximum temperatures found at central locations of the waste.

Hanson et al. (2013) improved the model used previously by changing the heat generation term. It was assumed that the waste has a finite amount of energy that can be expended. Therefore, over time, the same total amount of heat can be extracted from all waste in the landfill. To simulate this, heat generation was now a function of temperature and previous energy expenditure, as is detailed in Section 2.5.6. The onset and presence of heat due to decomposition was deemed more accurately represented by this model.

Zambra et al. (2013) formed a 2D thermal model that simulated temperatures in the waste pile as well as the surrounding and underlying soil. Within the waste pile, temperature

and oxygen concentration were solved for. Two heat generation terms were used: chemical heat generation (which was dependent upon oxygen concentration), and biological heat generation, which was dependent upon first-order kinetics of the microbial community. Zambra et al. (2013) examined the effects of the depth at which the waste pile was buried in the soil, primarily in terms of contaminating potential.

The work in this thesis builds off of the previous landfill energy budget modelling done by Bonany et al. (2013a, 2013b) and Megalla (2015). Bonany et al. (2013a) was the first to model the temperature profile at the Ste-Sophie, QC landfill. At the surface, incoming solar radiation and convection were considered. At the base, a prescribed temperature was used as a boundary condition, estimated as the temperature measured by the bottom temperature sensor located at the base. A specific heat of 1000 J/kg•K and thermal conductivity of 0.45 W/m•K for thawed waste and 0.025 W/m•K for frozen waste were used. Heat generation was based on a quadratic relation peaking at 18 W/m^3 as described in Section 2.5.6. The model was simulated and calibrated for the first 10.5 months of waste placement at the Ste-Sophie, QC landfill cell. Bonany et al. (2013a) computed a corresponding heat budget, as seen in Figure 5.

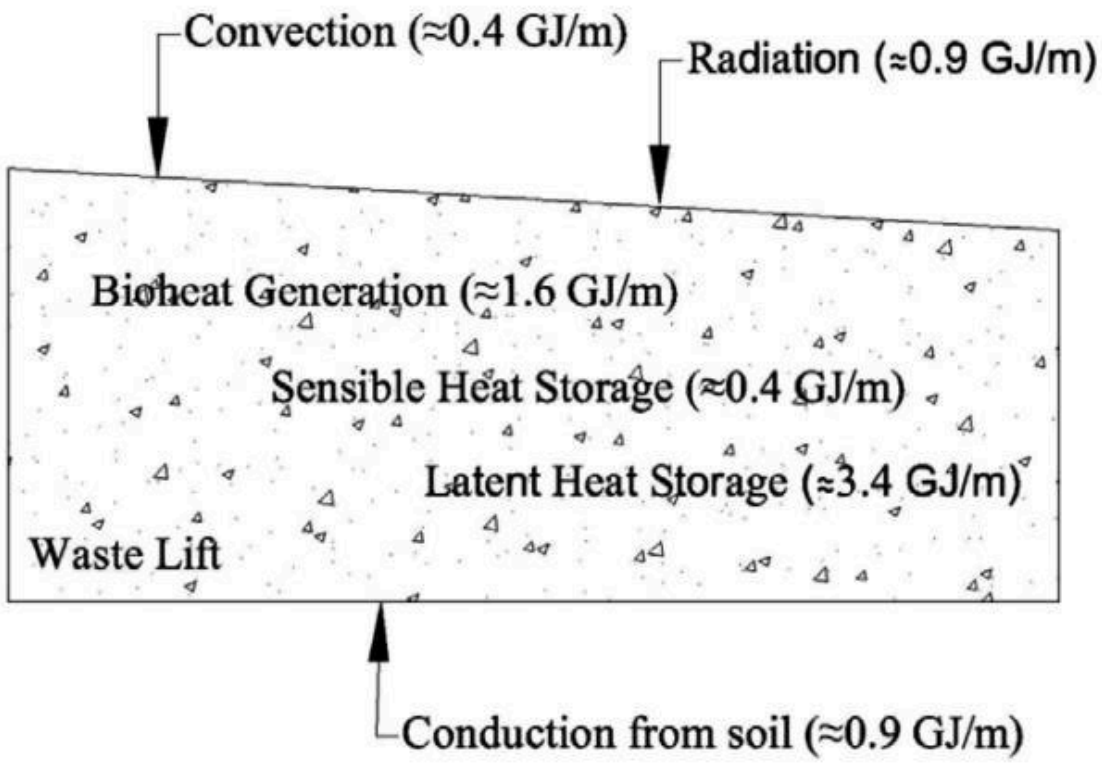

Figure 5: Heat Budget for the first 10.5 months of waste placement at the Ste-Sophie, QC landfill cell (with permission from Bonany, 2012)

Bonany et al. (2013b) made modifications to the model presented in Bonany et al. (2013a). A specific heat of 1400 J/kg•K was used and a thermal conductivity of 0.67 W/m•K was used throughout the landfill. Heat generation was broken down to aerobic (maximum 16.5 W/m^3) and anaerobic (maximum 0.3 W/m^3) generation. The first 19 months of waste placement in the Ste-Sophie, QC landfill cell were simulated. Modelling results showed that underlying soil could be a source of heat gain for wastes placed at cold temperatures. Waste was also shown to be a good insulator, with low thermal conductivity and a high latent heat of fusion, as waste placed at frozen temperatures continued to remain frozen for up to 18 months. Heat generation due to anaerobic activity was considered negligible compared to heat generation due to aerobic activity.

Megalla (2015) continued the work of Bonany et al. (2013a, 2013b) and made modifications to the above model. Megalla (2015) used a specific heat of 800 J/kg•K and a thermal conductivity of 0.3 W/m•K for the top meter of waste, and 0.67 W/m•K below. Terms for the heat generation were also changed. The top meter of waste was always considered to be the aerobic zone. In most cases, a corresponding peak aerobic heat generation rate of 5.0 W/m^3 was used, however in a waste lift placed during warm summer months where temperatures rose near 60^oC, a peak aerobic heat generation of 50 W/m^3 was used. Below the top meter was considered the anaerobic zone. A constant anaerobic heat generation of 0.3 W/m^3 for wastes at 10^oC or greater was used. This resulted in 44% of heat generation having come from the anaerobic zone. Megalla (2015) used the calibrated model to simulate an alternative waste placement strategy to illustrate the potential impact of waste placement on the temperature profile within the waste.

3.0 STE-SOPHIE LANDFILL EXPERIMENTAL SETUP & FIELD DATA

3.1 Experimental Set-up at the Ste-Sophie, Quebec Landfill

The research group of Dr. Paul Van Geel has been studying the Ste-Sophie landfill since 2009. The landfill is located approximately 30 km north of Montreal and takes in municipal solid waste, industrial, commercial, & institutional waste, construction & demolition waste, automotive waste, and contaminated soils from nearby areas. The landfill is permitted to receive up to 1.0 million tonnes of waste each year. Approximately 70 million tonnes of landfill gas (LFG) are collected each year at the site. Of the LFG that is collected, approximately half is transported to a nearby pulp & paper mill operated by Cascade Inc. and the other half is flared.

The landfill began filling a new cell located at the southern portion of Zone 4 of the site (Figure 6) in late 2009.

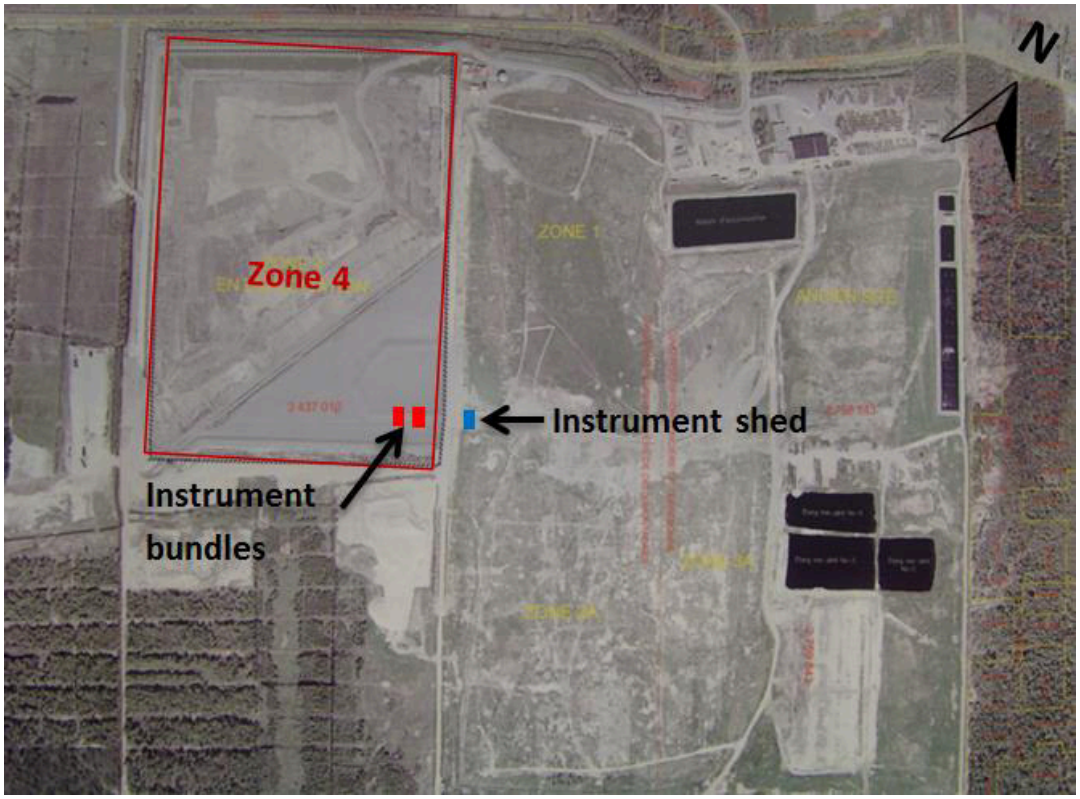

Figure 6: Overhead view of Ste-Sophie Landfill

This cell has been outfitted with 12 bundles of instrument sensors installed in two vertical columns throughout the depth of the waste in the approximate location depicted in Figure 6. Engineering drawings for the site are found in Appendix A. The instrument bundles are comprised of the following:

- 60 cm x 60 cm steel plate to hold all instruments.
- Oxygen sensor to measure oxygen concentration (% volume). These sensors are installed in sand that is placed above the instrument bundle. These sensors also measure temperature.
- Moisture & electrical conductivity sensor to measure moisture content. These sensors are installed in sand that is placed above the instrument bundle. The

moisture content in the sand is an estimate of the moisture content of the surrounding waste. These sensors also measure temperature.

- Total earth pressure cell (TEPC) to measure total overburden earth pressure. The TEPCs are mounted on the steel plate. These sensors also measure temperature.
- Vibrating wire piezometer to measure leachate mounding (bundles 1-4 only).
- Liquid settlement system to measure settlement. A transducer that measures pressure at the instrument bundle is hydraulically connected to a transducer that measures pressure at the instrument shed. The difference in pressure as the instrument bundle settles is used to calculate settlement. These sensors also measure temperature.
- Two hollow plastic lines that run from each instrument bundle to the instrument shed. These allow for drawing of leachate or landfill gas; or injection of air.

A photograph of an instrument bundle is shown in Figure 7.

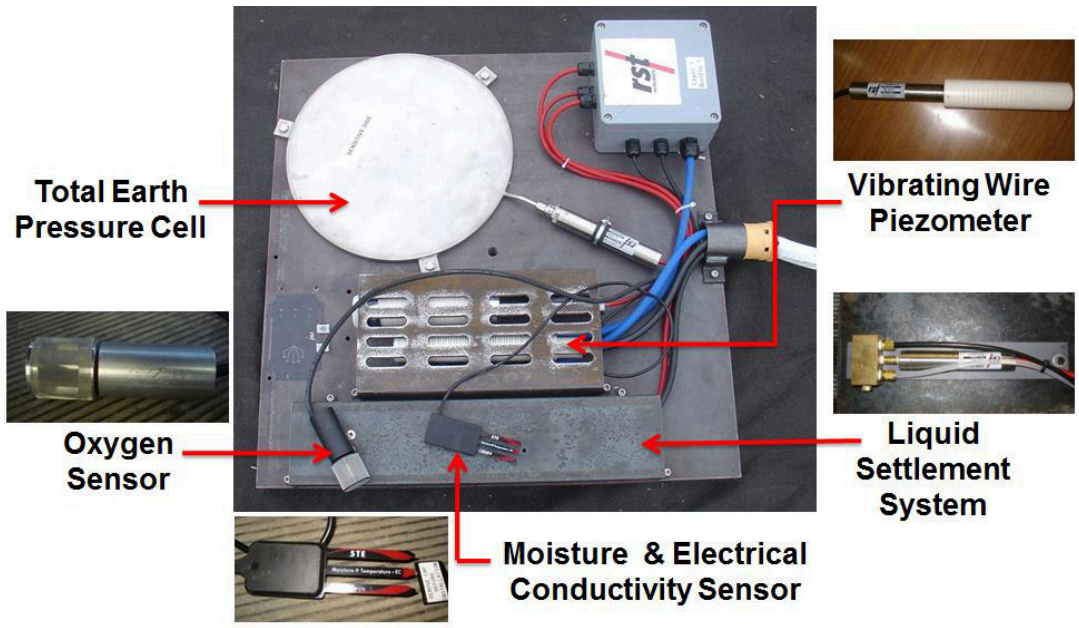

Figure 7: Instrument bundle used at the Ste-Sophie Landfill

The instrument bundles are connected by cables to a Campbell Scientific CR1000 FlexDAQ Datalogger that is housed in an instrument shed nearby. Data from the datalogger can be accessed remotely through wireless connection.

The bundles were installed progressively with the filling of the landfill. When installed, bundles were covered in 30-40 cm of sand for protection. Figure 8 shows the placement of the waste lifts and bundle locations within the waste over time. It is important to note that the waste lift heights shown are at the time of placement of each individual lift. The actual heights of the lifts are decreasing with settlement over time, as is shown in Section 3.4. Figure 9 shows a cross-sectional view of the landfill with bundle elevations as of April 2014.

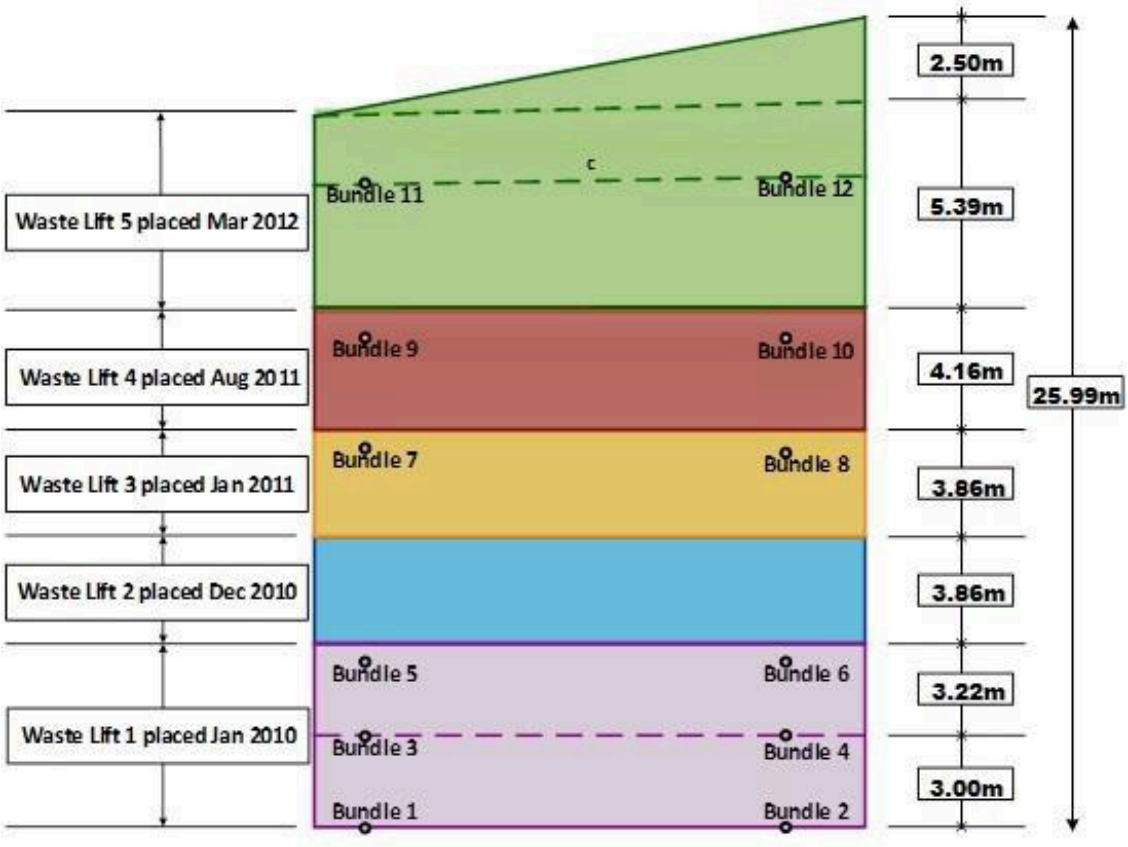

Figure 8: Waste Lift Heights and Bundle Locations

Point	Easting	Northing	Elevation	Survey Date
a	273109.3	5070968	75.142	May 2012
b	273109.3	5070968	76.542	June 2014
c	273057.1	5070937	91.557	June 2014
d	273051.1	5070940	92.284	June 2014
e	273045.4	5070925	94.703	June 2014
f	273036.5	5070930	94.253	June 2014
g	273127.1	5070987	76.205	Sept. 2009

Bundle	Northing Range	Easting Range	Elevation Range *
Column 1 (odd numbered bundles)	5070937 - 5070939	273056.4 - 273057.3	71.97 - 85.35
Column 2 (even numbered bundles)	5070925	273044.3 - 273045.4	71.68 - 85.34
Bundle 11	5070940	273051.1	90.85
Bundle 12	5070930	273036.5	89.97

* Elevation range taken as of April 2014

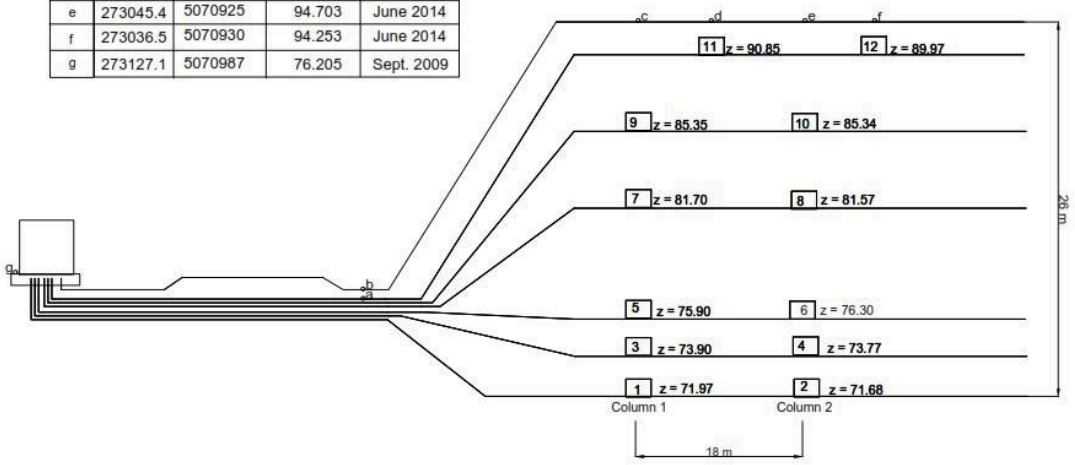

Figure 9: Cross Sectional View of Bundles in Landfill

Bundles 1 and 2 were placed at the base of the landfill, just above the leachate collection system, during below freezing temperatures and covered by frozen waste. The first waste lift was placed in January 2010. Bundles 3 and 4 were installed at the centre of the first waste lift approximately 3 m above the base of the landfill. Bundles 5 and 6 were installed in June 2010 approximately 0.75 m below the top of the first waste lift. The second waste lift was placed in December 2010 and the third waste lift was placed in January 2011. Bundles 7 and 8 were installed in January 2011 and after the placement of the third waste lift, approximately 0.75 m below the top of the lift. The fourth waste lift was placed in August 2011 and bundles 9 and 10 were subsequently installed approximately 1 m below the top of the lift. It is important to note that this was the first waste lift not placed during winter months. This was a request made to the landfill operators, as low temperatures in bundles 1-8 persisted for long periods of time (see Figure 10), after being placed at freezing temperatures. The fifth waste lift was placed in

March 2012. Bundles 11 and 12 were placed near the top of the fifth and final waste lift (Megalla, 2015). Within three months of the placement of bundle 12, and additional five meters of waste were placed above the even-numbered bundles.

Data collection from the bundles commenced November 9th, 2009. Table 4 shows the date that each set of bundles began reporting data.

Table 4: Date of Data Collection Commencement for Instrument Bundles

Bundles	Date of Data Collection Commencement
1 & 2	November 9th, 2009
3 & 4	January 16th, 2010
5 & 6	December 13th, 2010
7 & 8	January 28th, 2011
9 & 10	August 23rd, 2011
11 & 12	March 14th, 2012

The majority of instruments are still in good working condition even after up to over five years being entrained in the waste. The moisture & electrical conductivity sensors are the only sensors that failed within 6-12 months of installation and therefore do not provide adequate data to be analyzed. Temperature, oxygen, total earth pressure, leachate mounding, and settlement data continue to be downloaded and recorded. For the purposes of this thesis, temperature, oxygen, and settlement data are presented and analyzed in subsequent sections.

3.2 Temperature Field Data

Temperature data from November 9th, 2009 to May 5th, 2015 are shown in Figure 10.

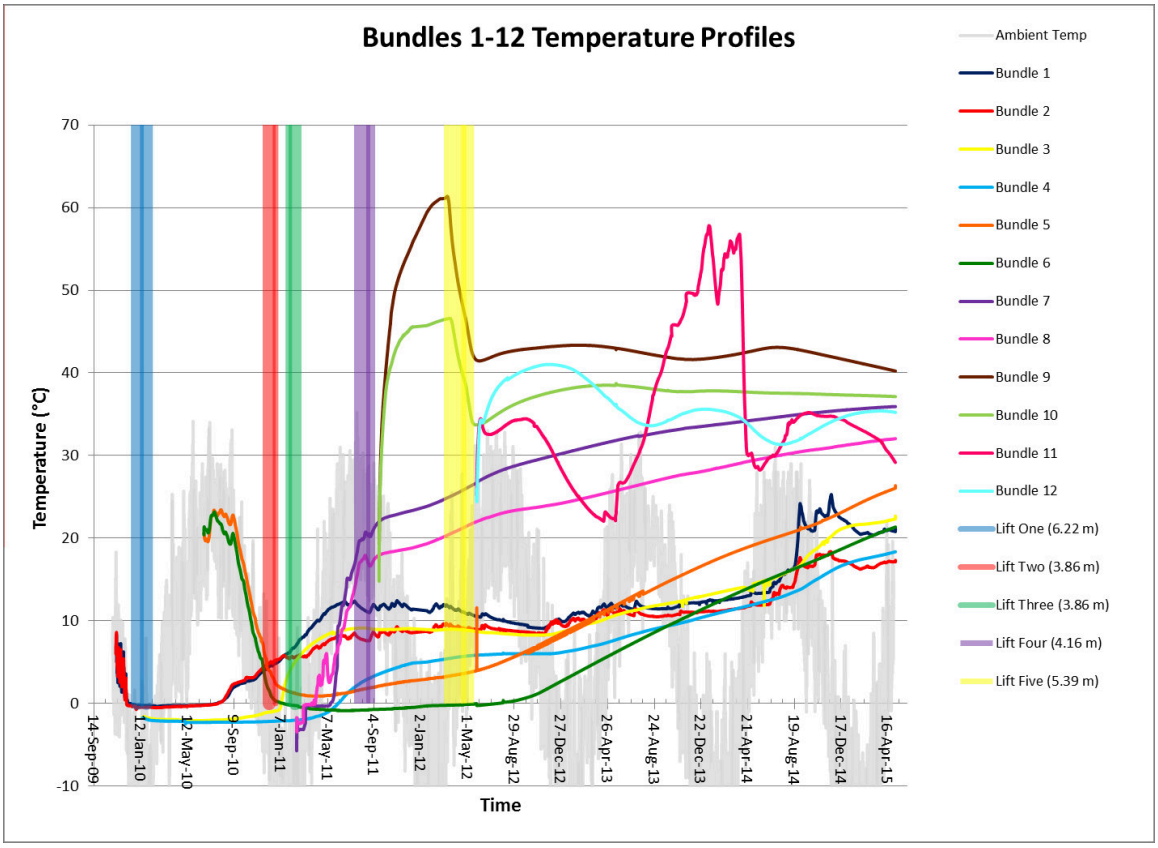

Figure 10: Temperature profiles of Bundles 1-12

Temperature profiles for all 12 bundles are shown as well as coloured vertical bars showing the times of waste lift placement, and the ambient temperature profile displayed in grey. From Figure 10, it can be seen that bundles 3 and 4 were placed in frozen waste and stayed at temperatures below zero for approximately one year, even though ambient temperatures in the summer rose up to approximately 30°C. The roughly 4 m of waste above the bundles provided enough insulation to not allow the waste to thaw at the centre of this waste lift. Bundles 5 and 6 were placed near the surface of the waste, and therefore followed the ambient temperature closely with a slight time lag. Once the second waste lift was placed in December 2010, when bundles 5 and 6 reported near 0°C temperatures, bundles 5 and 6 became insulated from the atmosphere by the second waste lift and remained at near 0°C temperatures. In the case of bundle 6, the waste stayed

frozen for over one and a half years. Bundles 7 and 8 were placed at the top of lift 3, when ambient temperatures were below freezing. These bundles rose in temperature, following the ambient temperature with a slight time lag, and then were insulated from the atmosphere by the placement of waste lift 4, at approximately 20^{o}C. Once insulated, the temperatures continued to steadily rise, even through cold winter months. Bundles 9 and 10 were installed near the top of waste lift 4 placed in warm conditions. It can be seen that temperatures for these bundles rise well above ambient temperatures (above 60^{o}C in the case of bundle 9). These high temperatures indicate that heat must be being generated in the waste. Looking at the oxygen data (Figure 11), it can be seen that oxygen is present at these bundles, and therefore it was assumed that these high temperatures must be generated from aerobic decomposition. Due to the heat generation and insulation from 0.5-1 m of material above, temperatures stay high even through the winter months. When the fifth waste lift was installed in March 2012, the source of oxygen from the atmosphere was cut off, and temperatures drop to approximately 40^{o}C over the course of only a few days. Bundles 11 and 12 were placed near the surface of the final waste lift, and similar to bundles 9 and 10, oxygen was available and resulted in aerobic heat generation. The large spike in temperature seen in bundle 11 spanning August 2013 - April 2014 correlates well with an increase in oxygen concentration. These oxygen spikes are due to landfill cover regrading activities in the area of bundle 11 that allowed oxygen to move through the surface waste to reach the area of bundle 11. It would be counterintuitive to expect oxygen concentrations to increase at bundle 11 after the placement of roughly four meters of waste above it under normal operating conditions.

3.3 Oxygen Field Data

Oxygen data from November 9th, 2009 to May 5th, 2015 are shown in Figure 11.

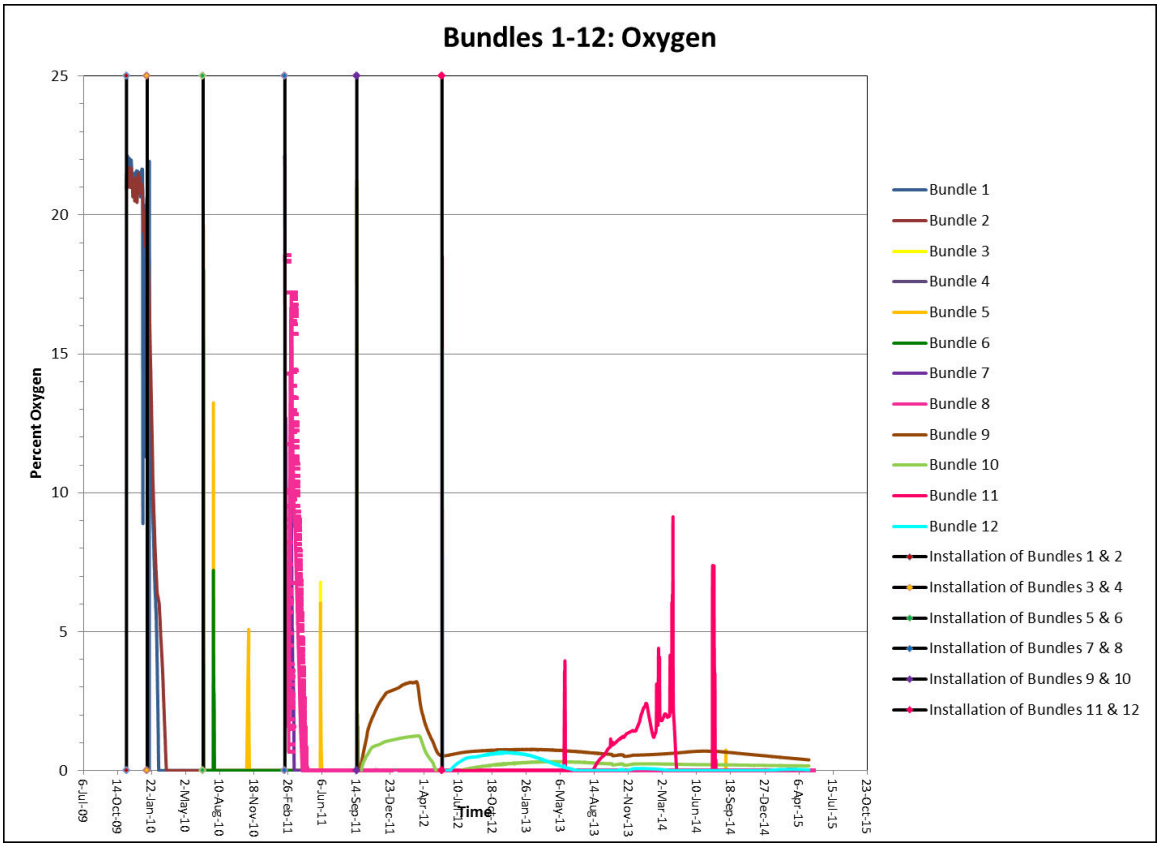

Figure 11: Oxygen Data for Bundles 1-12

In many bundles, it can be seen that oxygen is present for a very short period of time until the bundles are covered by waste. Bundles 9, 10, 11, and 12 show the presence of oxygen for a prolonged period of time. As was mentioned previously, the presence of oxygen at these bundles correlates with higher temperatures at these bundles, leading to the conclusion that aerobic activity must be ongoing at these locations. This is further explored in Section 4.5. The oxygen spikes reflect days when air was pumped out to the bundle to ensure the oxygen sensor was working. Note that the oxygen concentration declines rapidly as the oxygen migrates into the waste.

3.4 Settlement Field Data

Data from the liquid settlement system from November 9th, 2011 to May 5th, 2015 are shown in Figure 12. The coloured vertical bars represent the dates of waste lift placement.

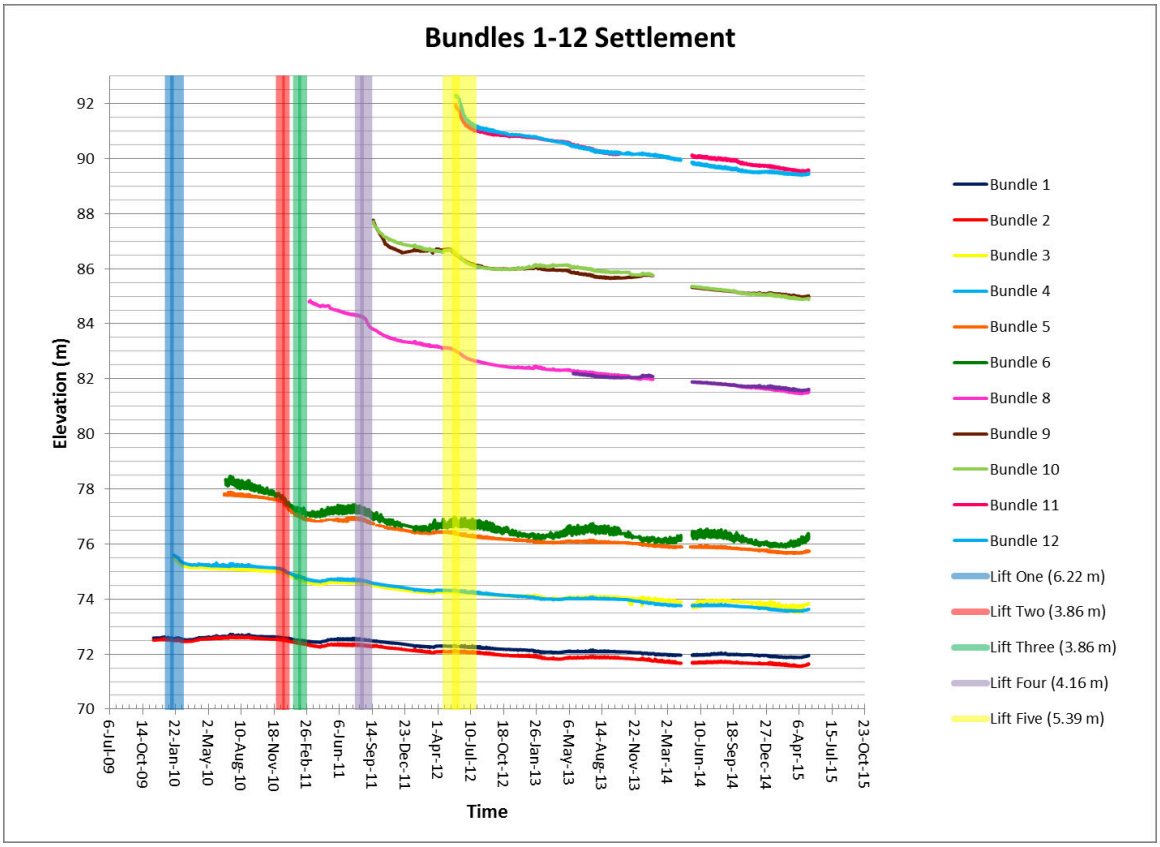

Figure 12: Settlement of Bundles 1-12

As can be seen in Figure 12, the landfill undergoes considerable settlement over time. Bundles 1 and 2, placed at the very base of the landfill undergo settlement due to the force of the placed waste on the underlying soil. The effects from waste lift placement can also be seen. At the placement of each lift, decreases in elevation can be realized due to the primary compression on underlying waste lifts (Marques, 2003). Van Geel & Murray (2015) investigated the settlement at the Ste-Sophie landfill, as discussed in Section 2.6.

4.0 LANDFILL QUASI-THERMAL-MECHANICAL-BIOLOGICAL CONCEPTUAL MODEL & NUMERICAL MODEL SETUP

The physical, chemical and biological processes that go on within a landfill are complex and intertwined. It is important to consider the relationship between all processes with respect to each other. Figure 13 shows the major links between all processes.

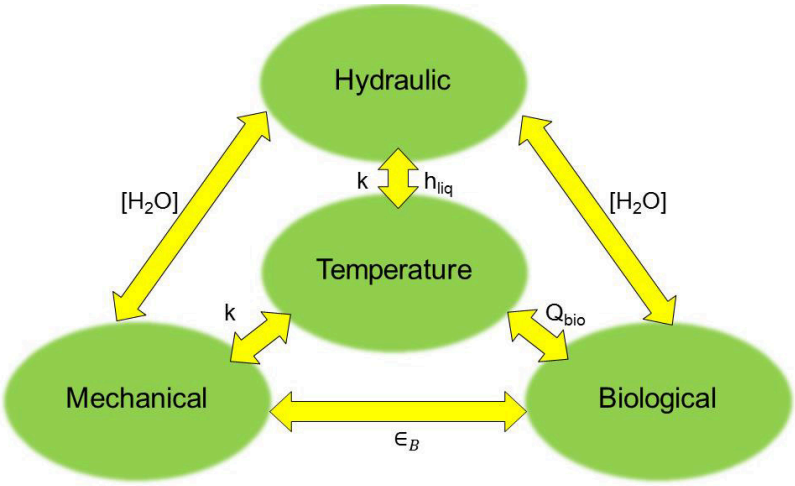

Figure 13: THMB Conceptual Model

For the purposes of this research, the contributions of hydraulic processes are not coupled into the model. Thermal, mechanical, and biological processes are all considered and all have an effect on each other. The mechanical settlement effects the thermal parameters of the waste, which has an effect on the overall temperature profile throughout the waste. Biological activity generates heat which affects the temperature, as well as increases settlement. The presence and rate of biological activity is dependent upon temperature, and temperature effects the structural properties of the waste that have an effect on mechanical settlement.

Figure 14 depicts the heat transfer processes ongoing in and around the landfill. Within the landfill, heat transfer is governed by conduction through the waste. At the surface,

net longwave radiation, convection, and incoming solar radiation control the surface heat flux. Below the landfill, heat can be released or gained due to conduction from underlying soil. Within the landfill, heat can be generated under aerobic and anaerobic conditions.

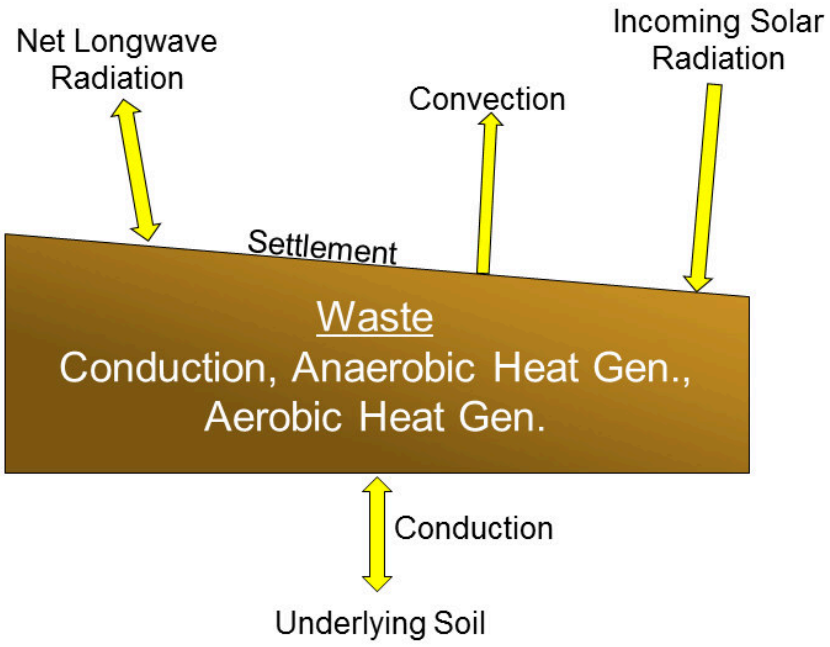

Figure 14: Conceptual Model of Heat Transfer Processes within and around Landfill

4.1 Heat Transfer within the Waste

Bonany (2012) developed a conceptual and numerical model for the heat transfer within the landfill. Megalla (2015) built upon this base model. The conceptual and numerical models presented in this thesis build on the work of both Bonany (2012) and Megalla (2015). The governing equation for heat transfer within the landfill is:

$$\nabla(k\nabla \mathrm{T}) + \mathrm{Q} = \rho C_p \frac{dT}{dt} \quad (\mathbf{19})$$

Where k [W/m•K] is the thermal conductivity of the waste, T [K] is the temperature of the waste, Q [W/m^3] is the heat generation in the waste due to biological activity, ρ [kg/m^3] is the bulk density of the waste, C_p [J/kg•K] is the specific heat, and t [s] is the time.

4.1.1 Specific Heat

The specific heat used in the heat transfer calculation is dependent upon the state of matter of the moisture in the waste according to the following piecewise equation:

$$C_p = \begin{cases} C_s & T < 271.55K \\ \dfrac{L}{\Delta T} & 271.55\ K < T < 272.55\ K \\ C_l & 272.55\ K < T \end{cases} \quad (\mathbf{20})$$

C_s is the specific heat for frozen waste, while C_l is the specific heat for non-frozen waste. From 271.55 K to 272.55 K, C_p is dependent upon L, which is the latent heat required to change the state of the liquid fraction from solid (frozen) to liquid or liquid to solid (Megalla, 2015). Megalla (2015) used a specific heat value of 800 J/kg•K, which is at the low end of the range of values found in the literature. An initial specific heat of 2000 J/kg•K was used in this model for both frozen and non-frozen waste(Hanson et al., 2013) A trial-and-error approach to minimize the sum of squared error between modelled bundle temperatures and actual bundle temperatures while varying the specific heat was then conducted to calibrate the model to Ste-Sophie field data. A specific heat of 2100 J/kg•K provided a better fit to the field data. A sensitivity analysis of specific heat is presented in Section 5.5. A latent heat value of 37.2 kJ/kg was used in this model, as was used by Megalla (2015).

4.1.2 Thermal Conductivity

The thermal conductivity of the waste was varied with depth and time in the model. The top meter of waste was assigned a thermal conductivity of 0.3 W/m•K. This value is similar to values used by Rowe et al. (2010) and Gholamifard (2008) for unsaturated wastes; and the same value used by Megalla (2015) for the top meter of waste. Below 1m, the thermal conductivity was allowed to vary linearly from a minimum thermal conductivity value of 0.3 W/m•K to a maximum thermal conductivity value at the base of the waste which was allowed to increase with time as waste lifts were added and settlement occurred. The variation of thermal conductivity with depth represents field conditions, where deeper wastes have greater density and moisture content; and therefore greater thermal conductivity. The settlement and compaction of waste over time also results in a thermal conductivity increase. The maximum thermal conductivity (at the base of the landfill) varied from 0.7 W/m•K (during the first simulation period) to 1.1 W/m•K (during the fifth and final simulation period). At the onset of each simulation period, the maximum thermal conductivity was increased by 0.1 W/m•K. Figure 15 gives a graphical representation of the varying thermal conductivity.

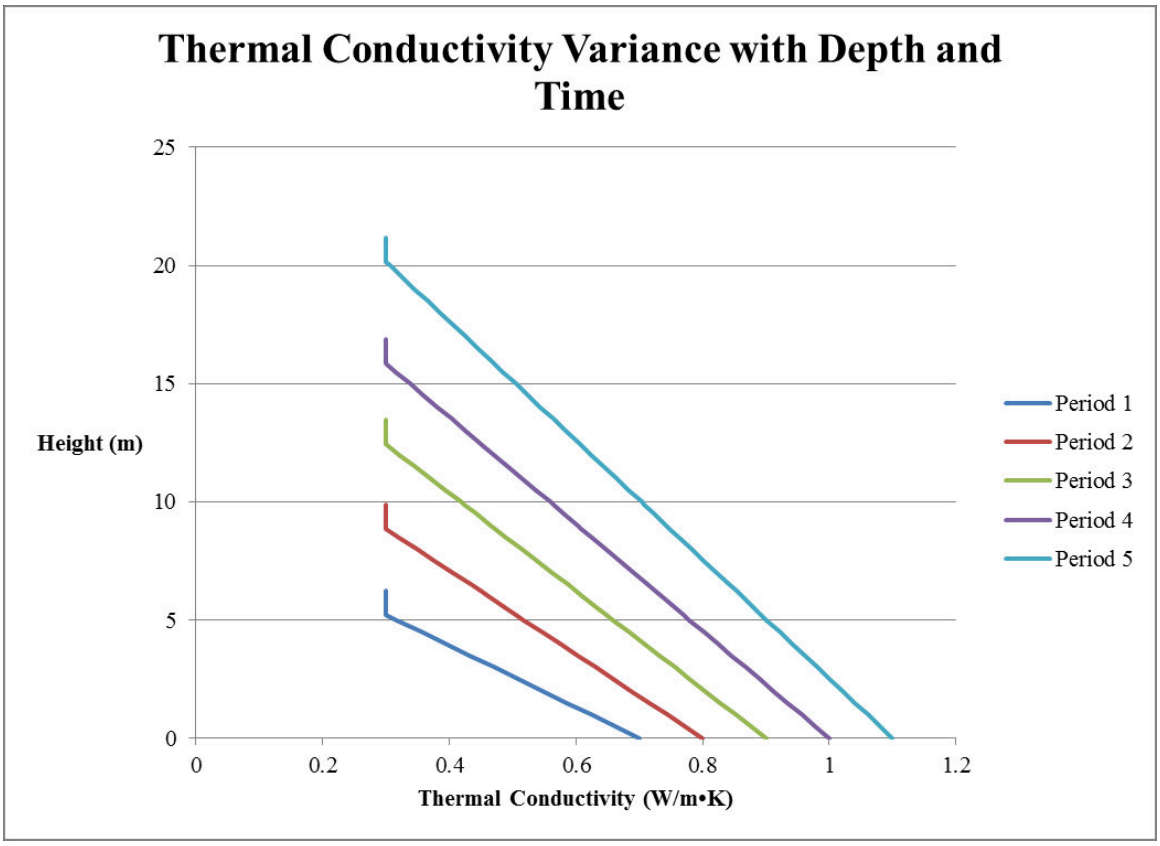

Figure 15: Thermal conductivity variance with depth and time

The maximum thermal conductivity values were selected based on a trial and error approach, minimizing the sum of squared error of the modelled bundle temperatures in comparison with the actual bundle temperatures. The range of thermal conductivities for wastes presented by Faitli et al. (2014) was used as a range in which maximum thermal conductivities could fall within.

Specific heat was not varied with depth in the final model as it was found to have considerably less effect on the overall model predictions (see sensitivity analysis in Section 5.5).

4.2 Conduction from Underlying Soil

Heat can be exchanged from the waste to the base soil below the waste, and vice-versa. In the numerical model, the lower boundary condition at the base of the landfill is a

prescribed temperature, taken as the temperatures recorded at bundle 1 which is located at the base of the landfill immediately above the leachate collection system.

4.3 Surface Heat Flux

The heat flux at the surface of the landfill is governed by the following equation:

$$\nabla(k\nabla T) = \varepsilon Q_o + h(T_{amb} - T_s) + \varepsilon\sigma(T_{amb}^4 - T_s{}^4) \quad (21)$$

The first term in Equation (21) represents the incoming shortwave solar radiation, the second term represents the convection at the surface, and the third term represents the net longwave radiation. ε is the surface emissivity, Q_o [W/m^2] is the net shortwave solar radiation, h [W/m^{2}K] is the convection coefficient, T_{amb} [K] is the ambient temperature, T_s [K] is the surface temperature, and σ [W/m^{2}K^4] is the Stefan-Boltzmann constant for blackbody radiation.

In the numerical model, a value of 0.9 is used for surface emissivity as was used by Megalla (2015). Net shortwave solar radiation is estimated as a function fitted to local solar radiation data from the nearby Mirabel Airport weather station. The convection coefficient is estimated based on the equation presented by Watmuff et al. (1977) (See Section 2.5.4). Wind velocity was estimated as a function fitted to local wind velocity data from the nearby Mirabel Airport weather station. The ambient temperature is taken as a sinusoidal function fitted to ambient temperature data from the nearby Mirabel Airport weather station. Surface temperature is an output of the numerical model.

4.4 Anaerobic Heat Generation Rate

The anaerobic heat generation rate is based on the work of Hanson et al. (2013), which is different than that used by Megalla (2015). The anaerobic heat generation is dependent upon the temperature and energy already expended from the waste. It is assumed that the

waste has a finite amount of energy that can be expended. Therefore, over time, the same total amount of heat can be extracted from all regions in the landfill. A detailed explanation of Hanson et al (2013)'s heat generation model can be found in Section 2.5.6.

From Hanson et al. (2013), the regressed parameters for Cell D and Cell B were both used to model the Ste-Sophie data. Cell D parameters provided a better fit to the Ste-Sophie data and therefore were used in the model. Hanson et al. (2013)'s exponential growth and decay function was used to first give heat generation dependent on waste age:

$$Q = A\left(\frac{t}{B_t + t}\right)\left(\frac{C_t}{C_t + t}\right)e^{-\sqrt{t/D}} \quad (\mathbf{22})$$

Where Q is the heat generation rate (W/m^3), t is the time (days), A is the peak heat generation rate factor (W/m^3), B_t and C_t are shape factors (days), and D is the decay rate factor (days). Parameters from Hanson et al. (2013) Cell D are provided in Table 5.

Table 5: Hanson Cell D Heat Generation Parameters

Parameter	Value
A	4.88
B_t	50
C_t	5000
D	180

This function was then scaled for temperature. Instead of using a dual-ramped temperature function as described in Section 2.5.6, which is difficult to set-up in COMSOL Multiphysics, a quadratic relation was developed to fit this function:

$$-0.000662\,T^2 + 0.414733\,T - 63.951196 \quad (\mathbf{23})$$

As was done in Hanson et al. (2013), Equations (22) and (23) were multiplied to give a 3D heat generation plot dependent on waste age and temperature. This 3D plot was then

integrated with time to give a plot of heat generation dependent upon expended energy at peak temperature, as seen in Figure 16.

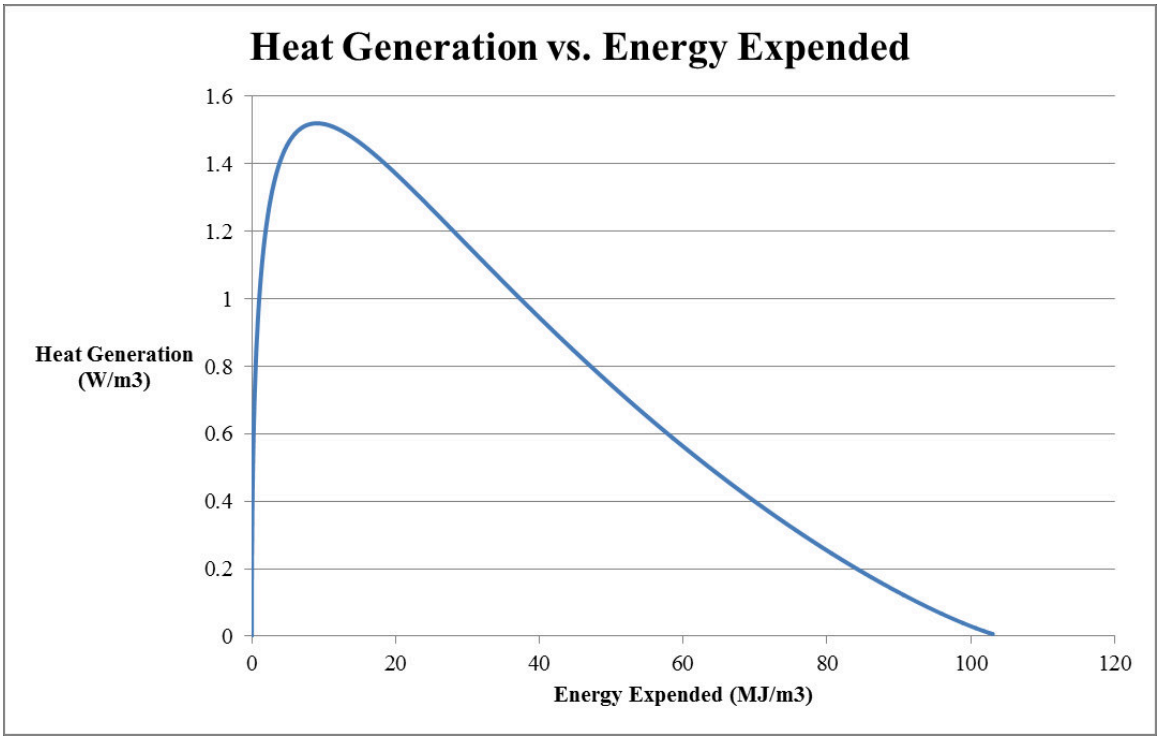

Figure 16: Heat Generation vs. Energy Expended

For modelling simplicity, this curve was fit to a polynomial equation ($R^2 = 0.971$):

$$Q = -1.530 * 10^{-10}E^6 + 5.549 * 10^{-8}E^5 - 7.878 * 10^{-6}E^4 + 5.513 * 10^{-4}E^3 - 1.948 * 10^{-2}E^2 + 0.2940E + 0.1 \quad (24)$$

Where E is the energy expended (MJ/m^3). This function was then scaled by the temperature function (Equation (23)) to create the final heat generation function dependent on energy expended and temperature. Figure 17 shows a 3D plot of this function. Note that below 0^{o}C and above 80^{o}C, no heat generation is considered.

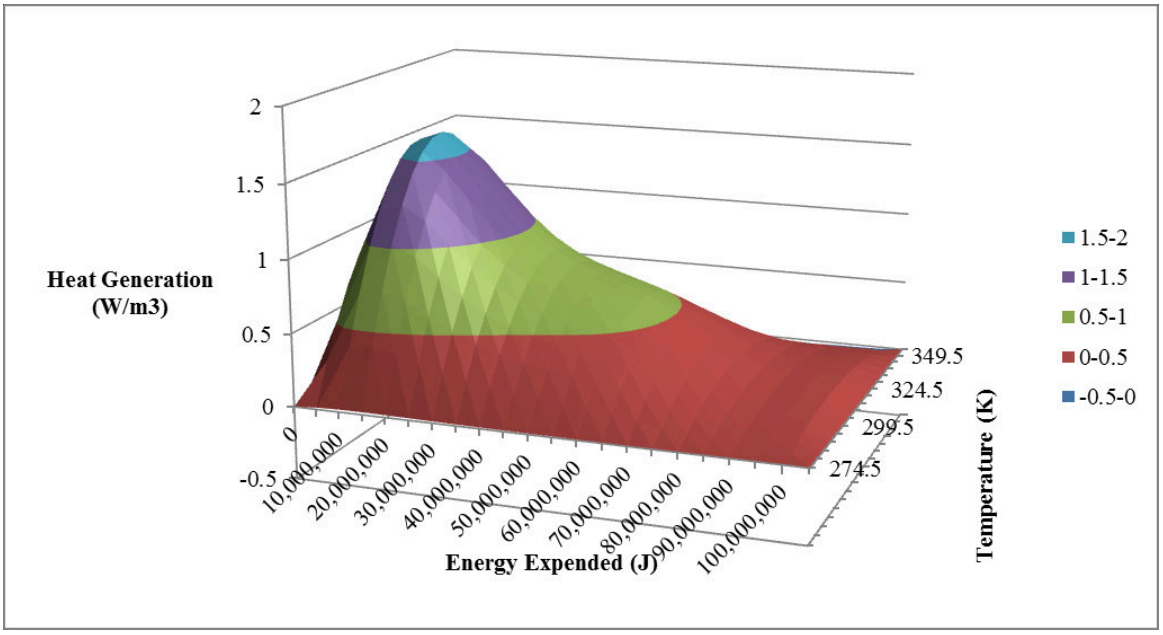

Figure 17: 3D Plot of heat generation dependent upon temperature and energy expended

In the numerical simulation, the cumulative energy expended was tracked throughout the entire space and time domain to use in the heat generation function.

Note that Hanson et al. (2013) uses this methodology to simulate aerobic and anaerobic heat generation. In this thesis, aerobic heat generation is modelled separately as seen in Section 4.5.

4.5 Aerobic Heat Generation Rate

The aerobic heat generation rate is different than that used by Megalla (2015). Looking at Figure 10 and Figure 11, it can be seen that there is a correlation between the concentration of oxygen (in Bundles 9-12) and temperature. These high temperatures are achieved due to ongoing aerobic activity while oxygen is present.

Figure 18 and Figure 19 show an expanded view of the data from Figure 10 and Figure 11 and a better view of the correlation between temperature and oxygen concentration for bundles 9 and 11 (since odd numbered bundles are modelled in this thesis).

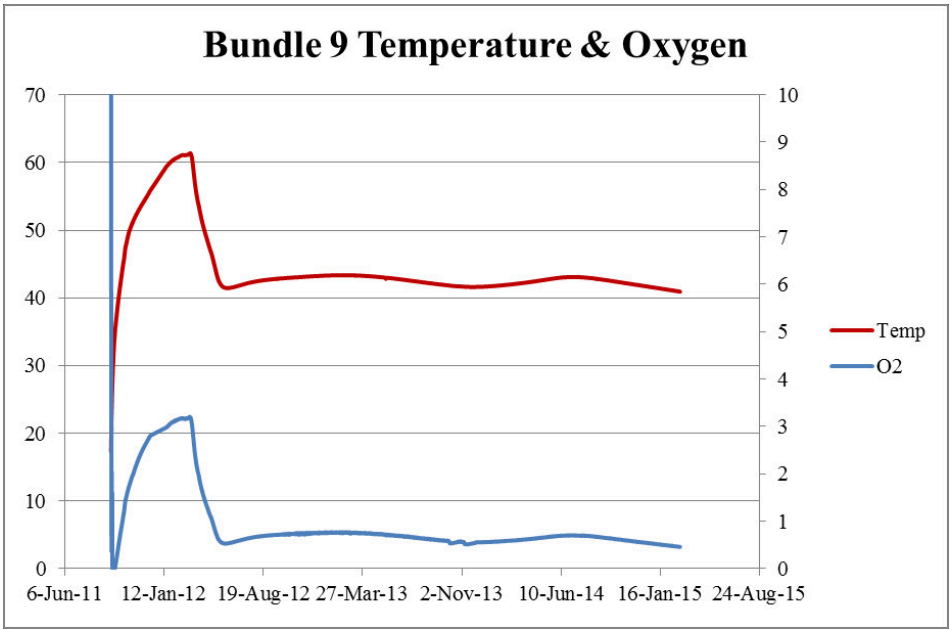

Figure 18: Bundle 9 Temperature & Oxygen Data

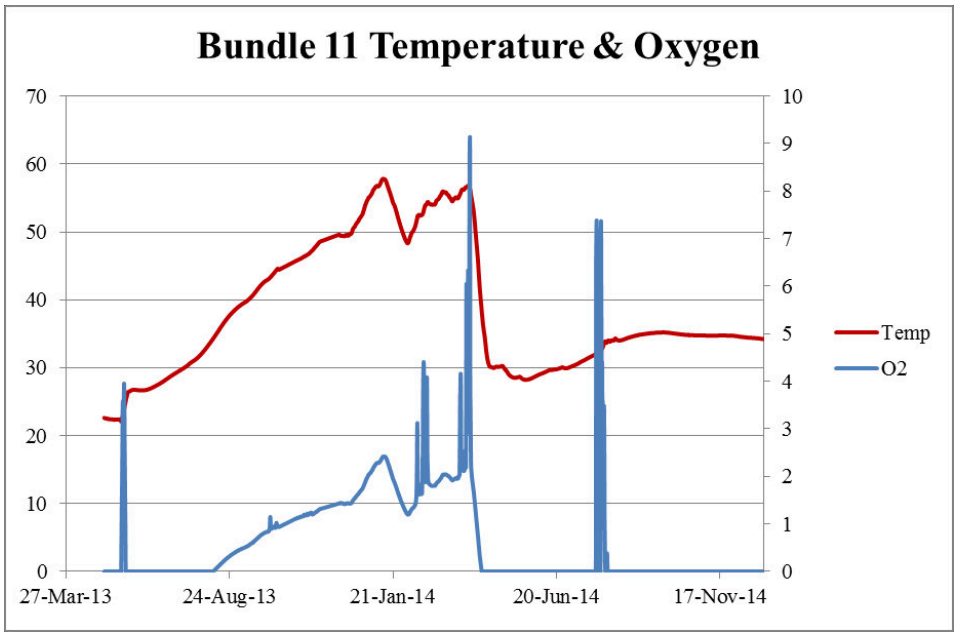

Figure 19: Bundle 11 Temperature & Oxygen Data

To estimate the heat generated by aerobic activity, the following empirical relation was used:

$$Q_{aer} = E_{O_2} * [O_2] \quad (25)$$

Where Q_{aer}[W/m^3] is the aerobic heat generation rate, E_{O_2} is an empirical coefficient calculated using a trial-and-error approach in the numerical model by best fitting the temperature data for bundles 9 and 11 during times where oxygen is present, and $[O_2]$ is the % concentration of oxygen. After trial-and-error analysis, a value of 14 was used for E_{O_2}. The maximum aerobic heat generation achieved in the simulation was 44.6 W/m^3. It was ensured that the maximum aerobic heat generation achieved in the simulation was within the accepted range from the literature. Neusinger et al. (2005) used a maximum heat generation value of 46.3 W/m^3 in landfill heat modelling. Zambra et al. (2011) found a maximum heat generation of 48 W/m^3 in a compost pile heating study.

4.6 Numerical Model Setup in COMSOL Multiphysics

To model the heat transfer and generation throughout the landfill, COMSOL Multiphysics (COMSOL) was used. COMSOL is a powerful modelling tool used to simulate physics based problems. Seeing as modelling the heat transfer and generation in a landfill is essentially a one-dimensional problem (effects from the edges are minimal), and the data from both the odd-numbered and even-numbered bundle columns were similar, a one-dimensional model was setup using the first column of instrument bundles (bundles 1, 3, 5, 7, 9, and 11). A similar approach was used by Bonany et al. (2013a, 2013b) and Megalla (2015).

The model is broken down into five simulation periods (Table 6). At the onset of each new period, a new waste lift is added to the model, corresponding to when a new waste lift was placed in the field.

Table 6: Model Simulation Periods

Simulation Period	Date Range	# of Days	Unsettled Height of Waste (m)
1	Jan 16, 2010 - Dec 12, 2010	331	6.22
2	Dec 13, 2010 - Jan 27, 2011	45	10.08
3	Jan 28, 2011 - Aug 22, 2011	207	13.94
4	Aug 23, 2011 - Mar 14, 2012	204	18.1
5	Mar 14, 2012 - Aug 31, 2014	900	23.49

At the onset of each simulation period, the final results from the previous simulation period are used as initial conditions for the new simulation period. The new waste lift is assigned a uniform initial temperature that it was placed at in field. The numerical model is governed by Equation (19) and incorporates all equations presented throughout Section 4.0.

Spatially, a one-dimensional mesh with finite elements of minimum possible size in COMSOL were used. Time steps of 7200s (2 hours) were used to solve the model. Settlement was also considered in the model (See Section 4.7). The model solution tracks position, temperature, energy expended, heat generation, and other properties for each mesh element over the entire time domain. To track all properties at the correct bundle locations, domain point probes were used. Domain point probes were inserted into the model at given mesh nodes corresponding to each of the bundles' initial placement location in the field. As the mesh deforms with time due to settlement, the mesh nodes move accordingly and the domain point probes are able to track desired properties at the bundle locations. The results at these domain point probes can then be used to compare to field data at the bundles.

4.7 Mechanical Settlement

The model presented by Van Geel & Murray (2015) was used to simulate settlement in this model. Van Geel & Murray (2015) performed regression analysis to determine settlement parameters to use in the composite compressibility model for municipal solid waste presented by Marques et al. (2003).

Using the parameters found by Van Geel & Murray (2015) (see Table 3), settlement was computed in COMSOL Multiphysics. To accommodate the instantaneous settlement in response to an applied load for each waste lift, an initial displacement of the model mesh was applied at the start of each of the five simulation periods for all waste lifts that have a new waste lift placed above them. The initial displacement follows the equation:

$$\Delta H_P = H_o C_C' \log\left(\frac{\Delta\sigma + \sigma_o}{\sigma_o}\right) \quad (\mathbf{26})$$

To accommodate time-dependant settlement (due to both mechanical creep and biological activity), each boundary mesh node in COMSOL Multiphysics (i.e. the top boundary of each waste lift) was assigned a moving mesh node velocity. A moving mesh node velocity is used to deform the mesh according to the movement of the node selected. Therefore, the derivative of the equations from the composite compressibility model that give the time-dependant displacement of the top of each waste lift must be taken to determine the velocity at which each waste lift decreases in height. Therefore, the boundary nodes move downward at a velocity that follows the equation:

$$v_{\Delta H_{C+B}} = \frac{d}{dt} H_o b \Delta\sigma\left(1 - e^{-ct'}\right) + \frac{d}{dt} H_o E_{DG}\left(1 - e^{-dt''}\right) \quad (\mathbf{27})$$

Settlement due to biological activity was only considered for the fourth and fifth waste lifts where anaerobic biodegradation occurred near the landfill surface and waste

temperatures rose to optimum levels for biodegradation. This is consistent with the method of Van Geel & Murray (2015).

The size of the mesh within each waste lift is kept uniform with depth but decreases over time as the overall mesh for each waste lift decreases in height. As mentioned previously, domain point probes inserted into the model at mesh nodes corresponding to the initial location of bundles in the field are able to track the position of the bundles over time.

5.0 LANDFILL QUASI-THERMAL-MECHANICAL-BIOLOGICAL MODEL RESULTS AND DISCUSSION

5.1 Mechanical Settlement

Figure 20 shows modelled settlement vs. the settlement data from the field settlement sensors.

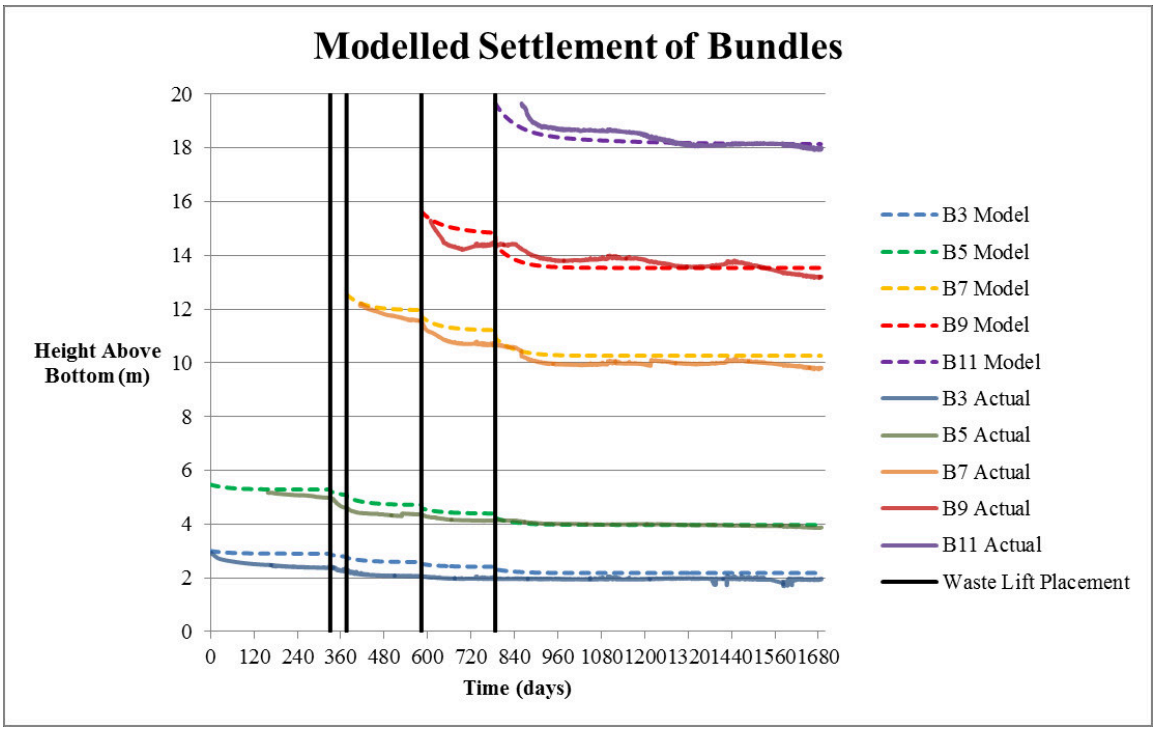

Figure 20: Actual and Modelled Settlement Values

From Figure 20 it can be seen that modelled settlement values fall close to those seen in the field. Sharp increases in settlement (decreases in height above the base of the model domain) at each bundle can be seen due to the placement of subsequent waste lifts due to primary compression in both the real and modelled data sets. Modelling the location of each bundle in the landfill over time allows for an accurate calibration of the thermal model. As the bundles (model nodes) move within the model, the temperature at each node can be predicted. Changes in depth as small as one meter can have large effects on the predicted temperature of the bundles, particularly those close to the surface and

ambient conditions (see Figure 23). Bonany (2012) and Megalla (2015) did not include settlement in their models and as a result, they could not directly account for the fact that the bundles move closer to the lower boundary with time. In their comparison with field data, Bonany (2012) and Megalla (2015) plotted the temperature data with time while manually adjusting the location of the bundles with time within their fixed mesh.

5.2 Numerical Model Results & Predicted Temperatures

Figure 21 shows the final modelled landfill temperature results. Predicted temperatures of odd numbered bundles 3 through 11, as well as the actual bundle temperatures and the ambient temperature, are plotted.

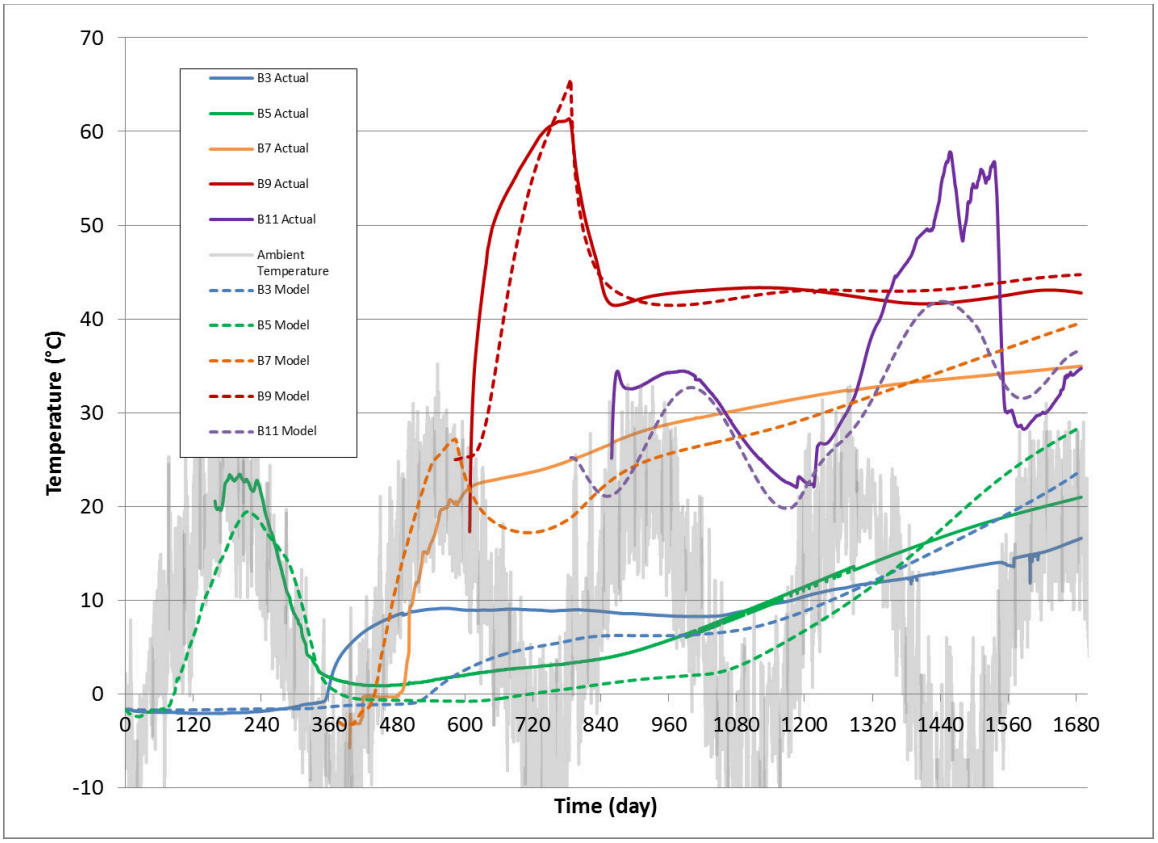

Figure 21: Actual and Modelled Odd-numbered Bundle Temperatures

Model predictions with respect to actual bundle temperatures are in good agreement. The modelled temperature at bundle 3 begins to rise above freezing shortly after the actual

temperature begins to rise above freezing. Towards the end of the simulation, the temperature of bundle 3 rises at a greater rate than the actual temperature. It should be noted that although the temperature appears to be rising at a rate much greater than the actual temperature, it is expected that this rate of increase will decline with time as the expended energy at the location of bundle 3 is past the peak heat generation on the anaerobic heat generation curve (Figure 17). The same holds true for bundles 5 and 7.

Modelled bundle 5 and 7 temperatures are also in good agreement with actual temperatures. As with bundle 3, the temperature towards the end of the simulation is overestimated at both bundles. Modelled bundle 7 temperatures are more closely correlated to ambient temperatures than field data are. Modelled bundle 7 temperatures also show a decrease due to the placement of an above colder waste lift (lift 4), whereas field data shows that bundle 7 did not decrease in temperature when waste lift 4 was placed above. This leads to the possible conclusion that bundle 7 may be deeper than 0.75 m below the surface of the third waste lift, and would therefore be greater insulated from above effects from ambient temperatures and waste lift 4.

Modelled bundle 9 and 11 temperatures are also in good agreement with actual temperatures. The presence of oxygen near bundle 9 during the fourth simulation period and near bundle 11 during the fifth simulation period play a large part in the modelling of these temperatures.

Figure 22 shows the simulated total expended energy at each of the bundle locations. The total expended energy feeds into the anaerobic heat generation term. It can be seen

that at all bundle locations, the expended energy is past the point where peak anaerobic heat generation is achieved (Figure 17).

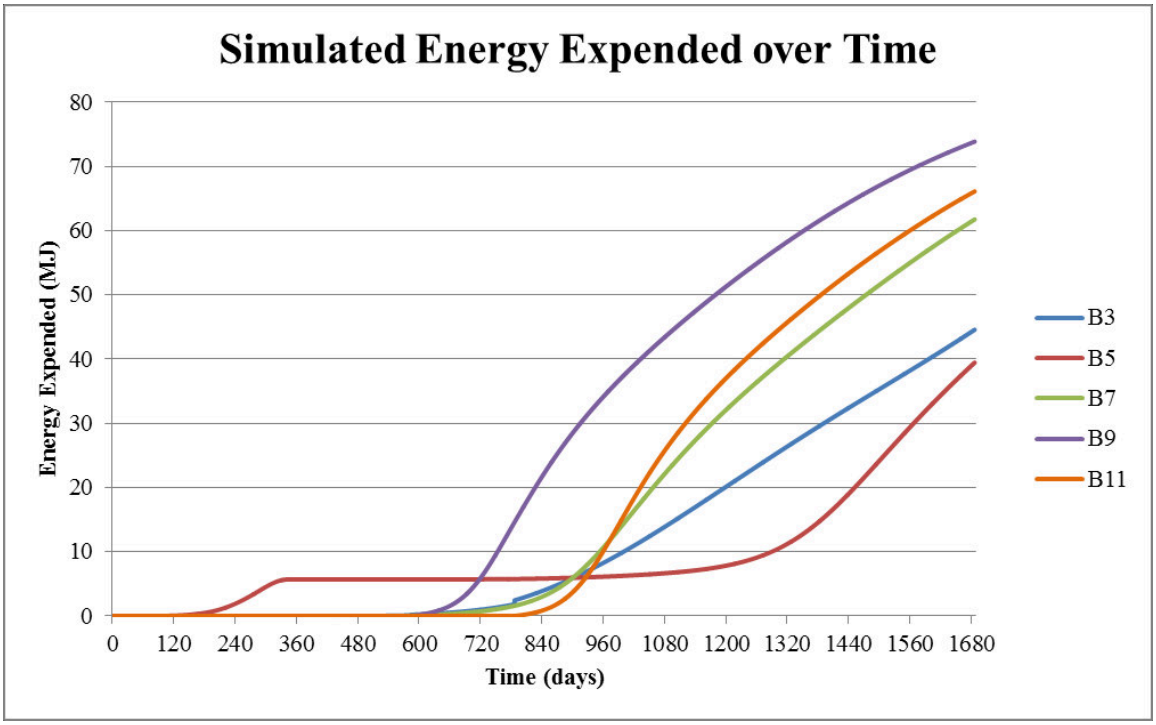

Figure 22: Expended energy at each of the bundle locations over time

An alternative graphical display of the temperature data is shown in Figure 23. Modelled temperature profiles of the landfill are shown at six different times. Measured bundle temperatures are displayed in each plot. It can be seen that a large amount of waste remains frozen 2-3 years after placement.

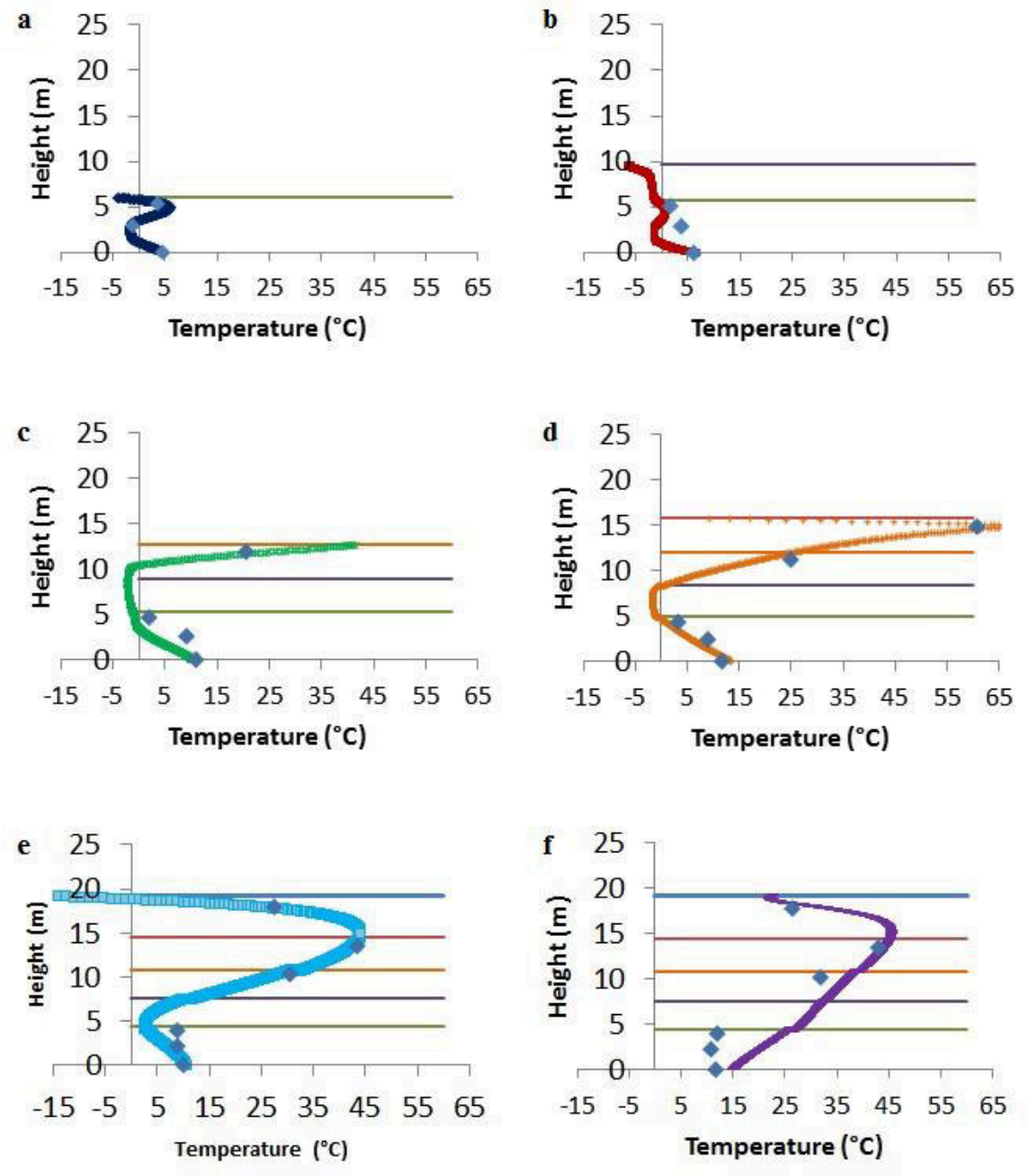

Figure 23: Temperature profiles with depth at the following dates: a) December 12, 2010; b) January 27, 2011; c) August 22, 2011; d) March 14, 2012; e) January 9, 2013; f) May 23, 2014

This model solution may not be unique, however it does provide a good idea as to the thermal properties, heat generation, and heat transfer processes affecting the landfill temperatures. Section 5.4 presents a heat budget calculated using the above model

solution. Section 5.5 presents a sensitivity analysis of the input thermal parameters and their effect on model predictions.

5.3 Comparison with Second Bundle Column

To partially validate the model the model was used to simulate temperatures of the second column of waste described in Section 3.0 (corresponding to the even-numbered bundles). The following changes to input parameters/data were made:

- Waste lift heights and bundle elevations were changed to values corresponding with data collected from the even-numbered bundles. This includes an additional five meters of waste placed in the fifth waste lift compared to what was placed above the first column of waste.
- The prescribed base temperature (bottom boundary condition) was taken from bundle 2.
- Oxygen concentrations from the even-numbered bundles were used as inputs for the aerobic heat generation term

Figure 24 shows the results of the simulated temperatures for the second waste column in comparison with field data for the even-numbered bundles.

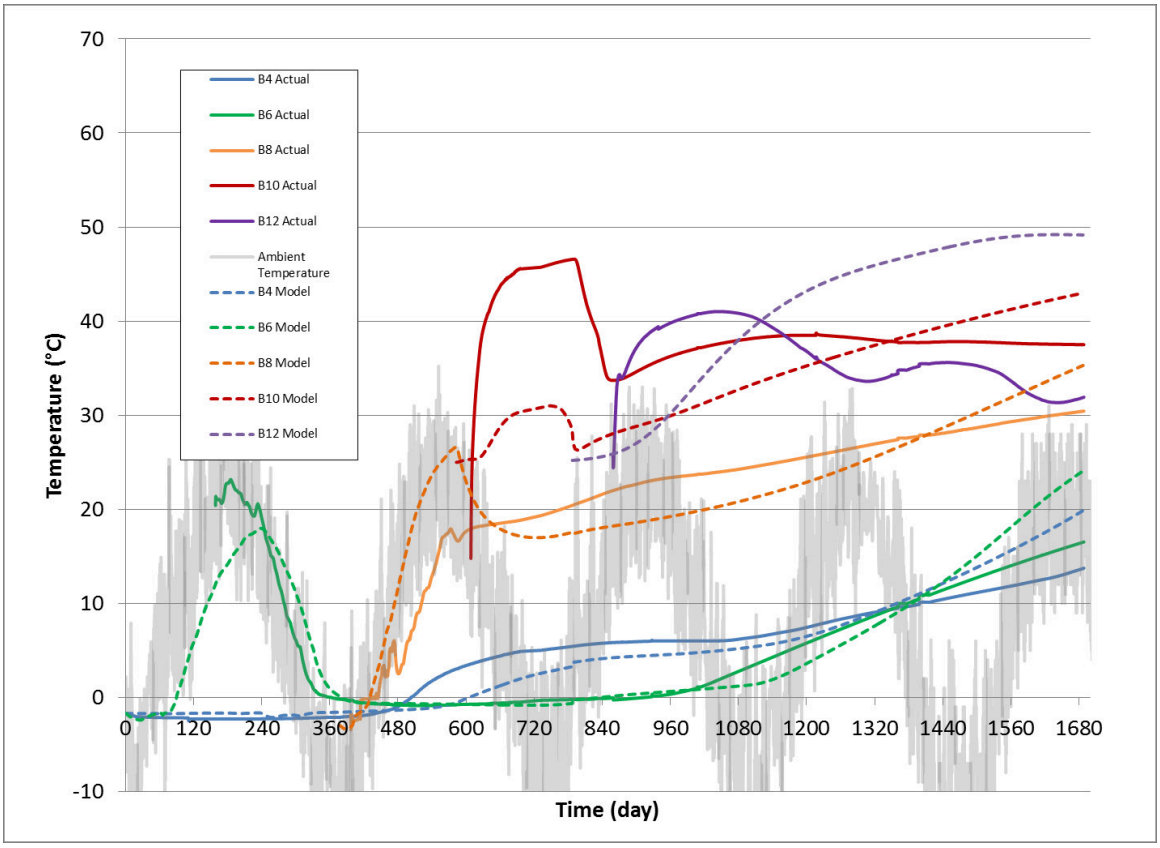

Figure 24: Actual and Modelled Even-numbered Bundle Temperatures

The model performed well through the first three simulation periods and for bundles 4, 6, and 8. A large discrepancy between modelled and field temperatures can be seen for bundles 10 and 12. There are a number of potential reasons for the discrepancy:

- The aerobic heat generation term appears to underestimate the amount of heat produced due to the presence of oxygen at bundle 10, after placement.
- Higher field temperatures (in comparison to modelled temperatures) during the fourth and beginning of the fifth simulation period for bundles 10 and 12 may be due to the conduction of heat from areas nearer to the side slope, such as the first column of waste (e.g. a two-dimensional problem). The first column of waste showed higher oxygen concentrations and higher temperatures. The higher

adjacent temperatures may have resulted in higher temperatures for the second column of waste, that could not be realized by the one-dimensional model.

- During the fifth simulation period, modelled temperatures rise at rates higher than what are seen in the field. This is likely due to the anaerobic heat generation term overestimating the amount of heat that is generated.

It is also important to note that although oxygen was present at bundle 12, no aerobic heat generation was realized in the model. Bundle 12 is located over one meter below the surface, and therefore the model does not consider any oxygen that may be present. In reality, there likely was aerobic activity ongoing at the location of bundle 12. The reason for the presence of oxygen at bundle 12 is potentially due to migration of oxygen from the side slope of the landfill due to advection or diffusion.

5.4 Heat Budget Analysis

An energy budget or heat budget was computed to analyze how much and when heat was transferred or generated in the landfill. The control volume for the analysis was the landfill volume, which changed from period to period. The calculations are based on a 1 m^2 column of waste and the following energy budget equation:

$$Q_{sensible} + Q_{latent} = Q_{conv} + Q_{sol} + Q_{long} + Q_{cond} + Q_{aer} + Q_{non-aer} \quad (28)$$

The results of the analysis are shown in Table 7.

Table 7: Heat Budget

Number of Days per Period	331	45	207	204	900	1687
Heat Term [MJ/m^2]	Period 1	Period 2	Period 3	Period 4	Period 5	Cumulative
Convection	-2337	-112	-1485	-1210	-6044	**-11189**
Solar Radiation	3739	154	2419	1250	7996	**15558**
Long Wave Radiation	-1280	-49	-824	-483	-2435	**-5070**
Net Heat Flux at Surface	122	-7	110	-442	-483	**-701**
Conduction from Soil Below	60	26	86	45	3	**220**
Net Heat Flux at Base	60	26	86	45	3	**220**
Aerobic Heat Generation	0	0	0	520	232	**752**
Anaerobic Heat Generation	7	0	8	136	1195	**1347**
Total Heat Generation	7	0	8	656	1428	**2099**
Latent Heat	153	40	59	80	122	**454**
Sensible Heat	36	-21	145	179	825	**1164**
Total Latent & Sensible Heat	189	19	203	259	947	**1617**

The amount of heat lost, gained, or transferred is shown for each period and the cumulative total over the entire 1687 day simulation period.

At the surface, the three methods of possible heat transfer in the model are convection (Q_{conv}), solar radiation (Q_{sol}) (always incoming), and net long wave radiation (Q_{long}). The cumulative heat gained or lost during each simulation period was calculated by integrating the respective heat fluxes over time. In all five periods, heat is lost through both convection and net long wave radiation, while gained through solar radiation. The resultant net heat flux at the surface (sum of heat transferred through the three methods) is relatively small in all five periods. During the first period, heat was gained at the surface due to the solar radiation outweighing the amount of heat lost through convection and longwave radiation. In the second period, heat was lost at the surface as this was during December 2010 and January 2011 where ambient temperatures were colder than surface waste temperatures. During the third period, which ranged from the end of January 2011 to the end of August 2011, heat was gained at the surface as this simulation

period primarily took place during Spring/Summer. Conversely, heat was lost at the surface during the fourth period as the period mainly covered the Fall/Winter months and a significant amount of heat was generated aerobically near the waste surface during this period. Due to the length of the fifth period (900 days), seasonal effects are diminished. As temperatures at the landfill surface rise due to heat generation in the landfill, the overall net heat flux at the surface is a loss to the atmosphere. It should be noted that during winter months snow may play a factor in the surface heat transfer processes but is not considered in the modelling. Snow cover increases the albedo effect on incoming solar radiation, which results in more reflection and less solar radiation reaching the landfill. Snow also insulates the landfill which would reduce the amount of heat transferred through convection and longwave radiation.

Conduction at the base of the landfill (Q_{cond}) was calculated using the thermal gradient between the base of the landfill and the model node at a height of 0.1 m. Conduction at the base resulted in a small heat gain in the landfill through the first four periods, while in the fifth period the waste at the bottom of the landfill was at a temperature greater than that of the underlying soil and therefore heat was transferred out of the landfill.

Aerobic heat generation (Q_{aer}) was assumed to only be possible in the top meter of waste in the model. It was calculated through an empirical relation (Equation (25)) tracked in the model and integrated over time to determine the overall aerobic heat generation for each period. Anaerobic heat generation (Q_{anaer}) was calculated using methods from Hanson et al.(2013) and was tracked in the model and integrated over time to determine the overall anaerobic heat generation for each period. Through the first three periods, minimal heat is generated in the landfill as all three waste lifts were placed in the winter

months and temperatures have not yet risen to values sufficient to support microbial activity. During the fourth and fifth periods, the presence of oxygen recorded at the instrument bundles close to the surface indicate that oxygen is migrating into the landfill by diffusion and potentially advection due to gas collection resulting in aerobic heat generation at the surface. The increased temperatures within the waste, coupled with increasing heat generation rates resulted in significant anaerobic heat gains as well. Cumulatively, aerobic heat generation resulted in 752 MJ/m^3 (36%) of heat generated while the anaerobic heat generation resulted in 1347 MJ/m^3 (64%) of heat generated during the 4.6 year period simulated.

Sensible heat stored ($Q_{sensible}$) was calculated using the equation:

$$Q_{sensible} = mC\Delta T \quad (\mathbf{29})$$

and the average initial temperature and final initial temperature for the entire domain for each period.

The latent heat for phase change was calculated using the assumption of energy conservation, and knowing all other terms in the energy budget equation:

$$Q_{latent} = Q_{conv} + Q_{sol} + Q_{long} + Q_{cond} + Q_{aer} + Q_{non-aer} - Q_{sensible} \quad (\mathbf{30})$$

To verify the energy balance equation, the latent heat calculated using Equation (30) was compared to the total energy needed to thaw the first three waste lifts which were placed under frozen conditions. The cumulate depth of the first three waste lifts was 13.94m. Given a latent heat term of 37.2 kJ/kg and a density of 930 kg/m^3, 454 MJ of energy

would be required. This confirms that Equation (30) does conserve energy and provide a reasonable energy balance.

During all periods except for the second period, sensible heat was stored in the landfill as there was a net increase in heat storage in the landfill. During the second period, the landfill decreased in average temperature due to the colder ambient temperatures. The latent heat value represents how much energy was used to thaw frozen waste. The fact that there was still latent heat required to thaw frozen waste in the fifth period shows how long waste can stay frozen within the landfill (upwards of 2-3 years). Through the entire 1687 day period, latent heat accounted for 454 MJ, compared to 1347 MJ of sensible heat stored in the waste.

5.5 Model Sensitivity Analysis

A sensitivity analysis was performed on the specific heat and thermal conductivity of the waste in the model. The goal of the sensitivity analysis was to provide an indication as to the effect that each of the above parameters has on the model predictions. Specific heat in the base model was 2100 J/kg•K. The model was tested with a specific heat of 1680 J/kg•K (-20% compared to the base model), 1890 J/kg•K (-10%), 2310 J/kg•K (+10%), and 2520 J/kg•K (+20%). The thermal conductivity of waste in the base model varied with time and space as described in Section 4.1.2. The average thermal conductivity over time and space in the base model was 0.6 W/m•K. The model was tested with a thermal conductivity that varied +/- 10% and 20% of the average thermal conductivity over the entire space and time domains. For example, when the model was varied by +10%, thermal conductivity across the entire domain was increased by 0.06 W/m•K. During the

first simulation period, thermal conductivity was therefore 0.36 W/m•K in the top meter; and varied from 0.36 W/m•K (at a depth of 1 m) to 0.76 W/m•K at the base. During the second simulation period, thermal conductivity was 0.36 W/m•K in the top meter; and varied from 0.36 W/m•K (at a depth of 1 m) to 0.86 W/m•K at the base. This methodology was followed for all simulation periods and sensitivity analysis model tests.

Table 8 shows the results of the sensitivity analysis. The sensitivity of each parameter variation was measured by comparing the squared error of each sensitivity analysis model run (with respect to the actual measured temperature data) to the squared error of the base model. Also displayed in the table are the increase in the total sum of squared error for all five bundle locations compared to the base model, and the increase in the sum of squared error for each of the five bundles and five simulation periods compared to the base model. Sum of squared error was used by calculating the squared error in model predictions vs. field temperatures once daily.

Table 8: Sensitivity Analysis Results

Parameter Varied	Parameter Variation	C_p (J/kg•K)	K (Top 1m; Gradient Below) (W/m•K)	Increase in Total Sum of Squared Error	Increase in B3 Squared Error	Increase in B5 Squared Error	Increase in B7 Squared Error	Increase in B9 Squared Error	Increase in B11 Squared Error	Increase in P1 Squared Error	Increase in P2 Squared Error	Increase in P3 Squared Error	Increase in P4 Squared Error	Increase in P5 Squared Error
Final Model		**2100**	**0.3; 0.3-(0.7-1.1)**	**N/A**	**N/A**	**N/A**	**N/A**	**N/A**	**N/A**	**N/A**	**N/A**	**N/A**	**N/A**	**N/A**
C_p	-20%	1680	0.3; 0.3-(0.7-1.1)	**36%**	55%	129%	106%	19%	-10%	-42%	-6%	21%	-8%	59%
	-10%	1890	0.3; 0.3-(0.7-1.1)	**7%**	21%	31%	15%	3%	-4%	-25%	-7%	-1%	-3%	14%
	+10%	2310	0.3; 0.3-(0.7-1.1)	**4%**	-19%	-10%	18%	5%	11%	3%	5%	-9%	4%	7%
	+20%	2520	0.3; 0.3-(0.7-1.1)	**14%**	-8%	17%	25%	12%	18%	19%	0%	-4%	9%	20%
K	-20%	2100	0.18; 0.18-(0.58-0.98)	**52%**	65%	67%	31%	155%	6%	173%	17%	-20%	73%	58%
	-10%	2100	0.24; 0.24-(0.64-1.04)	**2%**	1%	33%	-2%	27%	-15%	45%	6%	-7%	13%	-1%
	+10%	2100	0.36; 0.36-(0.76-1.16)	**21%**	-15%	-17%	30%	37%	34%	-35%	-25%	1%	11%	31%
	+20%	2100	0.42; 0.42-(0.82-1.22)	**54%**	15%	5%	28%	98%	70%	-57%	-31%	18%	40%	71%

As can be seen in Table 8, variations in model parameters from the base model results in poorer model predictions. Changes in thermal conductivity are more sensitive than changes in specific heat. From bundle to bundle and period to period, it can be seen that there is not a gradual relationship in greater variation in parameter inputs resulting in greater error/variation in model results. Due to the complexities in the model domain, variations in parameters can result in better or poorer model predictions at different locations and/or over different simulation periods.

On average, a change in specific heat of +/- 10% (+/- 210 J/kg•K) results in an increased total squared error of 6% compared to the base model. A change in specific heat of +/- 20% (+/- 420 J/kg•K) results in an increased total squared error of 25% compared to the base model. A change in thermal conductivity of +/- 10% (+/- 0.06 W/m•K) results in an increased total squared error of 12% compared to the base model. A change in thermal conductivity of +/- 20% (+/- 0.12 W/m•K) results in an increased total squared error of 53% compared to the base model. This shows that thermal conductivity has a greater effect than specific heat does on the model. In all cases, a 20% change in input thermal parameters results in roughly four times greater increase in total squared error in comparison with a 10% change in input thermal parameters.

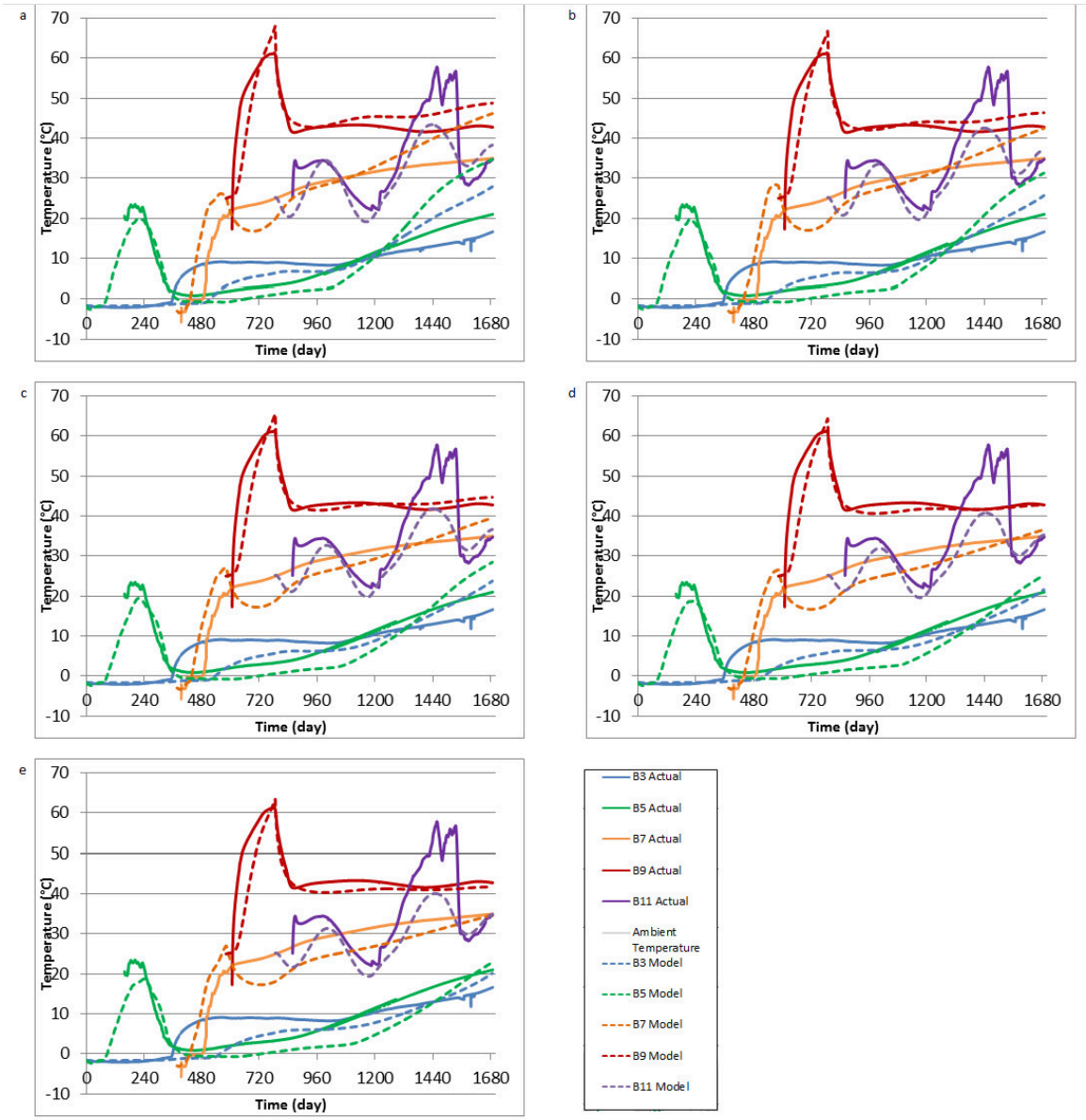

Figure 25: Specific Heat Sensitivity Analysis a) -20%, b) -10%, c) base model, d) +10%, e) +20%

Figure 25 shows the results of the model being run with the different specific heat values presented in Table 8. It can be seen that a lower specific heat value generally results in higher temperatures being generated throughout the model. This is logical, as a lower specific heat means that less energy is needed to increase the temperature of a material. For bundle 11, a lower specific heat value resulted in better model predictions than in the base model (as seen in Figure 25 and Table 8), however bundles 3, 5, and 7 showed

considerably worse predictions. For bundles 3 and 5, a higher specific heat value resulted in marginally better model predictions (a 10% increase in specific heat resulted in 19% and 10% less total squared error in comparison to the base model, respectively). This evidence suggests that the specific heat of the waste may vary from higher values near the base of the landfill to lower values near the landfill surface.

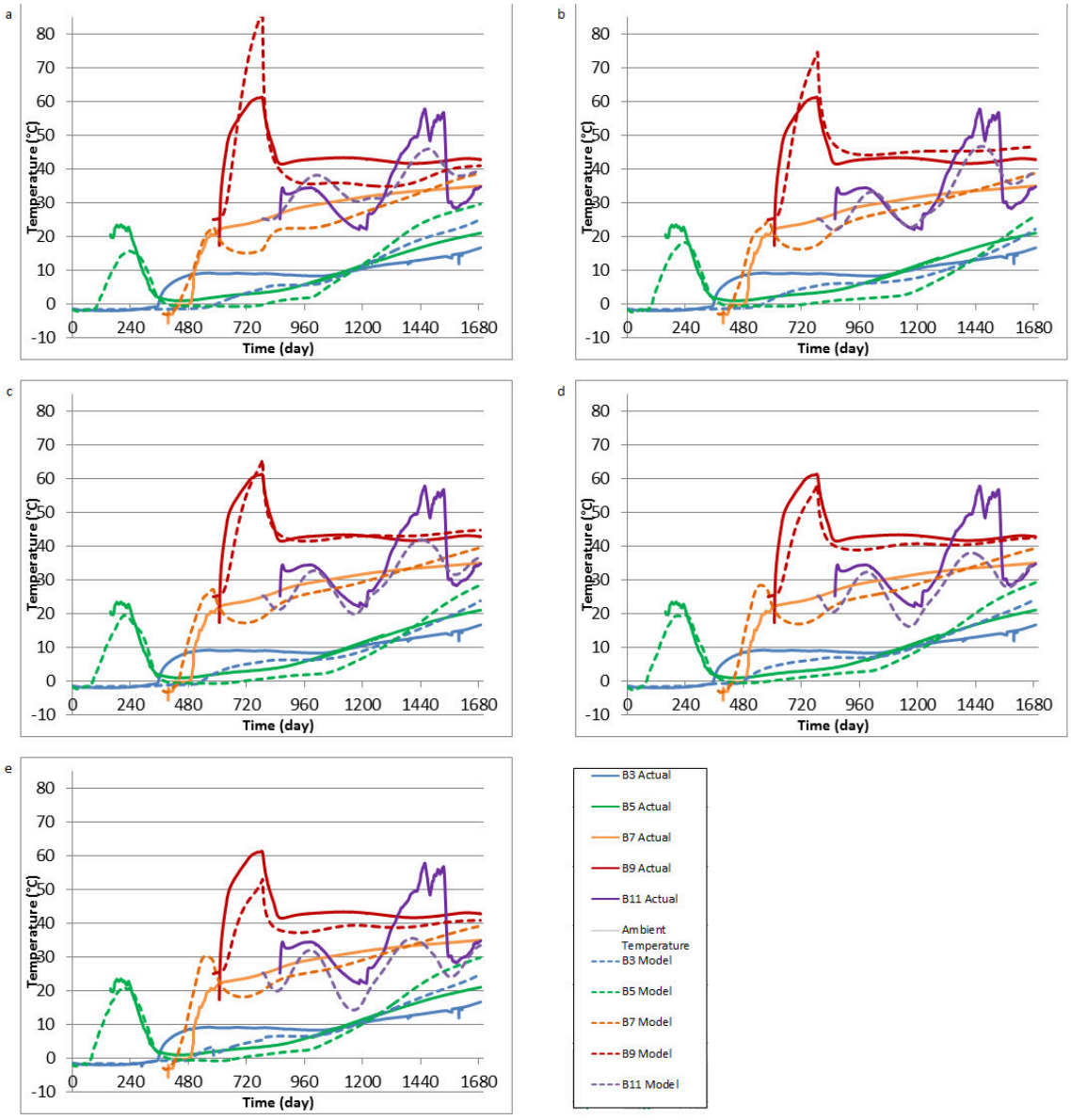

Figure 26: Thermal Conductivity Sensitivity Analysis a) -20%, b) -10%, c) base model, d) +10%, e) +20%

Figure 26 shows the results of the model being run with the different thermal conductivities presented in Table 8. When the thermal conductivity is altered, effects are more pronounced near the landfill surface than near the base of the landfill. This is due to the change in surface heat flux depending on the thermal conductivity. For the first three simulation periods, where minimal heat is generated in the upper portion of the landfill, reducing the thermal conductivity results in lower modelled temperatures at the surface due to less heat migrating downward from the warmer ambient temperatures at the surface. During the fourth and fifth simulation periods, where aerobic heat generation occurs in the upper portion of the landfill, less heat is lost through the surface, and therefore temperatures drive up well above the base model case. The opposite is true for increased thermal conductivity. At the base of the landfill, increasing the thermal conductivity by 10% results in better model predictions at the base of the landfill (15% and 17% reduced total squared error in bundle 3 and 5, respectively). Increasing the thermal conductivity does however produce poorer temperature predictions in the upper bundles (for a 10% increase in thermal conductivity, bundle 7, 9, and 11 had increased total squared error of 30%, 37%, and 34%, respectively). These negative effects were more pronounced with a 20% increase in thermal conductivity.

6.0 MODELLED AIR INJECTION TEST

One way to increase the temperature within the waste is to inject air and encourage aerobic biodegradation as this generates heat. This can be tested in the field at Ste-Sophie by pumping air out to an instrument bundle. A test of this nature could also be used to further calibrate and validate the model. Therefore, a simulation was conducted to estimate the potential impact on temperature of pumping air into the waste at an instrument bundle. This simulation assumed that all oxygen injected will be consumed and used by aerobic microbes. The energy production due to the consumption of oxygen was assumed to be 460 kJ/mol of oxygen (Yoshida et al., 1997). The test also assumes the heat generation to come from a point source. If oxygen was to be injected into the landfill it is likely that it would migrate both vertically and laterally due to diffusion and advection. The heat produced would come from the area that the oxygen migrates to. The simulation is done using an air injection pumping rate of 10 L/s for one week. This value was chosen as it reflects the approximate upper value of air injection that has been successfully pumped into the landfill by another researcher in Dr. Van Geel's research group. Note that the pumping rate would be greater in the field and is adjusted here given that the model only simulates heat transfer in the vertical direction. Assuming a $1m^2$ cross-sectional area, this results in a total heat generation of 26.08 MJ over the one week period. In the simulation, a heat source of 43 J/s is added at the beginning of the fifth simulation period at the interface of the 2^{nd} and 3^{rd} waste lifts (See Figure 27). In reality there would be a lag period from the time of oxygen injection to the time that aerobic microbes would start producing heat, however this is not considered in this study. Further study and experimentation are needed to determine whether field oxygen addition would result in activation or re-activation of aerobic microbes, and at what rate this may

occur at. Consideration of fire due to spontaneous combustion would also need to be taken.

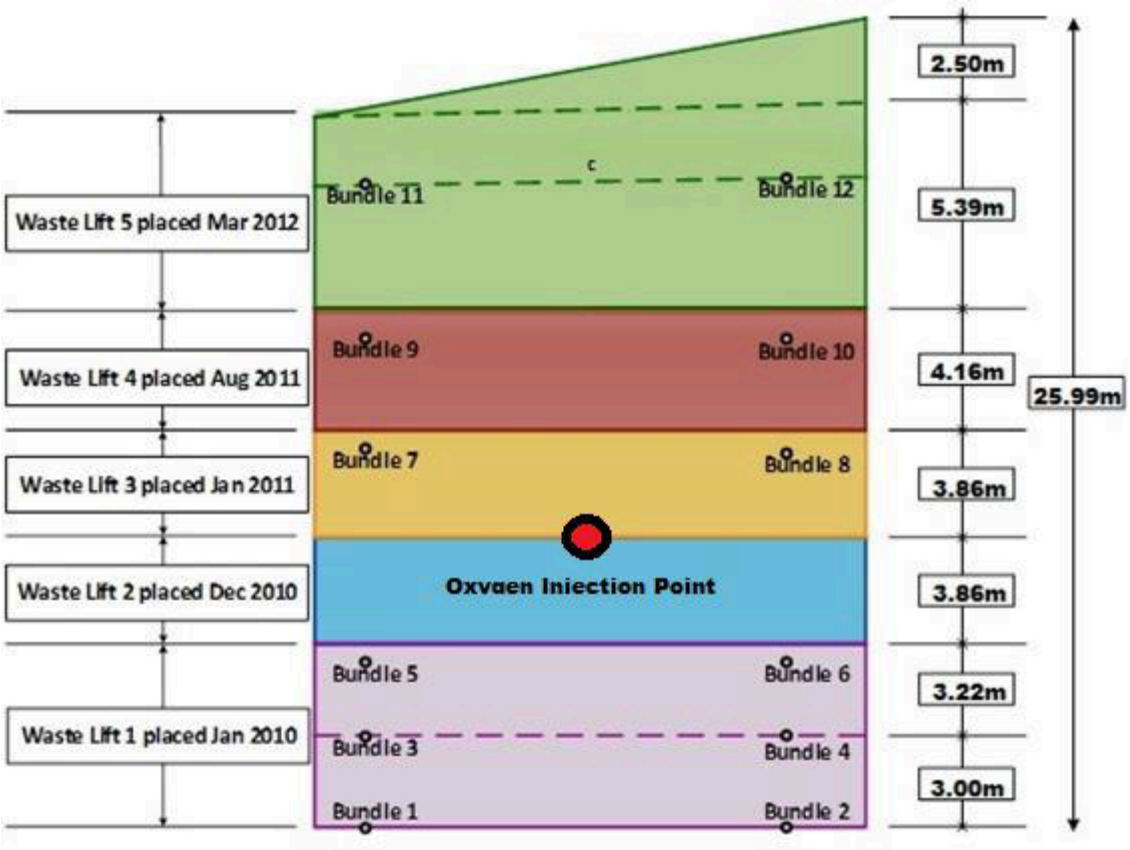

Figure 27: Oxygen Injection Point Source Location

Figure 28 shows the results of the air injection simulation. The field temperatures, base model case, and air injection simulation temperatures are shown. Temperatures in bundle 7 (roughly 3.5 m away) and bundle 5 (roughly 4 m away) rise by approximately 1°C compared to the base model case. The lag due to heat transfer from the heat source to these bundle locations can be seen. Minor temperature change is seen in bundles 3 and 9, while there is almost no effect seen in bundle 11 as it is separated by roughly 12 m of waste from the source point.

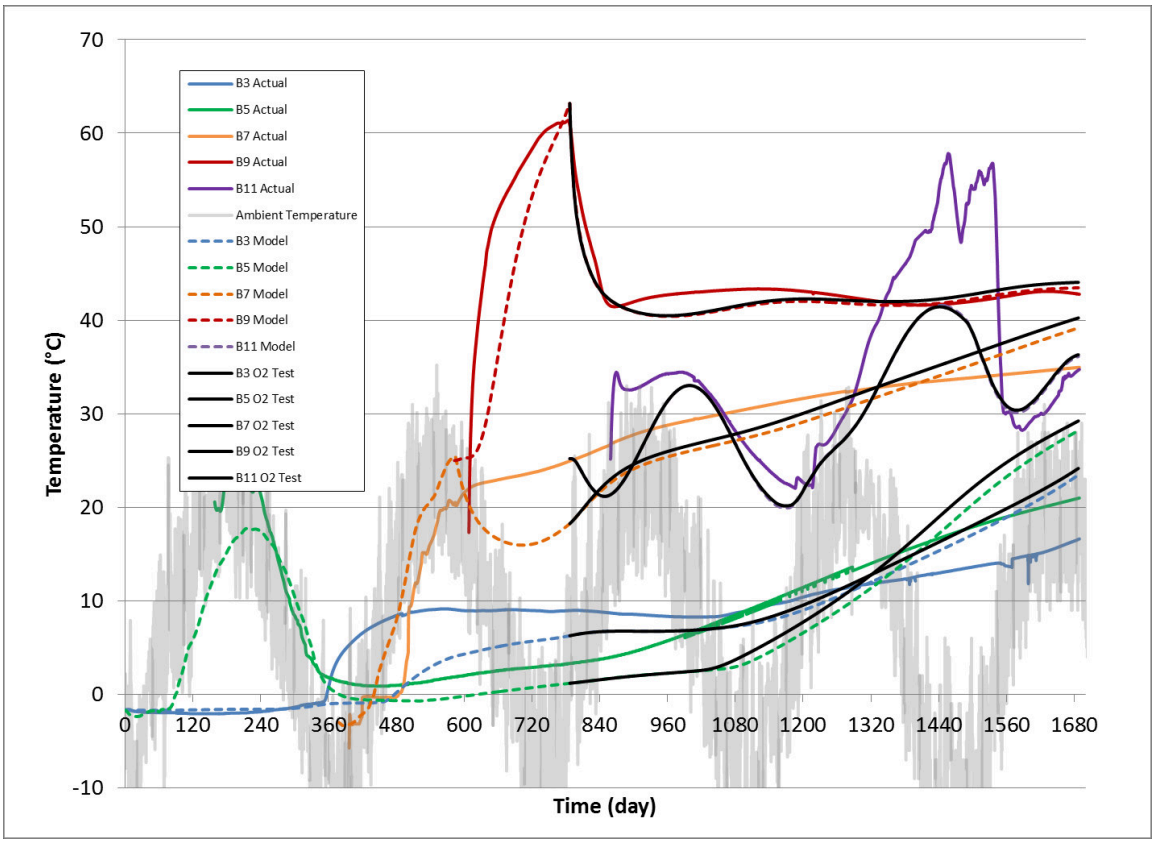

Figure 28: Oxygen Injection Test Results

As temperatures throughout the domain rise, anaerobic activity can also be promoted due to its temperature dependence. On the contrary, the addition of oxygen could halt anaerobic activity and after oxygen is depleted due to aerobic microbes, the re-activation of anaerobic microbes could be delayed. This topic has not been further researched.

The small amount of heat generated in this study due to the oxygen injection did not have a large effect on temperatures, however it does lay the foundation for an experiment of this nature in the field.

7.0 LANDFILL SURFACE STUDY

To date, there has not been any research performed on the effect of landfill cover systems on the heat transfer and heat generation processes occurring at the surface of a landfill. The goal of this study was two-fold: a) to give a better understanding of heat transfer processes at the landfill surface; and b) to analyze different interim landfill cover materials with respect to their potential for allowing oxygen diffusion into the landfill to maintain aerobic conditions and corresponding heat generation rates.

7.1 Surface Study Experimental Set-up

A landfill surface monitoring station was re-installed at the Ste-Sophie landfill. The initial design and installation of the surface station was completed by Alyssa Gladish as part of her MASc work. The initial installation was not very successful for a number of reasons and the station was reinstalled in May 2014. The surface monitoring station was installed approximately 500 m west of the location of instrument bundles 1-12 that are discussed in this thesis (see Appendix A for location on site engineering drawing).

The surface monitoring station was equipped with sensors to monitor the top meter of waste in three field interim cover pods. The station also was equipped with a weather station to monitor ambient conditions at the landfill surface. The equipment and sensors were fixed to a tripod located at the center of the three interim cover pods. Figure 29 shows an overhead schematic of the surface monitoring station. Figure 30 is a photograph showing the above-ground components of the surface monitoring station and the location of the three interim cover pods.

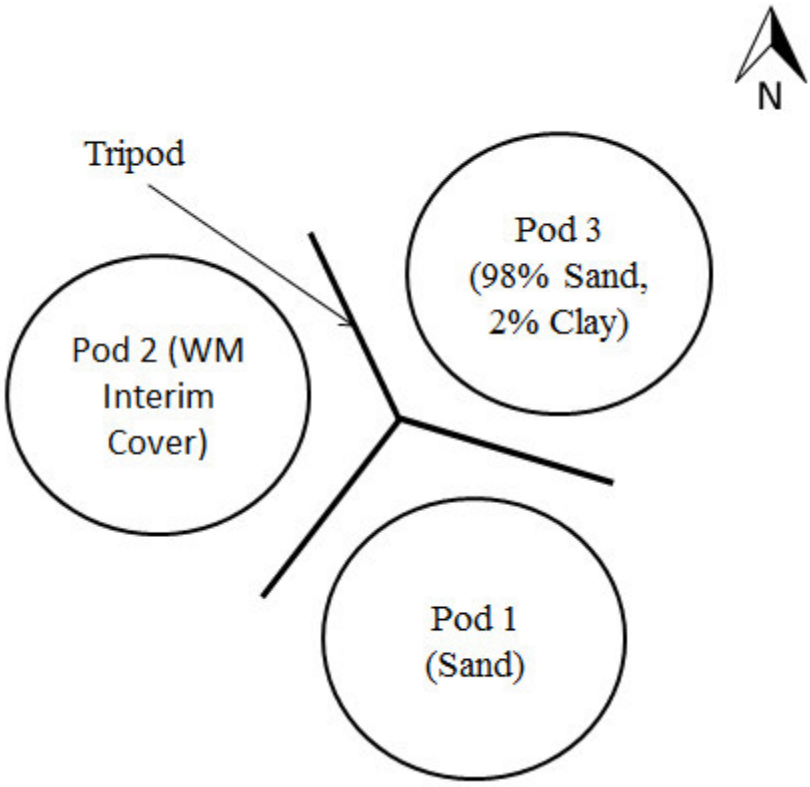

Figure 29: Overhead Schematic of Surface Monitoring Station Set-Up

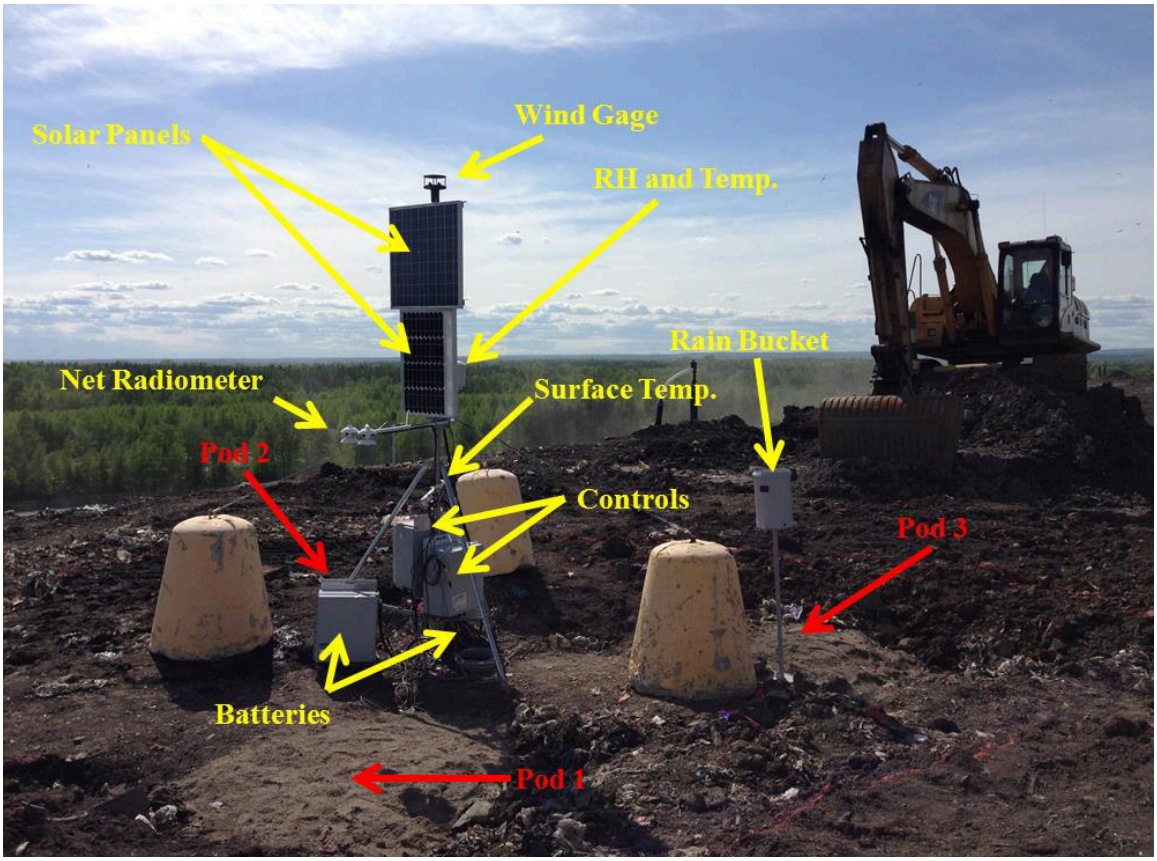

Figure 30: Surface Monitoring Station Set-Up

The above-ground components of the surface monitoring station include:

- A relative humidity and ambient temperature sensor
- An infrared net radiometer that measures the net short and long-wave radiation
- A surface temperature sensor
- A rain bucket to measure rainfall intensity and cumulative rainfall
- A sonic wind gage to measure wind velocity and direction
- Two batteries to provide power to the station controls and devices
- Two solar panels to provide power to the batteries
- Two control boxes that include a central data acquisition system that read the data from the sensors; terminal boxes for attaching sensors; and a modem to relay data.

Below the surface, the station was equipped with sensors to monitor three interim cover pods. Each interim cover pod included a 30 cm of interim cover material lying overtop the waste. Within each pod, the following sensors were installed:

- 3 oxygen sensors that also measure temperature. Originally installed at depths of 40 cm, 60 cm, and 75 cm. The top sensors in pods 1 and 3 were later moved to a depth of 15 cm (within the cover material). This is discussed in Section 7.2.
- 3 temperature thermistors. Installed at depths of 40 cm, 60 cm, and 75 cm.
- 1 heat flux plate (in pods 1 and 3 only). Installed at a depth of 60 cm.
- 2 moisture sensors. Installed at depths of 40 cm and 60 cm.

The system was installed on May 28th and 29th, 2014 in approximately one year old waste. To install the below-ground sensors, excavations of approximately one meter deep were made by an excavator (see (Left) Figure 31).

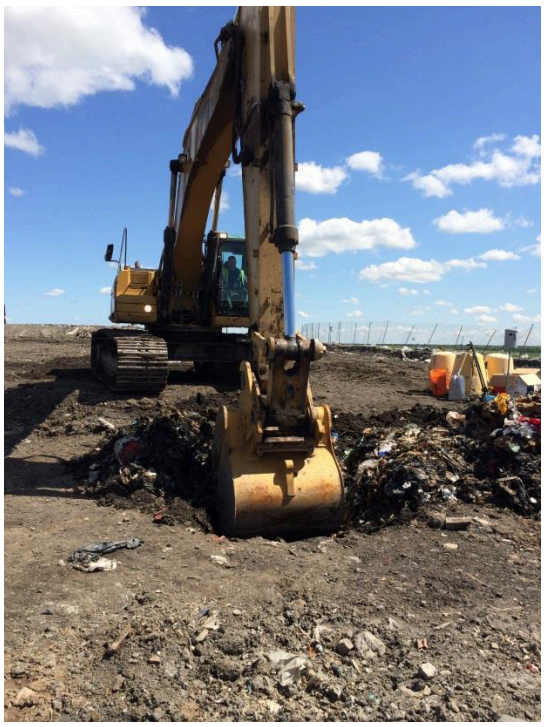
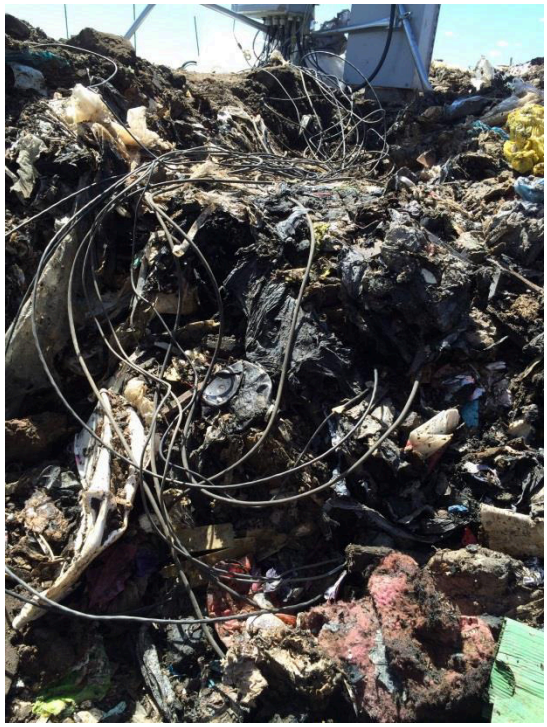

(Left) Figure 31: Excavation of waste pods
(Right) Figure 32: Sensor installation into excavated wall of waste pod

Sensors were placed into the excavated wall of waste closest to the central tripod (see (Left) Figure 31). Once the sensors were installed, waste was backfilled and compacted (by the excavator bucket) up to a depth of 30 cm below ground surface. Each of the three pods was then covered by 30 cm of different interim cover material (see Figure 34). Pod 1 was covered by clean sand. Pod 2 was covered by the interim cover that Waste Management (WM) was using in the location of the surface station. Pod 3 was covered with the same sand as pod 1 with 2% clay content (by mass). The grain size distribution for the clean sand used in pods 1 and 3 is shown in Figure 33. The clay used in pod 3 was kaolinite. The clay was weighed out on site and mixed in the excavator bucket.

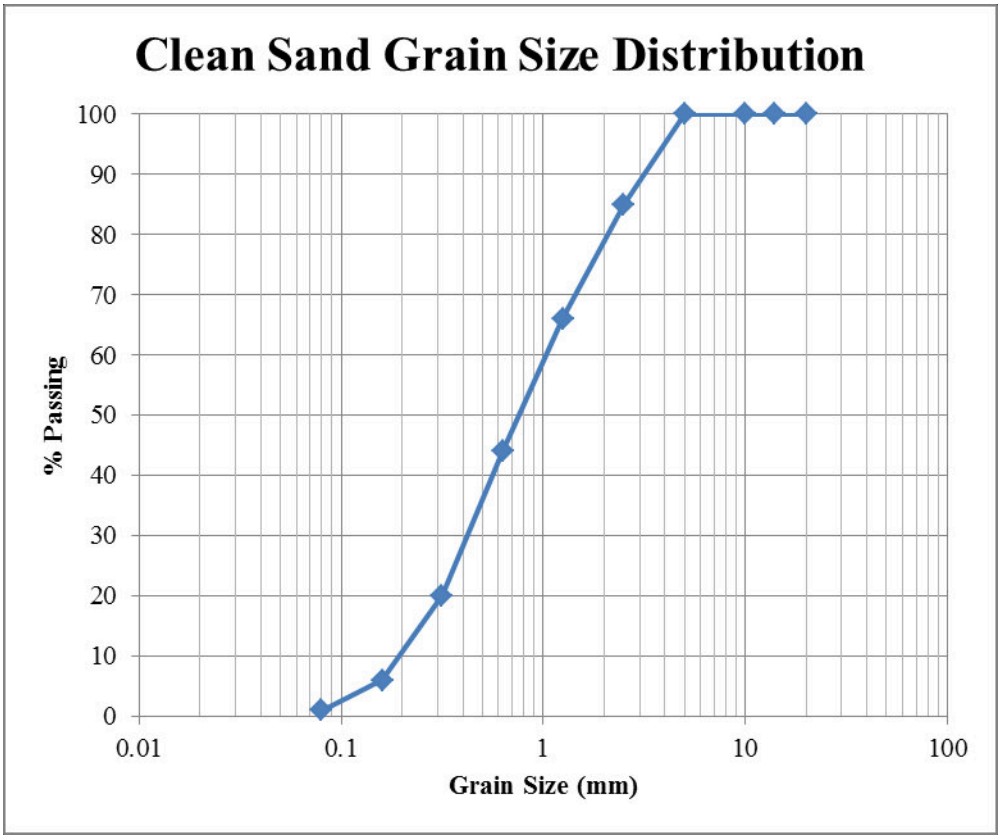

Figure 33: Clean sand grain size distribution

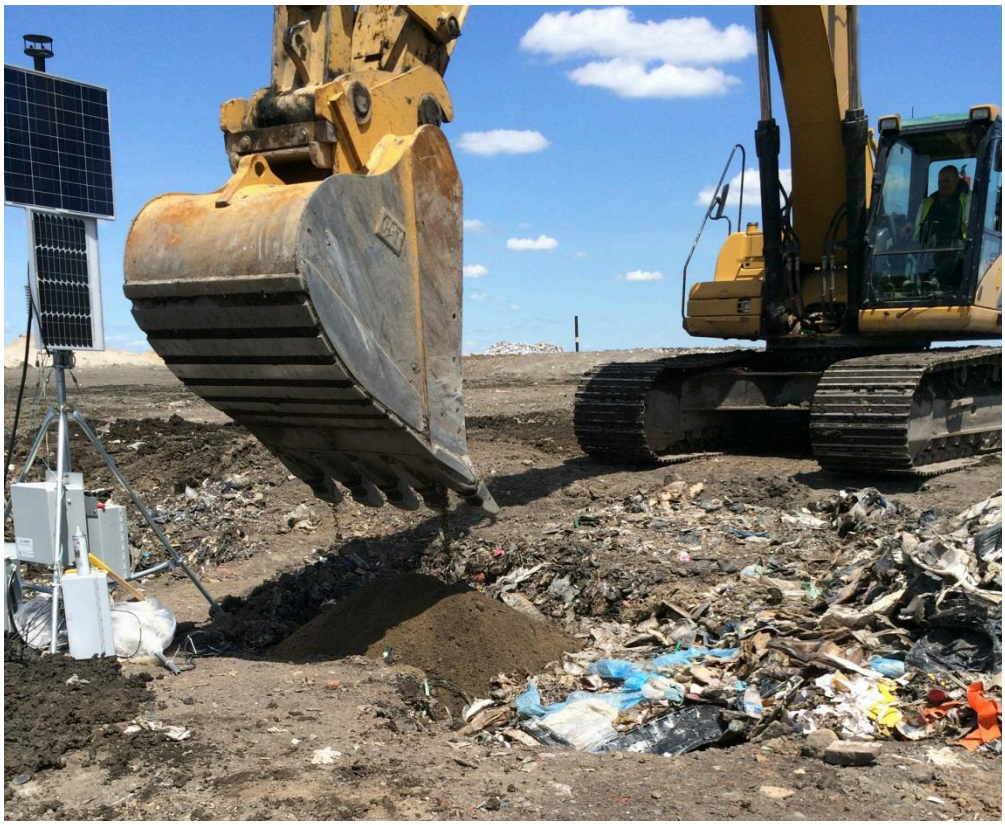

Figure 34: Filling of sand cover on pod 1

The goal of using three different covers was to monitor the differing waste conditions depending on the cover type. Gladish (2013) had installed the same surface monitoring station at a different location in the landfill that had a very dense, clayey interim cover. No oxygen was able to diffuse through the cover; and therefore, no aerobic activity occurred in the waste underneath the cover and no temperature effects were seen.

It was hypothesized that the sand and sand-clay covers would allow for oxygen diffusion; and therefore aerobic decomposition in the underlying waste. The mining industry commonly uses sand to cover mine waste tailings (Mackay, 1997). In the case of tailings, oxygen diffusion through the sand cover is not desired, however does occur.

The system was removed from the field on June 23rd, 2015 to allow WM to place another waste lift in that area Figure 35.

Figure 35: Surface monitoring station on June 23rd, 2015

7.2 Surface Study Results & Discussion

Preliminary data from the surface station is presented in this section.

Initially, it was observed that oxygen was more prevalent beneath the WM interim cover than the sand covers (Figure 36, Figure 37, Figure 38).

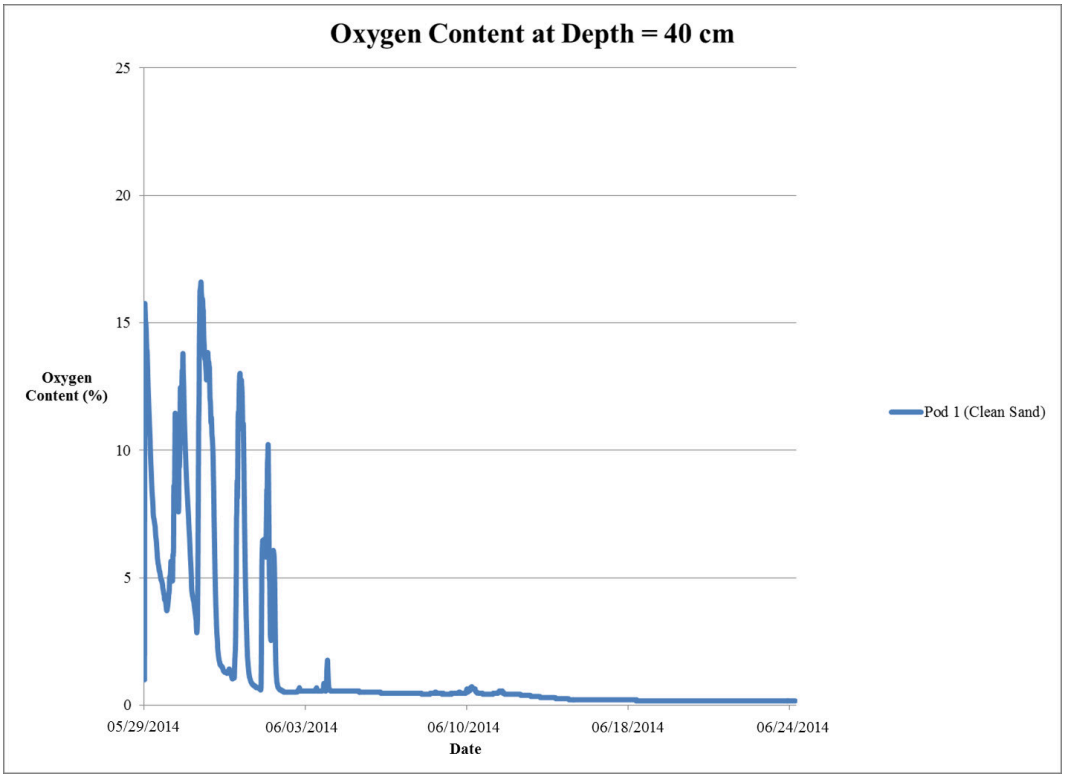

Figure 36: Oxygen Concentration at a Depth of 40 cm for Pod 1 (Clean Sand)

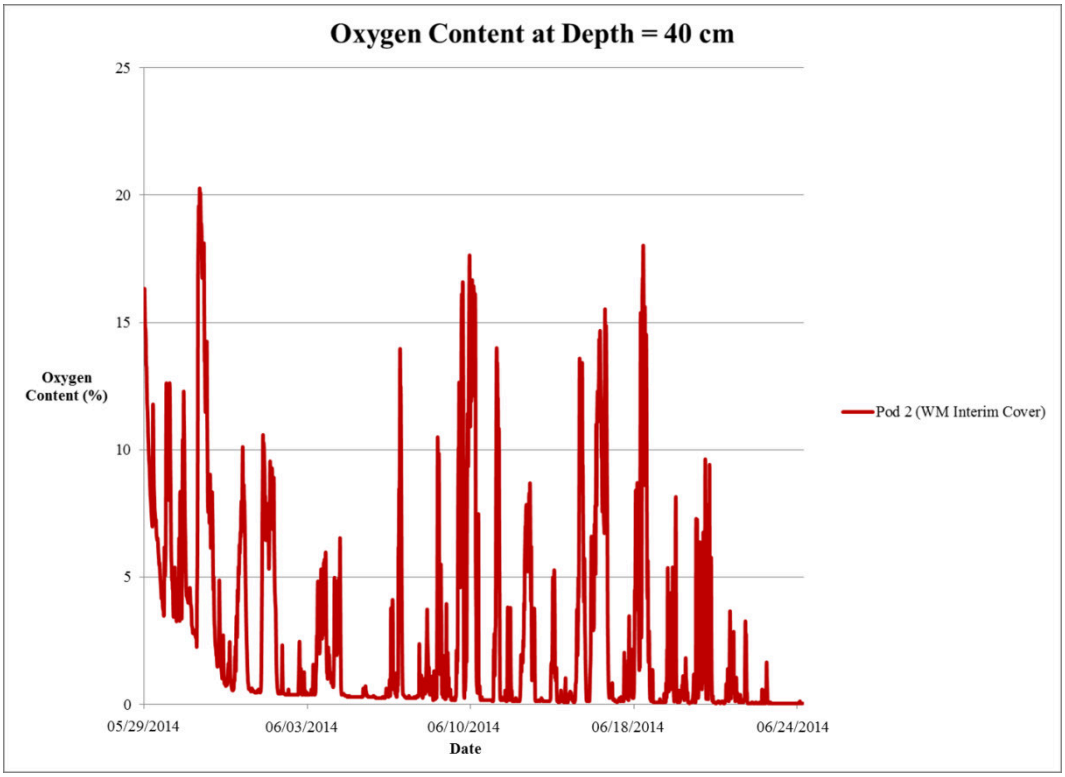

Figure 37: Oxygen Concentration at a Depth of 40 cm for Pod 2 (WM Interim Cover)

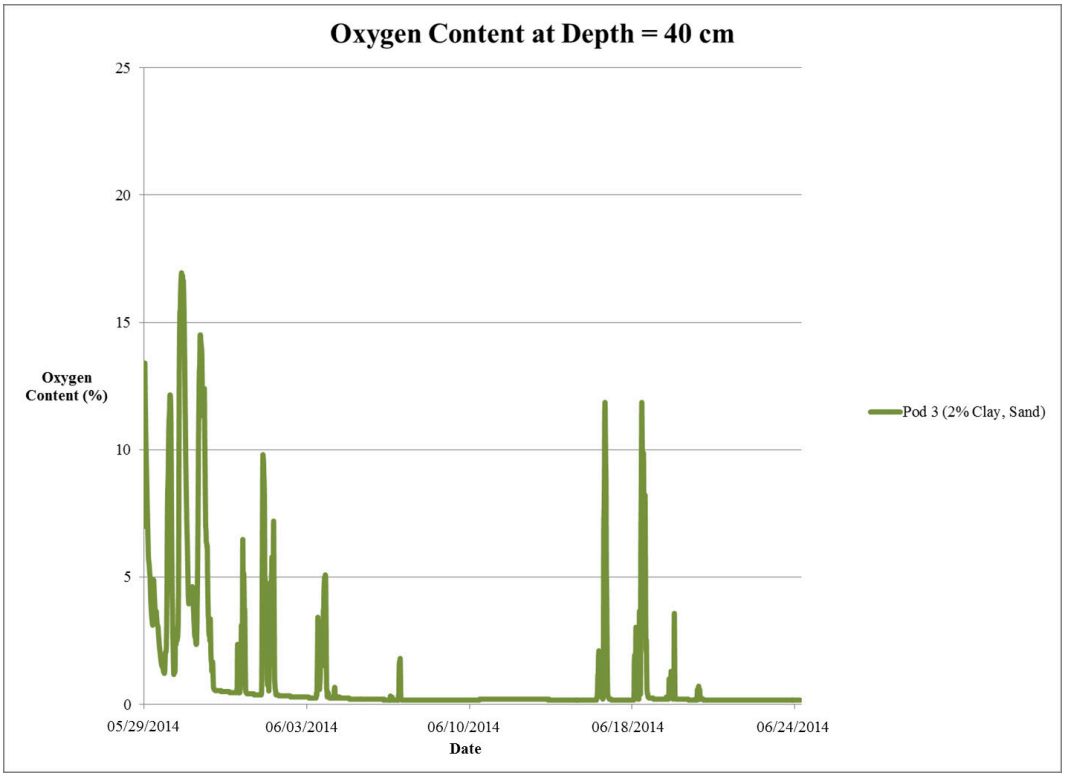

Figure 38: Oxygen Concentration at a Depth of 40 cm for Pod 3 (2% Clay, Sand)

After an initial five day period where each cover behaved similarly, the two sand covers indicated lower oxygen levels than the WM cover at a depth of 40 cm (10 cm below the cover). Upon investigation, the sand covers were saturated with water (Figure 39). The more compacted WM interim cover was not saturated and it was assumed that this may have been because the lower permeability of this material caused the water to pond and run-off the surface as opposed to infiltrating. In addition, the final grading of the WM interim cover was more conducive to run-off than the other two interim cover materials.

The diurnal fluctuations in oxygen recorded below the WM interim cover (pod 2) occurred during periods of high atmospheric pressure (and low relative humidity). This is a phenomenon known as barometric pumping, where an increase in atmospheric pressure results in subsurface motion of air in porous earth materials (Auer et al., 1996).

As a result of these findings, the top oxygen sensors in pods 1 and 3 were moved to a depth of 15 cm (within the cover) on July 15th, 2014 to examine conditions in the middle of these pod covers.

Figure 39: Pod 1 saturated cover (June 26, 2014). Pooled water is visible at a depth of 10 cm.

After the re-installation of the oxygen sensors in pods 1 and 3, it was found that oxygen rarely ever migrated to the middle of either of the sand covers (Figure 40). In all three pods, no oxygen was present at depths of 60 cm and 75 cm.

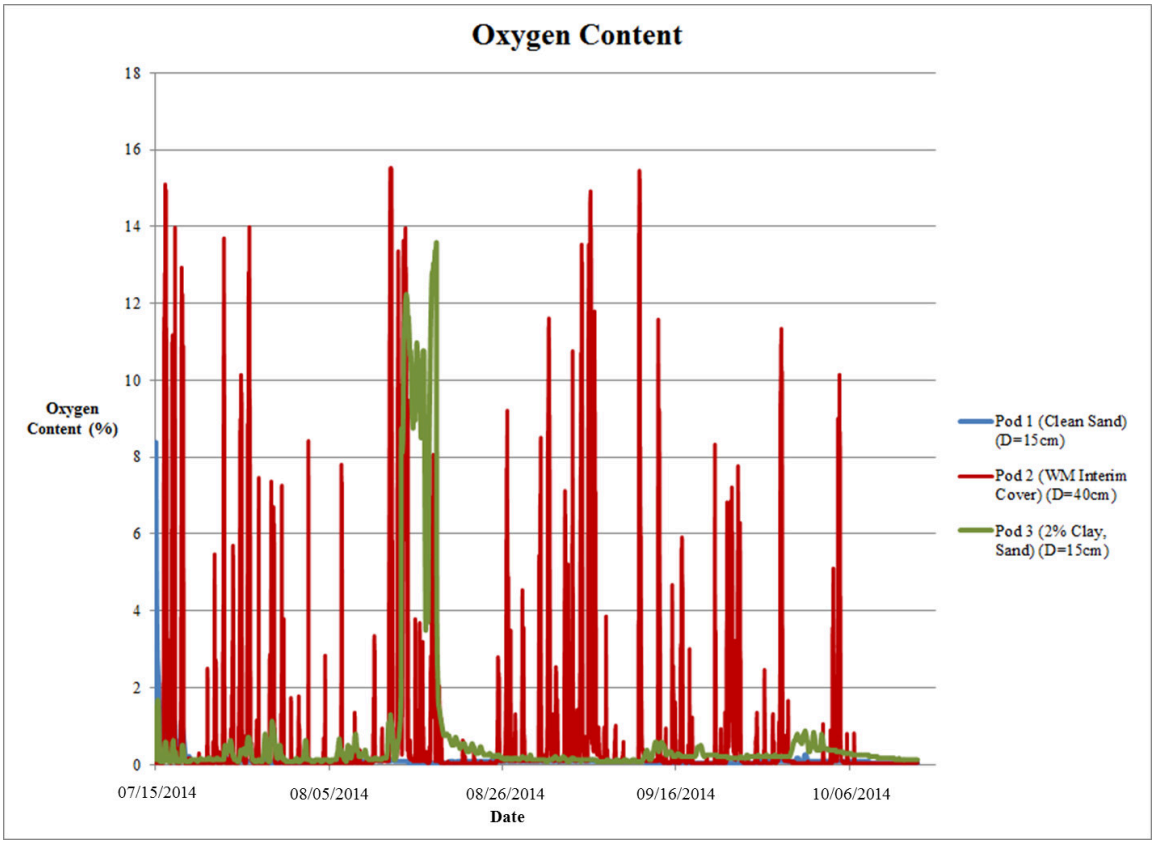

Figure 40: Oxygen content in the cover of pods 1 and 3 (D=15 cm) and just below the cover of pod 2 (D=40 cm)

The temperature profiles of each pod are plotted in Figure 41, Figure 42, and Figure 43. The 24 hour average ambient temperature is displayed for comparison. Data from the heat flux plot, as well as rainfall intensity, are plotted for pods 1 and 3. Heat flux is defined as positive in the downward direction.

Figure 44, Figure 45, and Figure 46 give a comparative view of the temperatures in each of the three pods at different depths. Ambient temperature is displayed for comparison.

Temperatures in the waste for all the pods are approximately 10^{o}C greater than the average ambient temperature. At a depth of 40 cm (10 cm below the cover material), waste temperatures in all three pods rose to temperatures above 35^{o}C at their peak. Temperatures this high are likely due to heat generation from biodegradation. Although

no oxygen is seen beneath pods 1 and 3, heat generated from aerobic decomposition in surrounding areas is likely to have transferred to the locations of pods 1 and 3.

No significant differences in temperatures are seen underneath the three different cover materials. If a larger scale experiment was conducted by covering larger areas with sand or the clay-sand mixture, it could be expected that the limited diffusion of oxygen through the saturated cover would result in less aerobic decomposition and therefore lower waste temperatures.

It can however be seen in pod 2 that rises in temperature do occur when sharp spikes in oxygen concentration are seen in the waste (Figure 47). This relationship is likely due to heat generation from aerobic biodegradation. High levels of oxygen are not sustained and therefore neither are the rises in temperature.

The heat flux data (Figure 41, Figure 43) shows that when rainfall occurs, waste temperatures decrease due to the downward advection of the rain (which is colder than the waste).

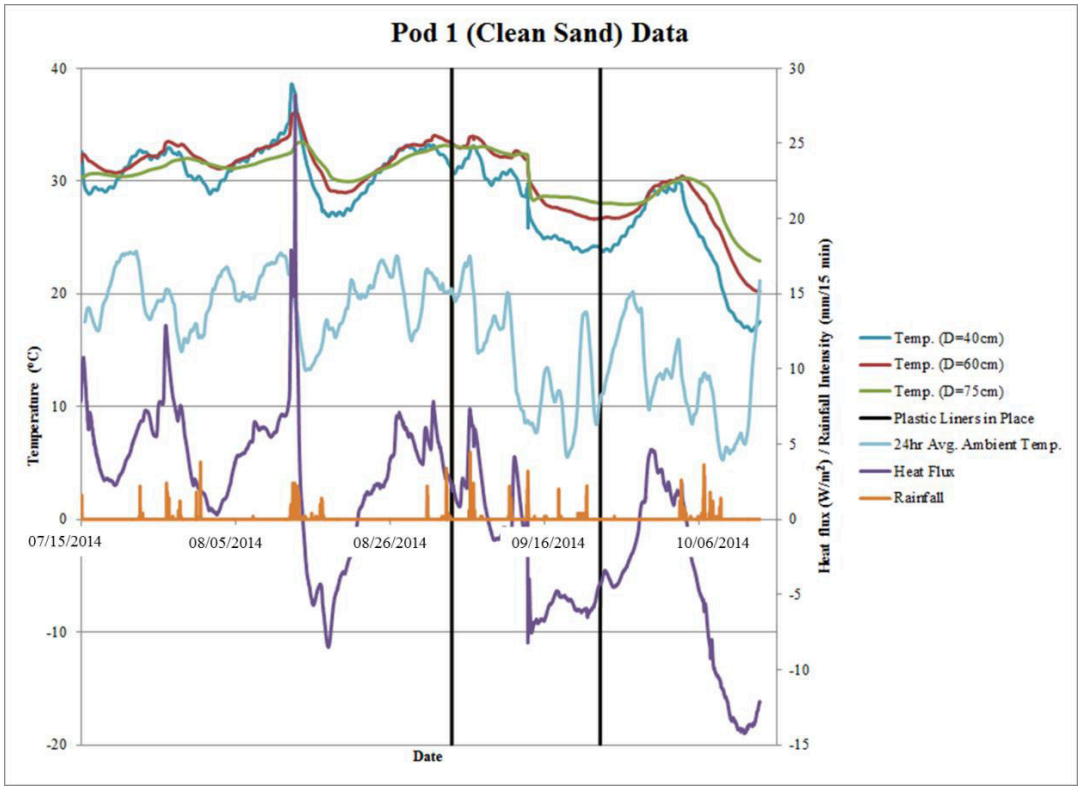

Figure 41: Pod 1 temperature, heat flux, and rainfall data

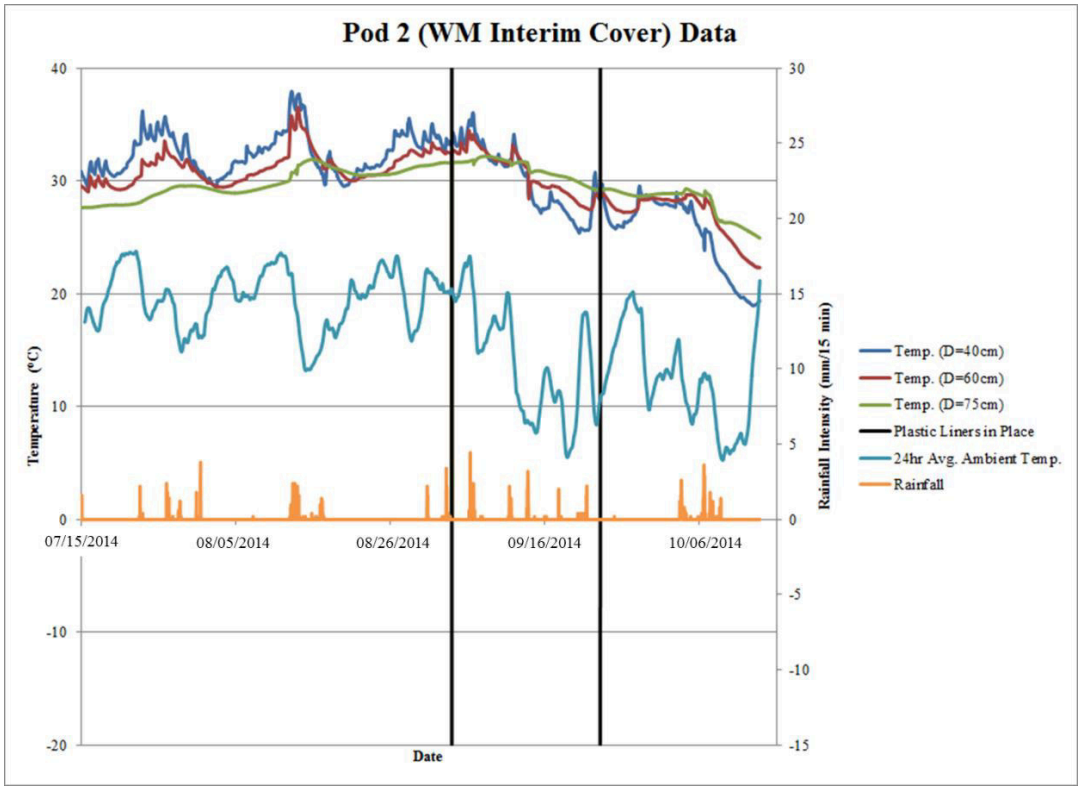

Figure 42: Pod 2 temperature data

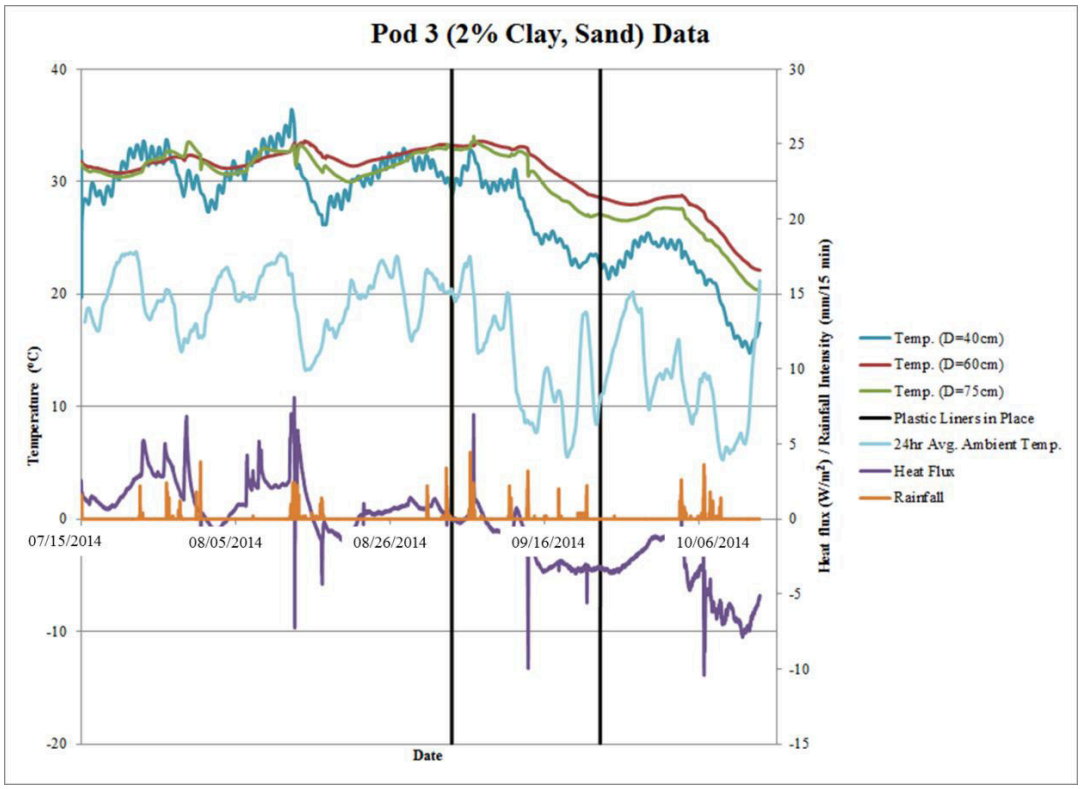

Figure 43: Pod 3 temperature, heat flux, and rainfall data

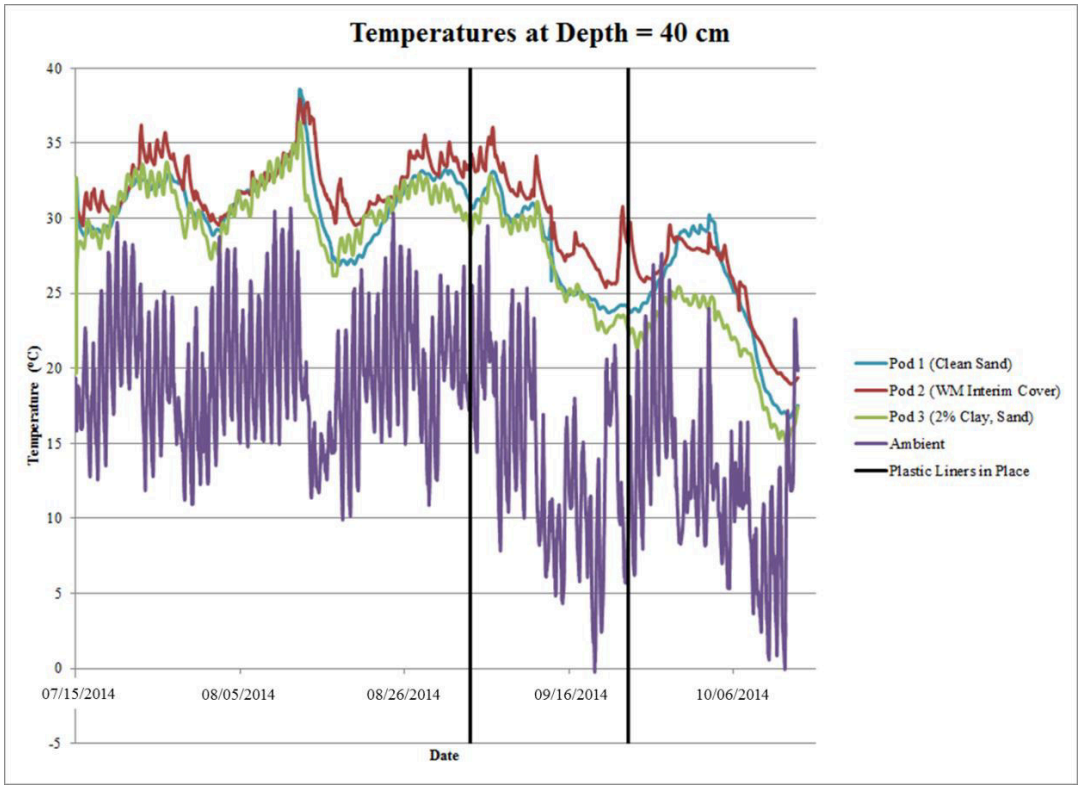

Figure 44: Temperatures at a depth of 40 cm in pods 1-3

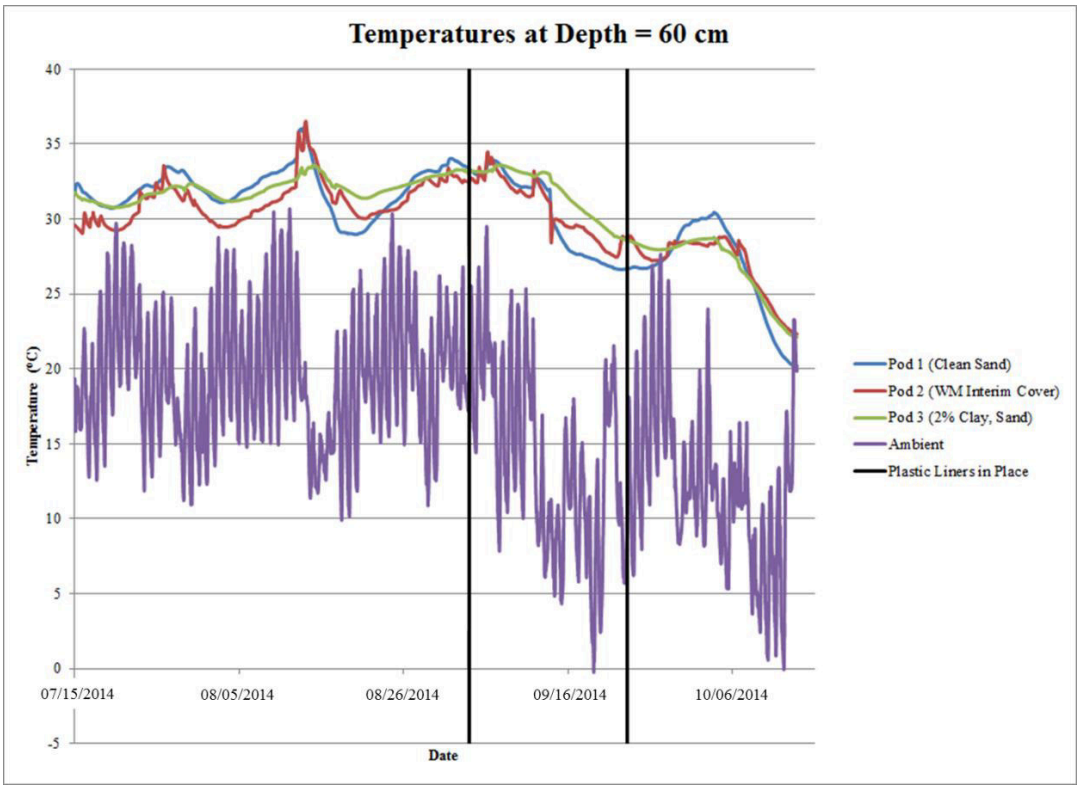

Figure 45: Temperatures at a depth of 60 cm in pods 1-3

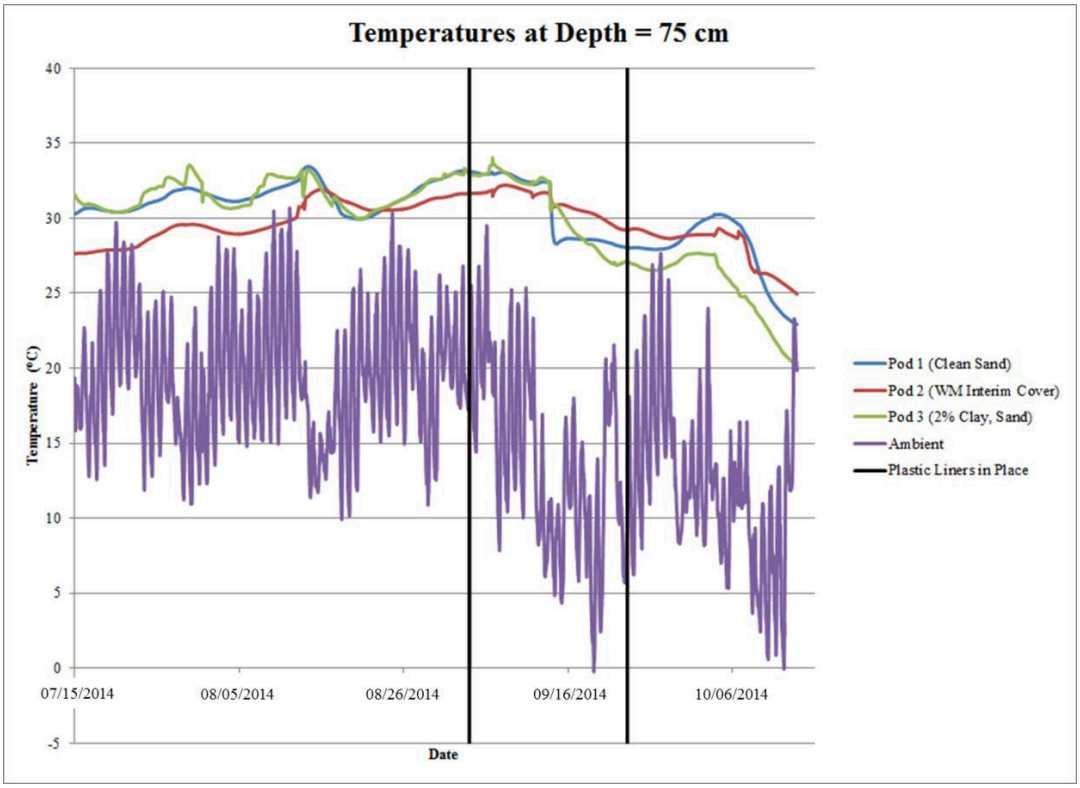

Figure 46: Temperatures at a depth of 75 cm in pods 1-3

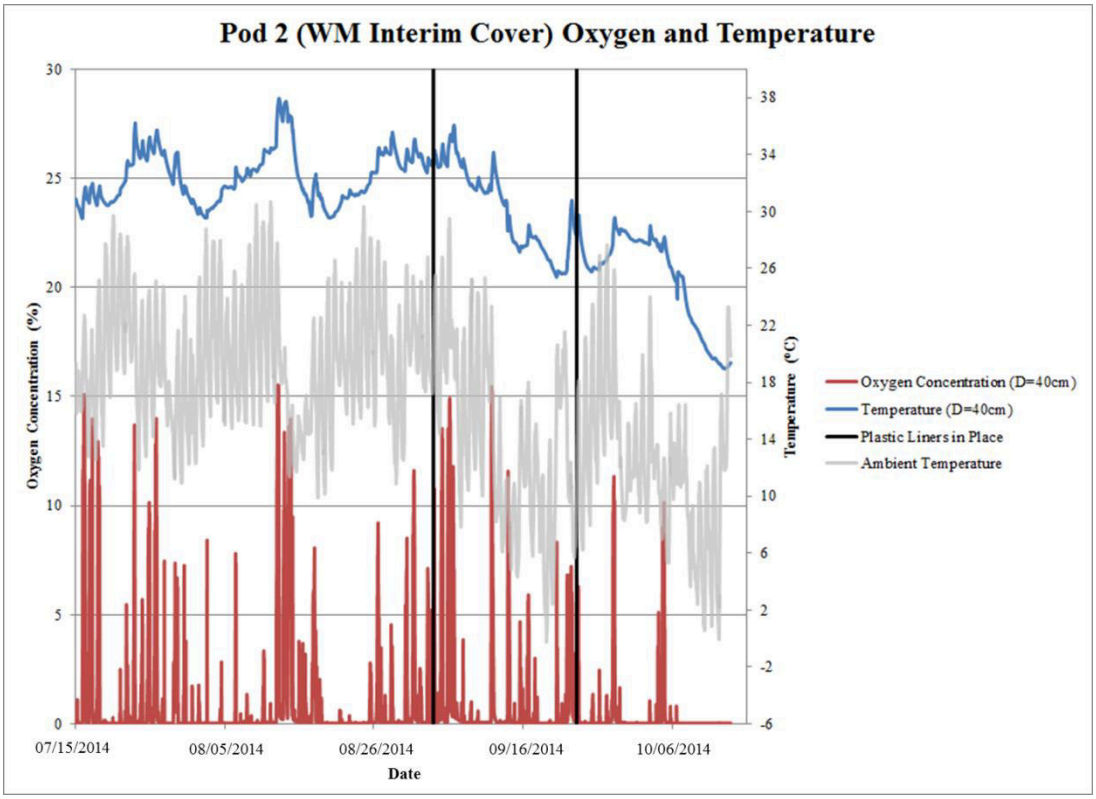

Figure 47: Pod 2 oxygen and temperature

From September 3rd to September 23rd, 2014, plastic liners were place above all of the pods and sealed with large rocks (Figure 48). This period is noted by black vertical bars on all plots. The experiment was designed to look at the effects of eliminating rainfall and minimizing the potential for oxygen migration through the cover. No changes in monitored parameters were found at the conclusion of the experiment. Oxygen fluctuations were still recorded at the oxygen sensor located 10 cm underneath the waste management interim cover in pod 2.

Figure 48: Plastic liner placed above pods

The surface monitoring station field data and the modelling of the data were originally the focus of the author's MASc research. When the data did not indicate the expected trends and the issues related to the data could not be resolved, it was decided by the author and his supervisor to shift the focus of the author's MASc to the modelling of the instrument bundle data.

8.0 CONCLUSIONS & RECOMMENDATIONS FOR FUTURE WORK

8.1 Conclusions

The Ste-Sophie, QC landfill was instrumented with sensors that have been successfully recording data for over five years. Temperatures in the waste have been found to rise to over 60^{o}C in locations where aerobic degradation is occurring. Frozen waste layers were found to stay frozen for one to two years after placement.

A one-dimensional conceptual and quasi-thermal-mechanical-biological numerical model was developed to simulate the landfill data. The model was used to gain a better understanding of the heat transfer and heat generation within the waste and at the upper (atmosphere) and lower (subsurface soil) boundaries of the vertical waste profile. Thermal conductivity was varied with depth in the model to replicate field conditions. Modelled temperatures were in good agreement with field data. The aerobic and anaerobic heat generation terms provided a more theoretically sound approach than what had previously been presented by Megalla (2015). Aerobic heat generation was directly linked to oxygen concentrations with good numerical model prediction in upper layers of waste where oxygen was present. Anaerobic heat generation was correlated to temperature and energy expenditure using a model proposed by Hanson et al. (2013), again resulting in good numerical predictions throughout the model domain. The model can be utilized as a tool to predict waste temperatures depending on the waste placement temperatures and waste filling schedule. Oxygen availability in upper regions would have to be estimated.

Settlement was included in the model by applying the equations developed by Van Geel & Murray (2015). The incorporation of settlement allowed for the tracking of bundle position over time. This in turn allowed for better comparison of the modelled temperatures with field data.

A heat budget was conducted for the vertical waste profile simulated. Over the 4.6 year simulation period, the net heat flux at the surface was negative, due to heat loss from convection and net longwave radiation exceeding heat gain from incoming solar radiation. A small amount of heat was gained through conduction at the base of the landfill over the first three years of simulation because the waste was placed under frozen conditions. As the landfill temperatures rose, heat was lost via conduction at the base. Aerobic heat accounted for 36% of all heat generation while anaerobic heat accounted for 64% of all heat generation during the 4.6 year simulation period. A total of 22% of the heat generated via aerobic and anaerobic conditions was needed to thaw frozen waste placed in the landfill (latent heat) as waste remained frozen for up to 3 years after initial placement, while 55% of the heat generated was stored as sensible heat increasing the waste temperatures. The remaining 23% was lost to the surrounding environment.

A sensitivity analysis was performed to analyze the effects of varying the model specific heat and thermal conductivity parameters. The model was more sensitive to variance in thermal conductivity than specific heat. Varying the thermal parameters provided different effects to the upper and lower regions of the waste, depending on whether the parameters were increased or decreased.

A model simulation was performed to evaluate the potential effects of injecting air into the waste allowing aerobic decomposition to occur. Assuming that all oxygen would be used by aerobic microbes to produce heat, an air injection rate of 10 L/s between the second and third waste lifts at the Ste-Sophie, QC landfill would result in 26.08 MJ of added heat. This heat resulted in temperatures at bundles 5 and 7 (4 and 3.5 m away, respectively) to rise approximately 1^{o}C. The small amount of heat generated in this study due to the oxygen injection did not have a large effect on temperatures, however it does give an idea as to the magnitude of the change in temperature that could occur if an experiment of this nature were conducted in the field to further calibrate the model. Increased temperatures due to aerobic activity could result in an increased rate at which subsequent anaerobic activity occurs.

A landfill surface study was initially performed as part of this research to analyze the effects of different interim cover materials on the heat budget at the landfill surface. The preliminary data collected from the surface instrument station did not follow what was expected at the outset of the study and therefore, in consultation with the author's supervisor, the research focus shifted to the modelling of the instrument bundle data.

8.2 Recommendations for Future Work

The following work could be undertaken to further improve the model and understanding of thermal processes in landfills:

- Coupling of hydraulic processes into the model. Information on the moisture profile throughout the waste would enable better representation of varying

thermal properties as well as the movement of leachate (which transfers heat) through the landfill.

- Creating a biological settlement term that is dependent upon temperature/biological activity. This would allow for improvements to waste settlement modelling, and potential revenue increases calculated for waste management operators due to settlement during the filling stages of the landfill.
- Validate or modify the aerobic heat generation term by calculating the oxygen flux through the cover as opposed to using the concentration of oxygen recorded at the bundle locations as a proxy for the amount of oxygen available for aerobic decomposition.
- Larger-scale air injection model simulation and corresponding field test.

REFERENCES

Ahring, B. K. (2003). Perspectives for anaerobic digestion. *Advances in biochemical engineering/biotechnology, 81*, 1-30.

Agency for Toxic Substances & Disease Registry (2001). Landfill Gas Basics. Available Online: < http://www.atsdr.cdc.gov/HAC/landfill/html/ch2.html>. Accessed June 1, 2015.

American Heritage Dictionary of the English Language, (2011). Fifth Edition.

Angelidaki, I., Ellegaard, L., Ahring, B. K. (2003). Applications of the anaerobic digestion process. *Advances in biochemical engineering/biotechnology, 82*, 1-33.

Auer, L.H., Rosenberg, N.D., Birdsell, K.H., Whitney, E.M. (1996). The effects of barometric pumping on contaminant transport. *Journal of Contaminant Hydrology*, 24(2), 145-166.

Babu1, G.L.S., Reddy, K.R., Chouskey, S.K, Kulkarni, H.S. (2010). Prediction of long-term municipal solid waste landfill settlement using constitutive model. *Practice Periodical of Hazardous, Toxic, and Radioactive Waste Management*, 33(5), 139-150.

Bareither, C. A., Wolfe, G. L., McMahon, K. D., Benson, C. H. (2013). Microbial diversity and dynamics during methane production from municipal solid waste. *Waste Management, 33*(10), 1982-1992.

Bjarngard, A., and Edgers, L. (1990). Settlement of municipal solid waste landfills. *Proceedings of the 13th Annual Madison Waste Conference*, Univ. of Wisconsin, Madison, Wis., 192–205.

Bonany, J.E. (2012). Heat budget for an anaerobic bioreactor landfill in sainte-sophie , Quebec , Canada. M.A.Sc. Thesis, Ottawa, Canada.

Bonany, J. E., Van Geel, P. J., Gunay, B. H., Isgor, B. (2013a). Heat budget for a waste lift placed under freezing conditions at a landfill operated in a northern climate. *Waste Management, 33*(5), 1-14.

Bonany, J. E., Van Geel, P. J., Gunay, B. H., Isgor, B. O. (2013b). Simulating waste temperatures in an operating landfill in Québec, Canada. *Waste Management & Research, 31*(7), 692-699.

Durmusoglu, E., Corapcioglu, M.Y., Tuncay, K. (2005). landfill settlement with decomposition and gas generation. *Journal of Environmental Engineering, 131(9)*, 1311-1321.

Edil, T. B., Ranguette, V. J., Wuellner, W. W. (1990). Settlement of municipal refuse. *Geotechnics of waste fills: Theory and practice*, STP1070, A. Landva and G. D. Knowles, eds., ASTM, West Conshohocken, Pa., 225–239.

El-Fadel, M. (1991). Modeling gas and heat generation and transport in sanitary landfills. Ph.D Thesis. Stanford University, California, USA.

El-Fadel, M. (1999). Simulating temperature variations in landfills. *Journal of Solid Waste Technology and Management, 26*(2), 78-86.

El-Fadel, M., Angelos, N., Findikakis, Leckie, J. O. (1996a). Estimating and enhancing methane yield from municipal solid waste. *Hazardous Waste & Hazardous Materials, 13*(3), 309-331.

El-Fadel, M., Findikakis, A. N., Leckie, J. O. (1996c). Numerical modelling of generation and transport of gas and heat in sanitary landfills II. model application. *Waste Management & Research, 14*(6), 537-551.

El-Fadel, M., Findikakis, A. N., Leckie, J. O. (1997). Numerical modelling of generation and transport of gas and heat in sanitary landfills III. sensitivity analysis. *Waste Management & Research, 15*(1), 87-102.

El-Fadel, M., Findikakis, A., Leckie, J. O. (1996d). Biochemical and physical processes in landfills. *Journal of Solid Waste Technology and Management, 23*(3), 131-143.

El-Fadel, M., Leckie, J. O., Findikakis, A. N. (1996b). Numerical modelling of generation and transport of gas and heat in landfills I. model formulation. *Waste Management & Research, 14*(5), 483-504.

El-Fadel, M., Shazbak, S., Saliby, E., Leckie, J. (1999). Comparative assessment of settlement models for municipal solid waste land- fill applications. *Waste Management & Resource*, 17(5), 347–368.

Faitli, J., Magyar, T., Erdelyi, A., Muranyi, A. (2014). Characterization of thermal properties of municipal solid waste landfills. *Waste Management*.

Gibson, R. E., Lo, K. Y. (1961). A theory of soils exhibiting secondary compression. Acta Polytech. Scand., C10, 1–15.

Giroux, L. (2014). State of Waste Management in Canada. Canadian Council of Ministers of Environment.

Gholamifard, S., Robert, E., Duquennoi, C. (2008). Modeling anaerobic bioreactor landfills in methanogenic phase: long term and short term behaviors. *Water Research, 42*(20), 5061-5071.

Gladish, A. (2013). Personal Communication.

Haarstrick, A., Hempel, D. C., Ostermann, L., Ahrens, H., Dinkler, D. (2001). Modelling of the biodegradation of organic matter in municipal landfills. *Waste management & research, 19*(4), 320-331.

Halvadakis, C.P. (1983). Methanogensis in solid-waste landfill bioreactors. Ph.D Thesis. Stanford University, California, USA.

Hanson, J. L., Edil, T. B., Yesiller, N. (2000). Thermal properties of high water content materials. *ASTM Special Technical Publication 1374 Geotechnics of High Water Content Materials*, (pp. 137-151). West Conshohocken, PA.

Hanson, J. L., Liu, W.-L., Yesiller, N. (2008). Analytical and numerical methodology for modeling temperatures in landfills. *Selected Sessions of GeoCongress 08: Geotechnics of Waste Management and Remediation*, (pp. 1-8). New Orleans, Louisiana.

Hanson, J. L., Oettle, N. K., Yesiller, N. (2010). Spatial and temporal temperature distributions in municipal solid waste landfills. *Journal of Environmental Engineering, 136*(8), 804-815.

Hanson, J. L., Yesiller, N., Kendall, L. A. (2005). Integrated temperature and gas analysis at a municipal solid waste landfill. *Proceedings of the 16th International Conference on Soil Mechanics & Geotechnical Engineering*, (pp. 2265-2268). Rotterdam, The Netherlands.

Hanson, J. L., Yesiller, N., Howard, K. A., Liu, W. -L., Cooper, S. P. (2006). Effects of placement conditions on decomposition of municipal solid wastes in cold regions. *Proceedings of the 13th International Conference on Cold Regions Engineering.*

Hanson, J. L., Yesiller, N., Onnen, M. T., Liu, W.-L., Oettle, N. K., Marinos, J. A. (2013). Development of numerical model for predicting heat generation and temperatures in MSW landfills. *Waste Management, 33*(10), 1967-2144.

Hedrick, D.B., White, D.C. (1993). Application of analytical microbial ecology to the anaerobic conversion of biomass to methane. *Biomass and Bioenergy, 5(3-4)*, 247-259.

Hettiarachchi, C. H., Meegoda, J., Hettiarachchi, P. (2009). Effects of gas and moisture on modeling of bioreactor landfill settlement. *Waste Management*, 29(3), 1018–1025.

Hoornweg, D., Bhada-Tata, P. (2012). A global review of solid waste management. *Urban Development Papers Knowledge Series,* The World Bank Urban Development and Local Government Unit. No.15.

Indiana Department of Environmental Management (2013). Use of Alternative Daily Cover at Landfills.

Karthikeyan, O. P., Joseph, K. (2007). Bioreactor landfills for sustainable solid waste management. *Proceedings of the National Conference on Sustainable Energy and Waste Management*, (pp. 112-123). Coimbatore, India.

Lanini, S., Houi, D., Aguilar, O., Lefebvre, X. (2001). The role of aerobic activity on refuse temperature rise: II. experimental and numerical modelling. *Waste Management & Research, 19*(1), 58-69.

Lefebvre, X., Lanini, S., Houi, D. (2000). The role of aerobic activity on refuse temperature rise, I. landfill experimental study. *Waste Management & Research, 18*(5), 444-452.

Mackay, P.L. (1997). Evaluation of oxygen diffusion in unsaturated soils. Master's Thesis, University of Western Ontario. London, Ontario.

Marques, A.C.M., Filz, G.M., Vilar, O.M. (2003). Composite compressibility model for municipal solid waste. *Journal of Geotechnical & Geoenvironmental Engineering*, 129(4), 372–378.

McAdams, W. H. (1954). *Heat Transmission*. 3rd Edition. New York: McGraw-Hill.

Megalla, D. (2015). Heat transfer model for an engineered landfill in Sainte-Sophie, Quebec, Canada. M.A.Sc. Thesis, Ottawa, Canada.

Megalla, D., Van Geel, P.J., Gladish, A., Gunay, B. (2014). Impacts of aerobic and anaerobic biodegradation on the heat budget for landfills operating in northern climates. *Proceedings of the Fifth International Symposium on Energy from Biomass and Waste*. San Servolo, Venice, Italy: CISA.

Moran, M.J., Shapiro, H.N. (2008). Fundamentals of Engineering Thermodynamics. 6th Edition. New Jersey: John Wiley & Sons Inc.

Murray, W. (1995). The Garbage Crisis: Traditional Solutions. *Government of Canada.* Available Online: < http://publications.gc.ca/Collection-R/LoPBdP/BP/bp407-e.htm>

Neusinger, R., Drach, V., Ebert, H. -P., Fricke, J. (2005). Computer simulations that illustrate the heat balance of landfills. *International Journal of Thermophysics, 26*(2), 519-530.

Park, H. I., Lee, S. R. (1997). Long-term settlement behavior of landfills with refuse decomposition." *Journal of Resource Management & Technology*, 24(4), 159–165.

Pirt, S.J. (1978). Aerobic and anaerobic microbial digestion in waste reclamation. *Journal of Resource Applied Chemistry & Biotechnology*, 28, 232-236.

Rees, J. F. (1980). Optimisation of methane production and refuse decomposition in landfills by temperature control. *Journal of Chemical Technology and Biotechnology, 30*(2), 458-465.

Rowe, R. K. (2011). Systems engineering: the design and operation of municipal solid waste landfills to minimize contamination of groundwater. *Geosynthetics International,* 18, No. 6, 391–404.

Rowe, R. K., Hoor, A., Pollard, A. (2010). Numerical examination of a method for reducing the temperature of municipal solid waste landfill liners. *Journal of Environmental Engineering, 136*(8), 794-804.

Sharma, H.D., Lewis, S.P. (1994). Waste Containment Systems, Waste Stabilization, and Landfills: Design and Evaluation. New York: John Wiley & Sons Inc.

Sowers, G. F. (1973). Settlement of waste disposal fills. *Proc., 8th Int. Conf. on Soil Mechanics and Foundation Engineering*, Moscow, Vol. 2(2), 207–210.

Townsend, T. G., Kumar, D., Ko, J. (2008). Bioreactor Landfill Operation: A Guide For Development, Implementation and Monitoring: version 1.0 (July1, 2008). Gainesville, FL.

United States E.P.A. (1998). Interpretations of waste management activities: recycling, combustion for energy recovery, treatment for destruction, waste stabilization and release. Office of Pollution Protection and Toxics. Revised August, 1999.

Van Geel, P.J., Murray, K.E. (2015). Simulating settlement during operations at a landfill with waste lifts placed under frozen conditions. *Waste Management (2015)*. 29 August 2015.

Vingerhoeds, E. (2011) Instrument installation and preliminary data in a full-scale anaerobic bioreactor landfill, Sainte-Sophie, Quebec, Canada. M.A.Sc. Thesis, Ottawa, Canada.

Ward, R. F. (1983). Temperature effects: methane generation from landfill samples. *Journal of Environmental Engineering, 109*, 979-981.

Warith, M. (2003). Solid waste management: new trends in landfill design. *Emirates Journal for Engineering Research, 8*(1), 61-70.

Waste-to-Energy Research and Technology Council (2009). Anaerobic Digestion Process. Available Online: <http://www.wtert.eu/default.asp?Menue=13&ShowDok=12>. Accessed June 1, 2015.

Warith, M. (2003). Soilid waste management: new trends in landfill design. *Emirates Journal for Engineering Research, 8*(1), 61-70.

Watmuff, J. H., Charters, W. W., Proctor, D. (1977). Solar and wind induced external coefficients - solar collectors. *Cooperation Mediterraneenne pour l'Energie Solaire*, Revue Internationale d'Heliotechnique, 2nd Quarter.

White, J.K., Beaven, R.P., Powrie, W., Knox, K. (2011). Leachate recirculation in a landfill: Some insights obtained from the development of a simple 1-D model. *Waste Mangement, 31*(2011), 1210-1221.

White, J.K., Beaven, R.P. (2013). Developments to a landfill process model folloiwng its application to two landfill modelling challenges. *Waste Mangement, 33*(2013), 1969-1981.

White, J.K., Nayagum, D., Beaven, R.P. (2014). A multi-component two-phase flow algorithm for use in landfill processes modelling. *Waste Mangement, 34*(2014), 1644-1656.

White, J.K., Robinson, J., Qingchao, R. (2004). Modelling the biochemical degradation of solid waste in landfills. *Waste Mangement, 24*(2004), 227-240.

Williams, G.M., Aitkenhead, N. (1991). Lessons from loscoe: the uncontrolled migration of landfill gas. *Quarterly Journal of Engineering Geology and Hydrogeology*, 24, 191-207

Yoshida, H., Rowe, R. (2003). Consideration of landfill liner temperature. *Proceedings of the Ninth International Waste Management and Landfill Symposium* (pp. 1-9). Cagliari, Italy: CISA.

Yoshida, H., Tanaka, N., Hozumi, H. (1997). Theoretical study on heat transport phenomena in a sanitary landfill. *Proceedings of the* Sixth International Waste Management and Landfill Symposium. Sardinia, Italy: CISA.

Zambra, C. E., Moraga, N. O., Escudey, M. (2011). Heat and mass transfer in unsaturated porous media: Moisture effects in compost piles self-heating. *International Journal of Heat and Mass Transfer, 54*(13-14), 2801-2810.

Zanetti, M.C., Manna, L., Genon, G. (1997). Biogas production evaluation by means of thermal balances. *Sixth International Waste Management and Landfill Symposium*. Italy: CISA.

APPENDIX A – ENGINEERING DRAWINGS

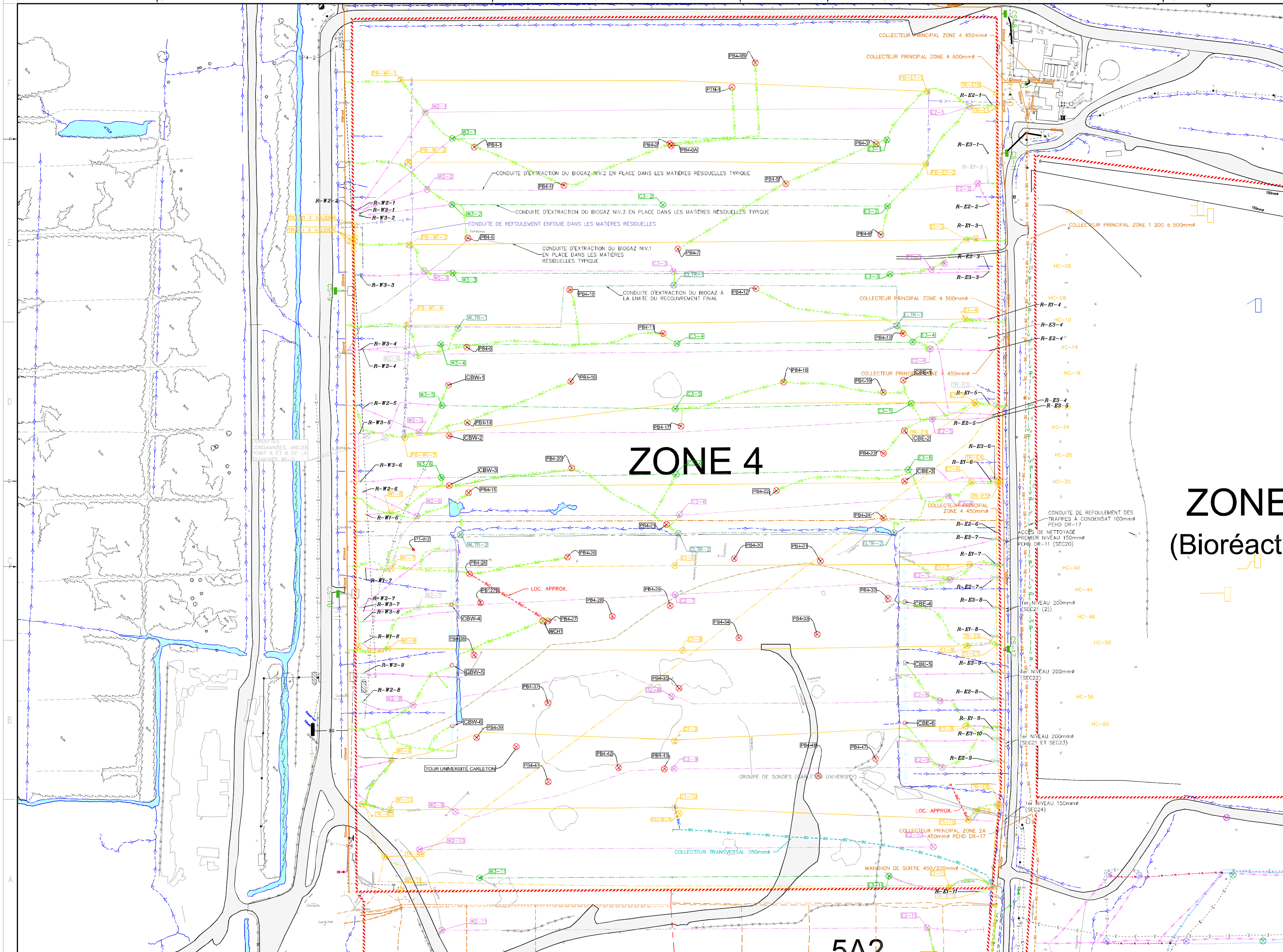

GENIVAR
5355, BOULEVARD DES GRADINS
QUÉBEC (QUÉBEC)
CANADA G2J 1C8
TÉLÉPHONE: 418 623-2254 TÉLÉCOPIEUR: 418 624-1857
WWW.GENIVAR.COM

NOTES:
À MOINS D'INDICATIONS CONTRAIRES, LES UNITÉS DE MESURE SONT EN MÈTRES.

RÉFÉRENCES:
LE FOND DE PLAN PROVIENT DE LA PLANIMÉTRIE RÉALISÉE PAR WSP À PARTIR DES PHOTOGRAPHIES AÉRIENNES. LA DATE DE LA PRISE DES PHOTOS EST LE 20 MAI 2014.

SYSTÈME DE COORDONNÉES PLANES DU QUÉBEC (SCoPQ), SYSTÈME DE RÉFÉRENCE GÉODÉSIQUE NAD 83, PROJECTION CARTOGRAPHIQUE MERCATOR TRANSVERSE MODIFIÉE (MTM) FUSEAU 8.

SCEAU:

CLIENT:
WASTE MANAGEMENT

PROJET:
LIEU D'ENFOUISSEMENT TECHNIQUE DE SAINTE-SOPHIE
TEL QUE CONSTRUIT GÉNÉRAL

PLAN CLÉ:

AVERTISSEMENT: COPYRIGHT:

ÉMISSION – RÉVISION:

ÉM	RÉ	DATE	DESCRIPTION
A		2014-10-21	POUR INFORMATION

NO PROJET: –
DATE: 2014-10-21
ÉCHELLE ORIGINALE: 1:1250
CONÇU PAR: Réjean Bouchard, Tech.
DESSINÉ PAR: Maxime Chaîné, tech., Julie Côté, tech., Catherine Fortin, tech.
VÉRIFIÉ PAR: Catherine Verrault M.Sc. M.Sc.A Jean Bernier, ing. M.Sc.

SI CETTE BARRE NE MESURE PAS 25mm, AJUSTER VOTRE ÉCHELLE DE TRAÇAGE.
25mm

DISCIPLINE:
LIEU D'ENFOUISSEMENT TECHNIQUE

TITRE:
PLAN D'ARRANGEMENT GÉNÉRAL DU RÉSEAU DE CAPTAGE DU BIOGAZ ZONE 4 ET 5

NUMÉRO DU FEUILLET:
TQC-LET-STE-SOPHIE_F05
FEUILLET #: 05 DE 06

ÉMISSION:
POUR INFORMATION
EN DATE DU: 2014-10-21
RÉV: A